



ज्ञान ज्योति से मार्गदर्शन

IRICEN Journal of Civil Engineering



Volume 22, No. 2

www.ircen.indianrailways.gov.in

September & December 2022



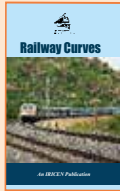
Indian Railways Institute of Civil Engineering, Pune

इरिसेन द्वारा प्रकाशित तकनीकी पुस्तके (TECHNICAL BOOKS PUBLISHED BY IRICEN)



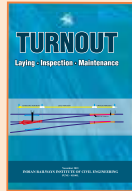
MECHANISED
TAMPING
&
STABILISATION

Rs. 150/-



Railway Curves

Rs. 130/-



Turnout

Rs. 100/-



Mechanised
Track Laying

Rs. 50/-



Non
Destructive
Testing of
Bridges

Rs. 80/-



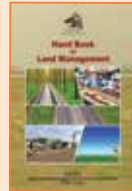
Compendium of
Judicial Verdicts

Rs. 80/-



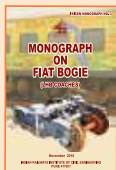
Compendium of
Schedule
Inspection

Rs. 80/-



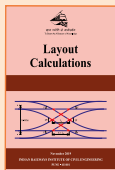
Hand Book
on
Land Management

Rs. 70/-



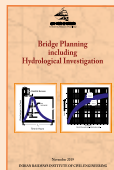
Monograph
on
Flat Bogie
(LHB Coaches)

Rs. 80/-



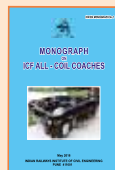
Layout
Calculations

Rs. 100/-



Bridge Planning
including
Hydrological
Investigation

Rs. 50/-



Monograph
ON
ICF ALL - COIL
COACHES

Rs. 60/-



Monograph
ON
CASNUB BOGIE

Rs. 60/-



Handbook
for
Track Maintenance

Rs. 500/-



Fundamentals of
Building Orientation
And Green
Building Features

Rs. 40/-



Welding
Techniques

Rs. 40/-



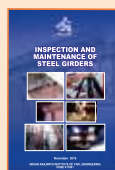
The Investigation
of Derailments

Rs. 100/-



Under Water
Inspection of Bridges

Rs. 80/-



Inspection and
Maintenance of
Steel Girders

Rs. 120/-



Construction And
Maintenance of
High Speed
Railway

Rs. 170/-



Bridge
Inspection &
Maintenance

Rs. 80/-



Hand Book
of
Land Management

Rs. 70/-



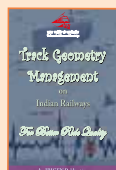
USFD
Testing of Rails
and Welds

Rs. 50/-



Bridge
Bearings

Rs. 60/-



Track Geometry
Management

Rs. 50/-



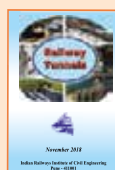
Signalling
For
Track Engineers

Rs. 70/-



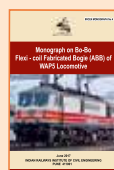
Rain Water
Harvesting

Rs. 30/-



Railway
Tunnels

Rs. 200/-



Monograph on Bo-Bo
Flexi-coil Fabricated
Bogie (ABB) of
WAPS Locomotive

Rs. 90/-



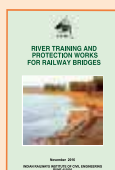
Geotechnical Testing
For Earthwork
In Railway Projects

Rs. 70/-



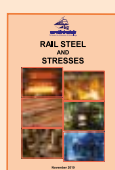
Handbook
of
Material
Testing

Rs. 50/-



River Training &
Protection works
for Railway
Bridges

Rs. 90/-



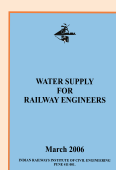
Rail Steel
And
Stresses

Rs. 50/-



Inspection,
Assessment,
Repairs &
Retrofitting Of
Masonry Arch
Bridges

Rs. 50/-



Water Supply
For
Railway
Engineers

Rs. 25/-



From Director General's Desk

Dear Readers,

In this edition of IRICEN journal, papers have been included on diverse topics. The first technical paper is about the new construction and methodology of full span girder launching under Ahmedabad- Mumbai High Speed Rail Project. The second paper is on the study and review of live load distribution factors for concrete girder bridges.

The third paper deals with the launching of 85m Open Web Girder with skew angle of 65 degree of a Road Over Bridge located in Mumbai Central Division of Western Railway. The fourth paper is related to Regirdering of existing span No. 28 to 30 of UP and DN lines of Wadibunder Bridge of CSTM-Kalyan section of Mumbai Division of Central Railway. This work was executed under adverse conditions having no approach road using an innovative method of launching.

The fifth paper talks about experimental and analytical study of benefits of using multi twin T girder prestressed concrete decks for Road Over Bridges. The sixth paper is “Uncracked reinforced concrete rectangular, circular and hollow circular columns under long term loading – A Review of Indian Bridge Codes” and the last paper is related to study and development of design charts for flexural members of Railway bridges.

I hope that the readers will find these papers and other articles contained in this edition relevant and useful. Any suggestions for making this journal more useful and contribution of technical papers for inclusion of forthcoming editions would be greatly appreciated. This will help in sharing and spreading knowledge and experience among Railway Engineers.

Pune

November 2022

(Ashok Kumar)

Director General

EDITORIAL BOARD**Shri Ashok Kumar**

Director General/IRICEN

Chairman**EDITING TEAM****Shri Ghansham Bansal**

Sr. Professor / Track-1

Executive Editor**Shri Avinash Kumar**

Professor / Track - 2

Executive Editor**Shri Shailendra Prakash**

Asst. Library & Inf. Officer

Assistant Editor**Shri Pravin Kotkar**

Sr. Instructor/Track-1

Editorial Assistant

The papers & articles express the opinions of the authors, and do not necessarily reflect the views of IRICEN editorial panel. The institute is not responsible for the statements or opinions published in its publication.

INDEX

1 - Full Span Launching Method under Ahmadabad Mumbai Bullet Train Project - A "Make in India" Initiative	03
Surendra Kumar Bansal, Chief Project Director, NWR Bhavna Singh, NICMAR Student Andrilla Roy, NICMAR Student A. H. More, NICMAR Student Sumeet Wankhede, NICMAR Student	
2 - Live Load Distribution Factors for Concrete Girder Bridges	12
Avinash Kumar, Prof. Track-II/IRICEN G.S. Yadav, Retd. Prof/IRICEN	
3 - Launching of Steel 85M Open Web Girder With 65 Degree Skew in Mumbai Central Division of Western Railway	17
Himanshu Sharma, Dy.CE/Design/WR Yogesh Kumar, Dy. CE/C/CCG Harish Meena, XEN/C/CCG	
4 - Regirdering of Existing Span No 28, 29, 30 & 30 Bp Up & Dn Lines of Wadibunder Bridge On CSTM-CLA (HB) Section In Mumbai Division	24
Nishith Kumar Mall, Dy.CE(Br.Line)HQ,CSMT Vivek Kumar, SSE/Bridge/C.Rly	
5 - Experimental Study and Discussion on Multi-Twin-T-Girder-Deck for Road Bridges over Railway	32
Dr.Geetha M. P., Retired AXEN/Design/ Southern Railway. Dr. Girija K., Professor, College of Engineering Trivandrum. S. Shanmughom, DEN/Special Works/ Madurai/ Southern Railway.	
6 - Uncracked Reinforced Concrete Rectangular, Circular and Hollow Circular Columns under Long Term Loading – A Review of Indian Bridge Codes	41
R.Sundaresan, SSE/Drg., CAO/CN/O/MS, S.Rly	
7 - Studies on Design Charts For RC Flexural Members of Railway Bridges.....	52
Dr. Amaravel. R, SSE/Designs/CN/BNC, S.W. Railway	
l) Literature Digest	60

Suggestion for improvement of IRICEN JOURNAL OF CIVIL ENGINEERING are welcome from the readers. Suggestions may be sent to mail@iricen.gov.in

Guidelines to contributors

Articles on the Railway Civil Engineering are welcome from the authors. The authors who are willing to contribute articles in the IRICEN Journal of Civil Engineering are requested to please go through the following guidelines :

1. The paper may be a review of conventional technology, possibilities of improvement in the technology or any other item which may be of interest to the readers. The paper should be reasonably detailed so that it could help the reader to understand the topic. The paper may contain analysis, design, construction, maintenance of railway civil engineering assets. The paper should be concise.
2. The journal is likely to be printed in a paper of size 215 mm X 280 mm. While sending the articles the author should write in 2 columns. Sketches, tables and figures should be accommodated in a 2 column set up only.
3. Author should send the original printout of photograph along with the digital copy of the photograph.
4. Soft copy as well as hard copy of article must be invariably sent to the editors of concerned subject.
5. Only selected articles will be included in the IRICEN Journal of Civil Engineering.

Full Span Launching Method under Ahmadabad Mumbai Bullet train project - A “Make in India” initiative

By
 Surendra Kumar Bansal¹,
 Bhavna Singh²,
 Andrilla Roy³,
 A.H. More⁴,
 Sumeet Wankhede⁵

ABSTRACT

This research paper highlights the new construction methodology and erection equipments used in the Full Span Launching Method (FSLM), its management and uncertainty mitigation under the Ahmedabad-Mumbai High Speed Rail Project.

Introduction:

Ahmadabad Mumbai High Speed Rail is the first project of its kind in India. The scope of this High Speed Rail (HSR) project is to construct a Double Track High Speed Rail connecting Mumbai with Ahmadabad. The total length is 508 km and includes 12 stations. The bullet train would operate at a speed of 320 kmph covering the distance of 508 km in 2 hrs and 7 minutes. [2]

The successful completion of this project will be the stepping stone for the development of high-speed rail network in India, which is expected to boost the economical growth of India and the development of satellite towns, resulting in the increase of the GDP rate of the country.

The project would be a big boost for the Indian construction industry in terms of works contracts as well as introduction of new technologies, as one of the main objectives of the project is “Make in India”.

The sequences of activities involved for the civil work under the full span box girder method of viaduct construction are as follows:

- Detailed Project Report
- Land Acquisition
- Geotechnical Investigation
- Piling
- Pile Cap
- Pier
- Pier Cap
- Precasting of superstructure elements
- Erection of the superstructure elements.

This research paper focuses primarily on resource management of the latest technologies and specialized equipment being used in the casting and erection of full span box girder (superstructure only).

The launching girder (LG) erects the Precast Span from the Gantry Transporter (GT) and places it at its final position. This method is designed to work on single-deck viaducts only. The precast post-tensioned full span box girder is shifted from casting bed to stacking bed with the help of Straddle Carrier.

The initial four spans are erected by Bridge Gantry. For balance spans, the erection is done by the launching girder.

Casting of Full Span Girder - Methodology:

Precast Yard set up:

- ❖ The Precast yard for full span girder fabrication shall consist of mainly:
- ❖ Mould assembly area.
- ❖ Girder Stacking area
- ❖ Rebar Jig location.
- ❖ Batching Plant.
- ❖ Ready Made Steel Plant.
- ❖ Plants and machinery Workshop.
- ❖ Labour colony.

A typical Precast yard at the site of High Speed Railway project is shown in Figure 1.

Mobilization of Materials and Machineries:

- ❖ After the completion of precast yard setup, the plants and machineries shall be mobilized immediately to their assigned location.
- ❖ The Machineries including the Straddle carrier, Gantry crane, Bridge Gantry, Gantry Transporter,

¹ Chief Project Director, NWR
^{2, 3, 4 & 5} NICMAR Student

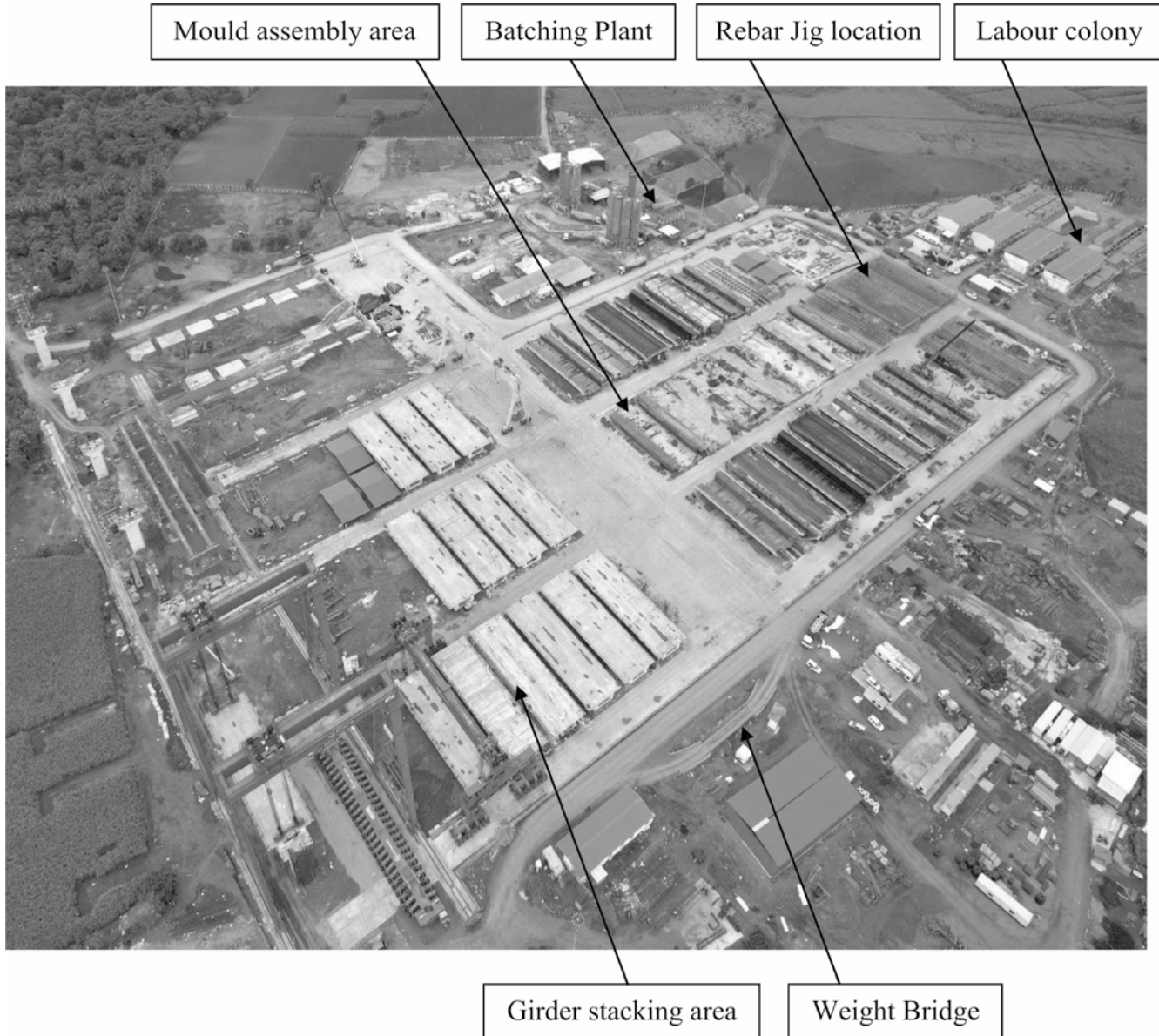


Figure 1: Precast Yard Layout (Source: HSR Site Photo)

batching plant, RMS plant machineries, Weigh Bridge, FSLM Mould, etc. has to be deployed at the yard.

Bed preparation for mould assembly:

- ❖ The soil below the casting bed shall be well compacted up to 90% compaction and the required thickness of ground Improvement shall be placed above it.
- ❖ Above the compacted soil the PCC levelling course of 100mm shall be cast.
- ❖ Above the PCC Levelling course, the RCC bed for the outer mould shall be cast.
- ❖ Pedestal and foundation for the Inner form parking area shall be prepared and levels shall be maintained correctly for smooth entry and exit of the Inner Form.

- ❖ All inserts for soffit form, Inner form, and Outer form shall be placed before concreting the casting bed.

The mould assembly area is shown in Figure 2.



Figure 2: Mould Assembly Area (Source: HSR Site Photo)

Assembly of formwork for girder casting:

- ❖ Fixing of prefabricated mould components i.e., outer form with soffit form mounted at a casted bed and inner form with pedestals at Inner form parking area.
- ❖ After fixing the Mould in position the horizontal and vertical alignment of the mould need to be checked in detail with the help of a surveyor to ensure the line and level of the mould.
Typical mould assembly is shown in Figure 3.



Figure 3: Assembling of Moulds (Source: HSR Site Photo)

Fixing & Assembly of Rebar Cage:

The Rebar cage shall be assembled in the Rebar Jigs as shown in Figure 4.



Figure 4: Tying of Rebar Cage (Source: HSR Site Photo)

Shifting and placement of pre-assembled reinforcement cage:

The reinforcement cage shall be lifted by a straddle carrier/crane using a lifting truss having multiple lifting points (Figure 5).



Figure 5: Shifting of Rebar Cage (Source: HSR Site Photo)

Sliding of the inner form:

- ❖ After the fixing of the prestressing components & all the required numbers of cover blocks, the alignment of the positioned reinforcement cage shall be checked.
- ❖ Bulkhead on both sides shall be installed and shall be locked properly.
- ❖ The Roller Supports will be fitted on the PVC Sleeves provided for the Air Vent hole for moving of inner form.
- ❖ The inner form shall be guided smoothly inside the already positioned reinforcement cage.
- ❖ After the completion of the fixing of the Inner form, the alignment of the reinforcement cage shall be verified. The arrangement is shown in Figure 6.



Figure 6: Sliding of Inner Mould (Source: HSR Site Photo)

Concreting of girders:

The Box girder shall be cast in a single pour (in layers) using the Boom placer (Figure 7), with the each concrete layer thickness not exceeding 300mm. Though the temperature of Concrete while pouring shall not exceed 40 as per Contract Specifications, however, Chiller Plant will be installed and a sprinkling of chilled water on aggregates will be envisaged during concreting to maintain the pouring temperature as per specifications.



Figure 7: Casting of full span girder (Source: HSR Site Photo)

Machineries / Equipment:

To encourage Aatma Nirbhar Bharat Abhiyan initiative, full span launching equipment of 1100MT capacity has been indigenously designed and manufactured by M/s Larsen & Toubro at Kanchipuram, Chennai. M/s L&T has partnered with 55 Micro-Small Medium Enterprises (MSME). This will expedite construction of high speed railway, as is the proven technology in metro and similar projects. Work has already begun on 325 km (in Gujarat state) out of 508 km corridor between Mumbai & Ahmadabad. For the construction of viaduct superstructures of 508 km long, Mumbai-Ahmadabad High-Speed Rail Project (MAHSR), the State-of-the-Art construction methodologies like Full Span Launching Methodology (FSLM) will be adopted. This technology will expedite the process of launching girders as the precast girders of full span length will be erected as a single piece for double track viaduct. FSLM is used world over as it is faster than the segment by segment launching method, usually adopted for the construction of viaducts for metro system. India is now coming in the select group of countries like Italy, Norway, Korea, and China which have been designing and manufacturing such equipment. This project will improve skill set in various rail construction technologies. Japanese counterparts will provide training to National High Speed Rail Corporation Limited employees and also to contractors. More than 6000 workers are already working at various construction sites for the project, thus creating employment opportunities for the local youth.

The standard precast Pre Stressed Concrete (PSC) Box Girders (weight ranging from 700 to 975 metric ton) of span 30, 35 and 45 meters will be launched by using FSLM methodology for the high speed corridor. The heaviest PSC Box

Girder weighing 975 MT and of 40 meter length will be used for the first time in the construction industry in India for MAHSR project. [3,4,5]

List of important Plant & Machinery deployed in the project shall be as shown in below table:

Sl. No.	Description	Remarks
1	DLT1100 Straddle Carrier	For Full span Lifting in Casting Yard
2	550 MT Bridge Gantry	For Full span Erection
3	Launching Girder 1100MT	Erection of full span girder
4	Girder Transporter 1100MT	Transportation of Full span girder over the erected span

Table 1: Specialized equipment used in erection

Straddle Carrier:

DLT1100 straddle carrier (Figure 9), which is used in the Indian high-speed railway project from Mumbai to Ahmadabad, involves full span box girders of various spans ranging from 30 m to 40 m, with a maximum weight of 1,100 tonnes. It is mainly composed of the main beam, leg, SC travelling mechanism, winch trolley, electrical system and hydraulic system.

The equipment consists of one DLT1100 straddle carrier which is intended to lift one piece of box girder for lift and transfer of box girders in the stacking yard.



Figure 9: Straddle Carrier (Source: HSR Site Photo)

Bridge Gantry:

The equipment (Figure 10) consists of two MG550 bridge gantries which work together to lift and transfer a box girder at the casting yard, project site cross line positions, cross-pier positions, as well as load the box girder onto the transporter.

The whole equipment consists of two MG550 bridge gantries: Bridge Gantry A and Bridge Gantry B. Through the joint operation, the two BG will fulfill the work such as the lifting of full-span precast concrete box girder from the stacking pedestal, the placing onto bridge deck girder transporter, and the installation and dismantling



Launching Girder

Bridge Gantry

Girder Transporter

Straddle Carrier

Figure 8: Specialised Equipments (Source: HSR Site Photo)

of transporter and launching gantry. Each bridge gantry consists of the main beam and two legs forming a gantry frame structure. The left leg is fixed with the main beam, the right leg is hinged to the main beam, and the main beam adopts a steel box beam structure. Under the legs, the BG travelling mechanism provides support and driving force, allowing each bridge gantry to run independently and two linked. Each Bridge Gantry has four travelling mechanisms. The transverse movement is completed by a winch trolley on the top surface of the main beam. The winch trolley supports the pulley block on the hook.



Figure 10: Bridge Gantry (Source: HSR Site Photo)

Launcher:

The main frame of the LG is a box girder structure, the upper part of the main frame is equipped with a winch trolley that can move longitudinally, and the trolley has a transverse movement function (Figure 11).



Figure 11: Launcher (Source: HSR Site Photo)

Girder transporter:

The girder transporter (Figure 12) carries a box girder on the erected bridge deck to complete the task from the prefabrication yard to the end of the launching gantry, so as to transfer of launching gantry between bridges by means of the girder transporter. The girder transporter is

designed to meet the requirement of transporting a 30-40m full span box girder (Max weight of 1100MT) from the bridge gantry access area to the launching girder area and feeding it to the launcher. The Girder transporter used in this project is DCY1100. It is mainly composed of frame, suspension assembly, driven axle, brake axle, steering system, power system, brake system, hydraulic system, cab and girder carrying system.



Figure 12: Girder Transporter (Source: HSR Site Photo) [8]

Erection & installation work methodology:

The sequence of erection is as below:

- Straddle Carrier shifts the girder from casting bed to stacking bed
- Bridge Gantry is then used to place the girder on top of the Gantry Transporter.
- Gantry Transporter moves over the erected span and carry the newly to be erected span to the launching girder
- Launching girder finally erects the span and then auto launch to next pier.
- ❖ Overall preparation of pier cap including bearing and stopper installation:

Pier cap is made ready by installing bearings and seismic stoppers (Figure 13) and ensuring their line and level as per the requirements.

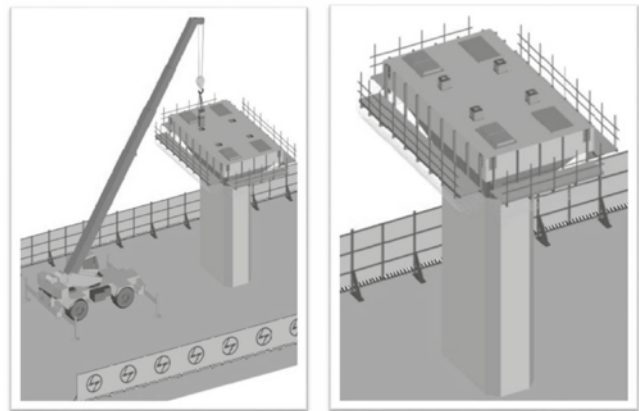


Figure 13: Installation of Stoppers and Bearings (Source: Project Manual)

Erection of first four full spans using bridge gantries:



Figure 14: Erection of first Full Span by Bridge Gantries (Source: HSR Site Photo)



Figure 15: Erection of first 4 nos. of Full Span by Bridge Gantries (Source: HSR Site Photo)

Assembly of launching girder and girder transporter on ground:



Figure 16: GT Main Box Girder Assembly at Ground Level at Casting Yard (Source: HSR Site Photo)

Erection of launching girder and girder

transporter over the erected deck at the casting yard location



Figure 17: Erection of LG and GT (Source: HSR Site Photo)

Erection of full span girder using launching girder and girder transporter



Figure 18: Feeding of full span girder by GT to LG (Source: HSR Site Photo)



Figure 19: Erection of Full Span Girder by LG (Source: HSR Site Photo)

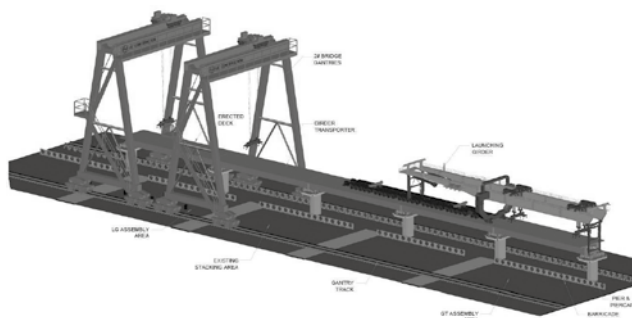


Figure 19: Erected Spans (Source: Project Manual)

Risk Identification and Control during HSR Project Execution

The various risks observed and controlled during the Mumbai Ahmadabad HSR project execution are as follows:

Sr. No.	Risk	Mitigation Measures
1	Time duration	As the project is on the fast track, completion of the work in the allotted time is most important. To ensure that required progress is achieved, proper planning is being done. To speed up the work, pre-casting of the superstructure is being used. During the time when foundation and substructure work was getting done, precasting of the superstructure is started on a war footing. To further reduce the time of construction, instead of segmental spans, precast Full span box girders weighing about 1000 MT are used in the majority of the stretches. This is the first time in India that full span precast box girders are being used in the superstructure of the viaduct.
2	Casting & Erection of Superstructure	Specialized equipments are being utilized for casting & erection of precast full spans. Specialized moulds are fabricated to accurately cast full span box girders in pre-cast yards in shortest possible time. Specially fabricated Straddle Carriers of capacity 1100 MT are being used to shift precast Full span box girders from moulds to stacking bed and then to the erection site. Two Bridge Gantries of each capacity of 550 MT are being used to erect the first 4 spans and further spans will be erected using a specially fabricated Over Head Launching Girder of

		1100 MT capacity. As the weight of girder is about 1000 MT and to avoid movement of same over poor load bearing Black Cotton soil, the girder is moved over already erected span using one of its kind 1100 MT girder transporter. Using this new method, the time cycle for completion of one span is reduced from 7- 8 days to 1 day.
3	Land acquisition in Gujarat	Proper coordination between National High Speed Rail Corporation Limited and Govt. of Gujarat resulted in fast land acquisition. Compensation was provided to the landowners. Moreover, education was also imparted to the landowners about the benefits of HSR.
4	Financing of the whole project	81% of the total construction cost i.e. 88,000 crore rupees given by Japan as aid to the Government of India, which is to be paid over 5 decades at an attractive interest rate with 15 years non- repayment moratorium.
5.	Land Strata: Black cotton soil	Black Cotton soil has poor load-bearing capacity. To overcome this, instead of an open foundation, pile foundation works are in progress. Piles of diameter 1200 mm to 1500 mm and lengths from 30 to 55 meters are cast for foundation works in the viaduct while for the station, the pile diameter ranges from 1200 mm to 1800mm with the depth ranging from 30 to 40 meters have been cast. Further proper geotechnical investigation works are being done to avoid any surprises/ uncertainties.

6	Access road	As most of the work is being done inside fields, access to the site is very difficult, particularly during the monsoon period. To overcome this challenge, proper access roads using GSM, WMM along with geogrid are being used.
---	-------------	--

Conclusion:

The method of casting & erecting Full span pre-stressed Box Girder is the latest and most efficient method for executing super structure works and is ideal for a big projects like High Speed rail project. Not only it reduces time of construction but also quality of work is much better than other methods.

As the whole box girder is casted in one go without need to join segments (as in segmental superstructure) and at ground level, we can achieve good finish of final product. Also, it is much easier to maintain geometry of super structure as all the alignment work of girder is done on ground not like in pre-cast segmental spans, where the alignment of each segment is done in hanging position. Further as casting of girder is independent of sub-structure, so we can keep casting girders as work for sub structure is going on. This helps to reduce execution time required for project. Compared to segmental super structure where segments are casted one by one either on long line bed or short line bed, casting of full span girder takes much less time as we do casting in one go.

When it comes to erection of super structure work, time required to erect one full span girder is quite less compared to other methods especially segmental super structure. We can easily erect 2 full span girders in a day compared to 4-5 days required to erect 1 complete segmental span. Also critical activities involved in erecting full span girder are much less compared to segmental spans resulting in far less chances of any accident happening at site during erection work.

Only problem in pre-cast full span box girder super superstructure is that we require numerous highly specialized machinery like molds, straddle carrier, Bridge Gantry, LG, Girder Transporter etc. They have increased capital cost but considering the enormous benefits of using this method, the net benefit far exceeds the capital cost of equipment.

We can conclude that in projects were execution

time is limited and even a slight delay in works result in huge loss not only for contractor but also for country, where we require good aesthetic view with excellent quality, Full span erection method is the best.

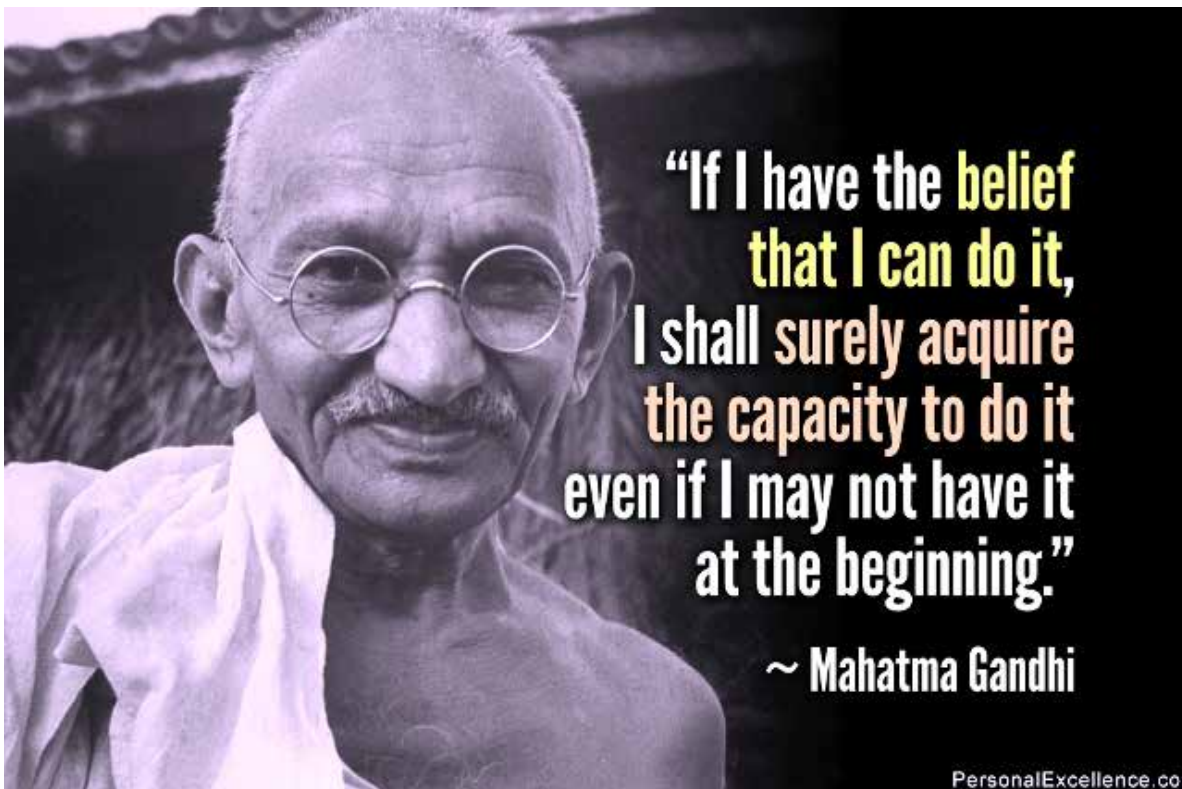
Acknowledgment

We acknowledge the generous support from Larsen & Toubro Construction Heavy Civil Infrastructure for allowing us to use their standard operating manual and site photos.

References

1. The Print (2022), ANI, New Delhi, ITP Available from: <<https://theprint.in/ani-pressreleases/18-billion-usd-japanese-low-cost-bullet-train-finance-without-the-fxrisk/794068/>> [Accessed 2nd May 2022].
2. National High Speed Rail, ITP Available from :< <https://www.nhsrcl.in/>> [Accessed 30th April 2022].
3. ITP Available from : <https://pib.gov.in/PressReleaseDetailm.aspx?PRID=1753529>> [Accessed 30th June 2022].
4. ITP Available from :<https://www.businesstoday.in/latest/economy/story/ashwinivaishnaw-flags-off-transporter-to-expedite-mumbai-ahmedabad-high-speed-railconstruction-306394-2021-09-10>> [Accessed 4th July 2022].
5. ITP Available from : <https://www.railpost.in/rail-min-flags-off-lts-india-made-1100ton-full-span-launching-equipment-for-mumbai-ahmedabad-high-speed-rail/>> [Accessed 6th July 2022].
6. Tai, J C, et.al. (2010) “Full Span Precast and Launching Construction in Taiwan’s High Speed Rail Project.” Proceedings of the 2010 Joint Rail Conference. Volume 1. Urbana, Illinois, USA. pp. 167-173. ASME. <https://doi.org/10.1115/JRC2010-36096>
7. IABSE Working Group No. 6 (2018). “Precast balanced cantilever erection by launching gantry”. ICE Publishing.
8. National High Speed Rail, ITP Available from : <https://www.linkedin.com/company/bullettrain/> [Accessed 25th May 2022].

□□□



Live Load Distribution Factors for Concrete Girder Bridges

By
Avinash Kumar¹
G.S Yadav²

ABSTRACT

This paper presents an evaluation of live-load distribution factors in flexure for a reinforced concrete girder bridge. The response of superstructure consisting of seven RC longitudinal girders with deck slab was measured during static live load test by placing a set of loaded trucks in three different lanes. The distribution of live load moment obtained from load test are compared with result of Finite Element Model developed in MIDAS software as well as with the distribution factor calculated from Courbon's method and AASHTO Load and Resistance Factor Design (LRFD) code. Load distribution factors (LDF) obtained from Finite Element Model are consistent with the results of load test. It is observed that the Courbon's method overestimates the LDF of outer girders when the eccentricity of loads about centre of deck is more and underestimates the LDF for inner girders when the eccentricity of loads is less. It is found that the distribution factors recommended in AASHTO LRFD provision are conservative for interior girders.

Introduction

Computing the response of a girder bridge to live loads is a complex task. The moment demand for a particular girder depends on the magnitude and location of the imposed loads and on the configuration of longitudinal as well as cross girders. The design moment in the girder will vary with girder spacing, span length, flexural stiffness, torsional stiffness, and on the properties of the deck and diaphragms. The presence of skew further complicates the task of estimation of the design moment.

Instead of going for complex three-dimensional analysis, live load distribution factor suggested by any method or code for different wheel load positions is commonly used by Bridge Designers to estimate the maximum moment in individual girders. To simplify the design process, many bridge codes, such as the AASHTO- Load and Resistance Factor Design (LRFD) treat the longitudinal and transverse effects of wheel loads as uncoupled phenomena. In such type of analysis, the design live-load moment is first estimated for single girder by performing moving load analysis for critical combination of lanes. Design moments of individual girders (exterior and interior girders) are then evaluated by multiplying appropriated live load distribution factor to the calculated design bending moment of single girder.

Courbon's Method for Load Distribution factor (LDF)

Courbon's method is one of the most popular classical methods for determining the distribution

factor of live loads for deck with slab and girders arrangements. It is widely used to calculate the distribution factor as calculation is simple and can be done manually. In this method, the cross girders or diaphragms are assumed to be infinitely stiff. Courbon's method is applicable for the following situation

- The ratio of span to width of deck is greater than 2 but less than 4.
- The longitudinal girders are interconnected by at least five symmetrically spaced cross girders.
- The cross girder extends to a depth of at least 0.75 times the depth of the longitudinal girders.

In case of a single concentric load or a group of symmetrical loads, the deflection of all the girders becomes equal but when the loads are placed eccentrically with respect to the centre line of the deck, the deflection of all the girders does not remain the same but the outer girder of the loaded side becomes more deflected than the next interior girder. The distribution factor of girders as per this method is as under

$$R_x = \left(\frac{\sum W}{n} \right) \left[1 + \frac{\sum I}{\sum d_x^2 I} \right] d_x e \quad (1)$$

Where,

R_x is the reaction factor for the girder under consideration,

I is the Moment of Inertia of longitudinal girder, d_x is the distance of the girder under consideration from the centre of deck, $\sum W$ is the total of concentrated live loads, n is number of longitudinal girders and e is eccentricity of live loads with respect to the

¹ Prof. Track-II/IRICEN,

² Retd. Prof/IRICEN

centre of deck.

IRC 21-2000 allows application of Courbon's method if the effective width of deck is less than half the span and stiffness of cross girders are much more than the stiffness of longitudinal girders. Recommendation for estimation of live load distribution factors for longitudinal girders was given in clause 305.12 of IRC 21-2000 for both Bending moment and Shear Force. IRC 21 is a Standard specification and code of practice for Road bridges for Cement Concrete based on working stress method. Now this code has been withdrawn and it is recommended to perform the analysis and design of bridges by IRC 112, which is recent IRC code and is based on limit state method. In the new code no specific recommendations are given for estimation of live load distribution factor.

AASHTO Specification for Distribution factor

The American Association of State Highway and Transportation Officials is a standards setting body which publishes specifications, test protocols, and guidelines that are used in highway design and construction throughout the United States.

In bridge design, calculation of maximum design moment due to live load for different combinations of lanes is required to determine and design section of deck slab and girders. The problem is three-dimensional and involves complex behaviour of load transfer from concrete slab to concrete or steel girders. The AASHTO bridge specification suggests many methods to analyse such bridges, i.e., finite element analysis, grillage analysis, and a load distribution factor (LDF) equation.

The LDF equation is introduced to facilitate in determination of maximum moment in the girders. Finite element analysis (FEA) is an accurate method, but it requires much effort in data preparation, bridge modelling and analysis, and interpretation of results. With the LDF equation, the maximum moments in individual girders (interior and exterior) are obtained by multiplying a value obtained from LDF equation suggested by AASHTO LRDF to the moment obtained from one-dimensional bridge analysis considering single girder.

Load Distribution factor as per AASHTO-LRFD for RC slab girder type deck as under

(i) For Interior Girders [in SI Unit]

One design Lane Loaded

$$LDF = 0.06 + \left(\frac{S}{4300}\right)^{0.4} \left(\frac{S}{L}\right)^{0.3} \left(\frac{K_g}{Lt_s^3}\right)^{0.1} \quad (2)$$

Two or more design lanes loaded

$$LDF = 0.075 + \left(\frac{S}{2900}\right)^{0.6} \left(\frac{S}{L}\right)^{0.2} \left(\frac{K_g}{Lt_s^3}\right)^{0.1} \quad (3)$$

(ii) For Exterior Girder

One Design Lane Loaded – Use Lever Rule

Two Design lane loaded condition

LRF = e (LDF of interior girder)

Where, $e = 0.77 + \frac{d_e}{2800} \geq 1.0$

d_e is positive if the girder is inside barrier, other wide negative

Here, S is girder spacing, L is span Length, t_s is slab thickness, d_e is the distance from the centre of the exterior beam and the inside edge of the curb or barrier and K_g is longitudinal stiffness parameter, Where

$$K_g = n(I_g + e_g^2 A)$$

Here, n is modular ratio (Egirder/Edeck), I_g is the Moment of Inertia of the girder, e_g is the girder eccentricity, distance of the girder from the centre of the deck and A is the girder area.

Description of live Load Test

Live Load test was performed on the superstructure of Road Over Bridge, ROB located at Pratapnagar Vadodara Western Railway. The superstructure of the ROB consists of seven longitudinal Reinforced concrete girders with reinforced concrete deck slab. The span length of longitudinal girder is 16.19 m and the thickness of deck slab is 150 mm. The roadway is of three lanes having width of 11.31 m and 1.83 m footpath is provided on both sides. Load test was performed by placing two loaded trucks with gross weight of 350 KN each back-to-back in longitudinal direction symmetrically about the centre of deck. The positions of axles of the loaded truck are depicted in figure 2. The trucks were placed in three different lanes to see the impact of position of loads on live load distribution factors of the longitudinal girders. The position of trucks for different lanes are shown in figure 3. The deflections at the centre of each girder were measured for all three load positions using dial gauges.



Figure 1 Road Over Bridge at Pratapnagar, Vadodara



Figure 2. Load test with set of Two trucks, lane-1

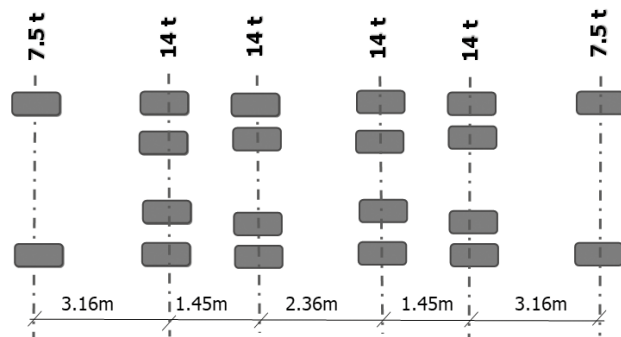


Fig 3. Position of Axles of Live Load

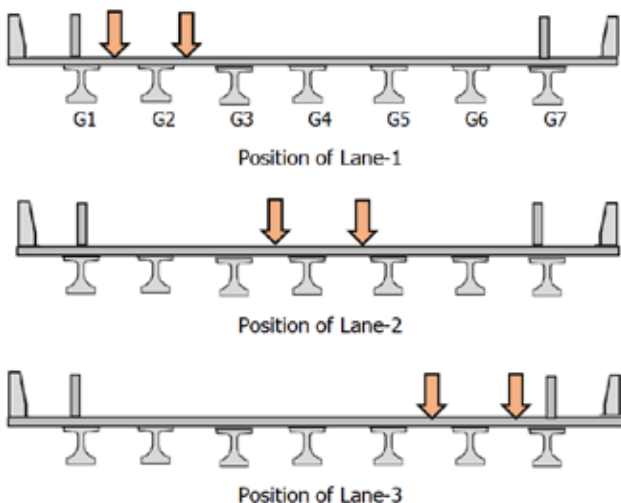


Fig 4 Placement of trucks in three different lanes

Finite Element Model

A finite element model of the superstructure is developed to evaluate the live load distribution factors across the girders in MIDAS software. The model must be sufficiently accurate to capture the true behaviour of girders under live loads. The main longitudinal girders as well as cross girders are modelled as space frame element (beam element) with 7 degrees of freedom at each node (7 DOF are 3 translation, 3 rotational and 1 torsional). Deck slab is modelled as plate element. The plate elements and cross beam elements are connected to the main longitudinal beam elements at their actual locations by using offset connection. Three-dimensional view of finite element model of MIDAS software for load positions of lane numbers 1 and 2 are depicted in figure 5.

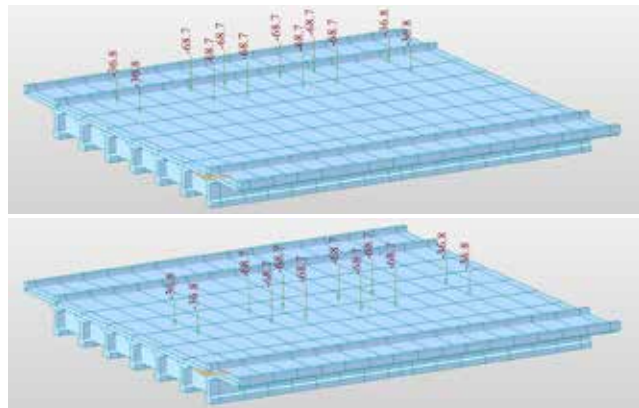


Fig 5. Finite Element Model with Live Load Lane positions 1 and 2

Result and Analysis

Load distribution factors for three positions of live loads are shown in table 1. The three different load positions of loads are depicted in figure 3 and the position of different axles and their load values are shown in figure 2. In load position 1 (lane 1), the test load is placed on the left side of deck, just above the location of girder-1 and girde-2 as shown in figure 4, hence more loads will be taken by girder-1 and girder-2. The live load distribution factor in this case will be more for girder-1 and girder-2. Similarly in case of load position-2 (lane-2) and load position 3 (lane-3), the live load distribution factors of middle girders and right-side girders will be more. The value of load distribution will depend on the exact position of load, stiffness of slab and cross girders if the stiffness of longitudinal girders are approximately same. The distribution factor for lane-1 and lane-3 of load test are found to be approximately same when compared with the values obtained from finite element analysis and Courbon's method. In Courbon's method, the load distribution factor will

always be more for exterior girder than interior girder irrespective of the position of live load as the method is like rivet theory. This can also be concluded by observing the pattern of variation of load distributions of girders G1 to G7 for lane position 1 and 3, as the variation of LDF is linear and increasing or decreasing from one side to other depending on the load positions. For lane position 2, since there is no eccentricity of load about the centre of deck, load distribution factor calculated from Courbon's method is constant for all girders. Hence in load position 2, the values calculated from Courbon's method are not matching with the values obtained from load tests. The values obtained from FE analysis are similar to the results calculated from load test. This indicates that if the eccentricity of loads about the deck is more, the Courbon's method estimates approximately reasonable values of load distribution factors but if the eccentricity is less, it underestimates the load distribution factors. It is also reported in literature that the Courbon's method overestimates the value of LDF for outer girder and underestimate value of LDF for inner girder. The comparison of the values of LDFs obtained from Load test, Finite Element Method and Courbon's method are depicted in table 3 and figure 6. The Results of Finite Element Analysis are matching with the results of load tests in all three different lane positions. The Courbon's method gives similar results for lane 1 and 3 but gives lesser values for lane-2 when compared with the results obtained from FE analysis and load tests.

Parametric study of the impact of stiffness of cross beams on load distribution factors of longitudinal girders is also done by changing the stiffness of cross beams in finite element model from 0K to 2K with an increase of 0.5K. Here K is taken as the stiffness of present cross beam. The study is done for lane-1 and lane-2 loadings and the distribution factors are compared. It is found that the load distribution factors increase in girders just under the load as the stiffness of

cross beam decreases as depicted in figure 7.

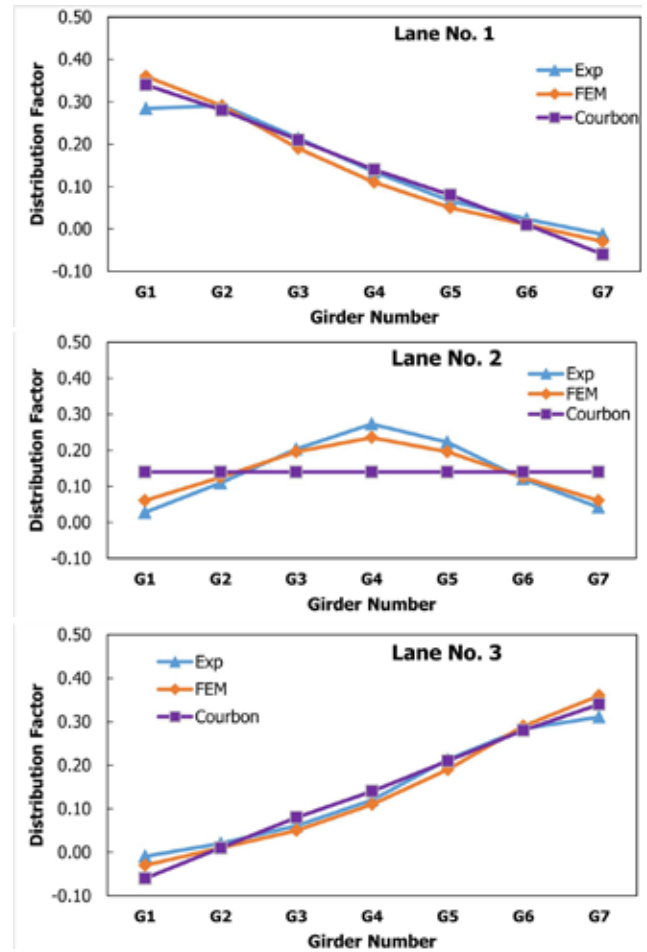


Fig 6. Comparison of Distribution Factors from different methods

Maximum load distribution factors are 0.38 and 0.36 for exterior and interior girders (G1 and G2) for lane-1 loading when there are no cross beams. In this case the distribution of load will occur only through deck slab connected to the top flange of girders it is found that the values of load distribution factors for girders G1 and G2 are 1.25% and 19.86% higher if compared with the load distribution factors with the present case (with K stiffness of cross beam). The maximum load distribution factor for lane position-2 is found

Table 1. Load distribution factors for three different lanes of Loading

Girder No.	Lane-1			Lane-2			Lane-3		
	Exp	FEM	Courbon	Exp	FEM	Courbon	Exp	FEM	Courbon
G1	0.28	0.36	0.34	0.03	0.06	0.14	-0.01	-0.03	-0.06
G2	0.29	0.29	0.28	0.11	0.13	0.14	0.02	0.01	0.01
G3	0.21	0.19	0.21	0.20	0.20	0.14	0.06	0.05	0.08
G4	0.13	0.11	0.14	0.27	0.24	0.14	0.12	0.11	0.14
G5	0.07	0.05	0.08	0.22	0.20	0.14	0.21	0.19	0.21
G6	0.02	0.01	0.01	0.12	0.13	0.14	0.28	0.29	0.28
G7	-0.01	-0.03	-0.06	0.04	0.06	0.14	0.31	0.36	0.34

*Exp- Load Test, FEM- Finite Element Model, Courbon- Courbon's Method

to be 0.33 for girder G4 when there are no cross beams. The value is 41.15% higher compared to the present case with K stiffness of cross beam.

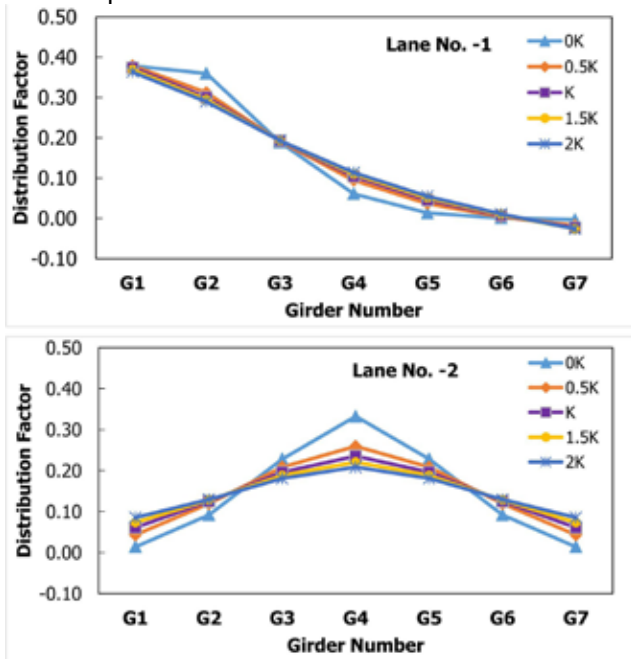


Fig 7. Distribution factor for different stiffness of cross beams

Live load distribution factors are also calculated from the provisions given in AASHTO LRDF-2019 as mentioned in equation 2 for interior girder for single lane loading. The value of live load distribution factor for exterior girder is also calculated from Lever Rule as recommended by AASHTO for single lane loading. The load distribution factors (LDF) is maximum distribution factors for all positions of live loads for interior girders and depends on the load position for exterior girder if Lever rule is used. Maximum load distribution factors obtained from Load test, Finite Element Analysis, Courbon's method are compared with the values calculated from AASHTO LRFD. The value calculated from AASHTO for exterior girder is close to the values obtained from FEM and load test, but values calculated for interior girder is much more than the values obtained from Load test and Finite Element Analysis.

Girder	Maximum Load Distribution Factor			
	Exp	FEM	Courbon	AASHTO
Exterior	0.31	0.36	0.34	0.37
Interior	0.29	0.29	0.28	0.48

*Exp- Load Test, FEM- Finite Element Model, Courbon-Courbon's Method

Conclusions

- 1 Courbon's method gives more accurate values of Load distribution factor if the eccentricity of loads about the centre of deck is large and gives very low values of LDF if the eccentricity of loads is

less. Courbon's method overestimate the load on exterior girders and underestimate the loads on interior girders.

- 2 Finite Element Analysis yields more accurate results of load distribution factors if the true behaviour is captured by the FE model by considering appropriate elements, boundary conditions with desired degree of freedoms.
- 3 Load distribution factor calculated from AASHTO LRDF for single lane loading yields more conservative results for interior girders.
- 4 Stiffness of cross beams changes the load distribution factors considerably. Maximum load distribution factor of girders lying just under the wheel loads increases as the stiffness decreases and vice versa.
- 5 Type of analysis and Methods to be used for estimation of load distribution factors was mentioned in old code, IRC 21. Nothing is mentioned regarding LDF in new IRC code, IRC 112. How to calculate load distribution factors should be mentioned in the IRC code like AASHTO for uniformity. At present designers calculate LDF as per their wish and understanding. Courbon's method is commonly used for calculation of LDF for bridge girders.

References

- 1 Richard M. Barker, Jay A. Puckett, Design of Highway Bridges, An LRFD Approach, John Wiley & Sons, Inc., Hoboken, New Jersey
- 2 AASHTO (2019). LRFD Bridge Design Specifications, 6th ed., American Association of State Highway and Transportation Officials, Washington, DC
- 3 IRC 112-2019, Code of Practice for Concrete Road Bridges, Indian Road Congress, New Delhi
- 4 IRC 21-2000, Code of Practice for Road bridges for Cement Concrete, Indian Road Congress, New Delhi.
- 5 Paul J Barr, Marc O. Eberhard and John F Stanton, Live Load Distribution Factor in Prestressed Concrete Girder Bridge, Journal of Bridge Engineering, Vol 6 No.5, September/October 2001
- 6 Zahar Yousif and Riyadh Hindi, AASHTO-LRDF Live Load Distribution for Beam-and-slab Bridges: Limitation and Applicability, Journal of Bridge Engineering, Vol 12. No.6, November/December 2007.
- 7 Kitjapat Phuvoravan, Load Distribution factor equation for Steel Girder Bridges in LRFD Design, Symposium on Infrastructure Development and the Environment 2006, 7-8 December 2006, SEAMEO-INNOTECH, University of the Philippines, Diliman, Quezon City, Philippines.
- 8 E. C Hambly, Bridge Deck Behaviour, CRC Press, Taylor and Francis.

Launching of Steel 85M Open Web Girder with 65 Degree Skew in Mumbai Central Division of Western Railway

By
Himanshu Sharma¹
Yogesh Kumar²
Harish Meena³

ABSTRACT

The old Delisle ROB, which was more than 100 years old, was found unsafe in 2018 for structural health of girders, revised loading standards and volume of road traffic. The mammoth work of dismantling and rebuilding of railway portion was entrusted to Western Railway and the work of rebuilding of approaches will be executed by Brihan Mumbai Municipal Corporation (BMC). The railway could complete the dismantling work by February 2019 in short span of 4-5 months. The existing bridge structure was having two spans with one intermediate steel support between two running lines on either sides. The proposed structure to replace the existing is 2x85m OWG with skew angle of 65 degrees. Apart from designing such mammoth OWG with such high skew angle, challenge was to launch the same over busiest suburban railway lines.



Introduction and Salient Features of the Proposed Structure

With no space in between tracks for providing an intermediate pier and skew alignment of the approach roads, single span of 82.167m at

65-degree skew only possible span arrangement. Keeping the clearance for the tracks below the ROB and levels of approach roads frozen due to limited available length of approaches in the busiest part of the Mumbai city, Open

¹ Dy.CE/Design/WR,

² Dy. CE/C/CCG

³ XEN/C/CCG

Web Girder was the only option that could be adopted. Separate OWG to be provided for each carriageway having road width of 11.0m and 2.0m wide footpath on outer side of each OWG. This was the first time in India, an open web girder with long span and such high skew angle was proposed for any bridge. The design of the Bridge was approved by RDSO with third party proof check was carried by IIT Bombay. The salient details of each proposed OWG are as:

1. Total Length of the Span
 - a. Overall length of OWG :85.5m
 - b. Effective Span (C/c of bearing) :82.167m
2. Height of Through Truss :12.00m
3. Width of Through Truss
 - a. C/c of truss : 1 3 . 0 0 m (SQ)
 - b. Overall : 1 4 . 0 0 m (SQ)
 - c. Clear : 1 2 . 0 0 m (SQ)
4. Weight of Through Truss :1050MT

Launching Methodology and challenges faced:

The girders were fabricated in the RDSO approved workshop and to be erected at site before launching. Subsequent to the start of fabrication, launching scheme was to be prepared and approved and this was the most challenging aspect of the project. Various issues and complications due to site constraints and due to geometry of the structure were encountered and all such problems were effectively resolved. Detailed commentary of major issues encountered at site and their resolution are listed below: -

Space Constraint and Retained Approach:

To minimize the height of staging required for supporting the Open Web Girder during assembly, it was decided to retain the approach on lower pannel mono station end of the bridge. Due to space constraints and unavailability of approach on the extended alignment of OWG for assembly of both spans, it was decided to assemble both the OWG one by one. As approach road width was limited, the girder was planned for erection on one side of the road and space left on the other side for movement of cranes and heavy machinery. It was planned such that once one OWG is launched, it will be slewed to its position, thus making way for launching of the other girder.

There was obligatory provision to keep open both the access roads to lower pannel station for pedestrian movement which are adjacent to the retained approach. Hence, all activities related to assembly of OWG, storage of fabricated OWG members was contained on the approach road only. This resulted in very less availability of space for any ancillary activity and required very precise planning for sequencing of the execution for erection and launching.



Fig: Assembly of OWG in retained approach road

Need for Fully Supported Launching and Retention of Old Intermediate Support with Modifications

Following 2 options were available to launch the OWG across railway tracks.

- A. The assembled OWG to be attached with adequate length launching nose at front end and launch the OWG along with nose by cantilevering some of the portion of main girder in railway span.
- B. The assembled OWG to be launched on the top of relieving girder (Temporary girder) which is supported on the existing steel substructure in railway track portion.

In option 'A' due to requirement of about 60m length launching nose to counterbalance the overturning of girder and observing difficulty in placement of lateral bracing to connect both launching nose trusses in transverse directions due to very high skew angle, this option was ruled out. The option of providing rolling supports on the top of existing ROB substructure to reduce length of launching nose was also ruled out due to inadequacy of the existing column supports to carry horizontal forces which will transfer at top in longitudinal directions due to the rolling friction during the launching of OWG.

The feasibility of 2nd option was ascertained with three spans of temporary girders over running lines and one approach span. To enable this arrangement, it was decided to assess the strength of existing bridge (Old Delisle bridge) retained intermediate substructure in railway portion to carry vertical loads during launching of OWG through temporary girders and act as an intermediate support. As the structure of the retained support had very less rigidity in the direction of the proposed rolling even after strengthening, it was critical to restrict the transfer of any horizontal force while rolling of OWG. To restrict the horizontal forces, the temporary girders were anchored on the constructed abutments on both ends, which were designed to take horizontal forces. In addition to the that, sliding spherical bearings were erected above the retained intermediate supports to rule out any force transfer in the horizontal direction or transfer any induced moments to the structure.



Fig: Retained substructure as temporary intermediate support

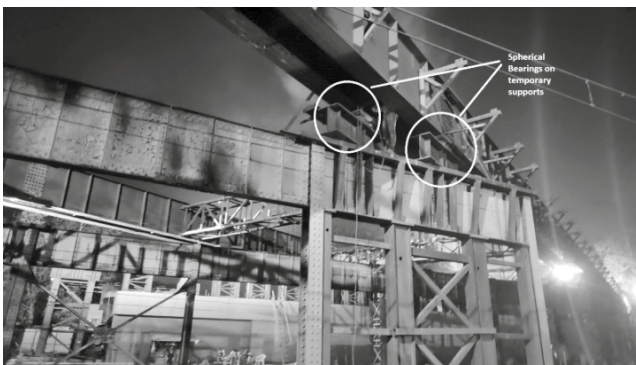


Fig:- Spherical Bearings on retained temporary supports

Design of Temporary Girders with Skew Arrangement:-

The design of temporary girders to be used for launching of the OWG are to be designed keeping in mind the effect of such high skew angle of the OWG and subsequent transfer of forces due to deflection in the temporary girders. To rule out any offloading of rollers, the entire arrangement was modeled in Staad.Pro and movement of the OWG on temporary girders was modeled to ascertain the stresses and loads on the supports, rollers and temporary girders during the course of launching. This modeling was also instrumental in designing of the trestles, their foundation and capacity required of the rollers.

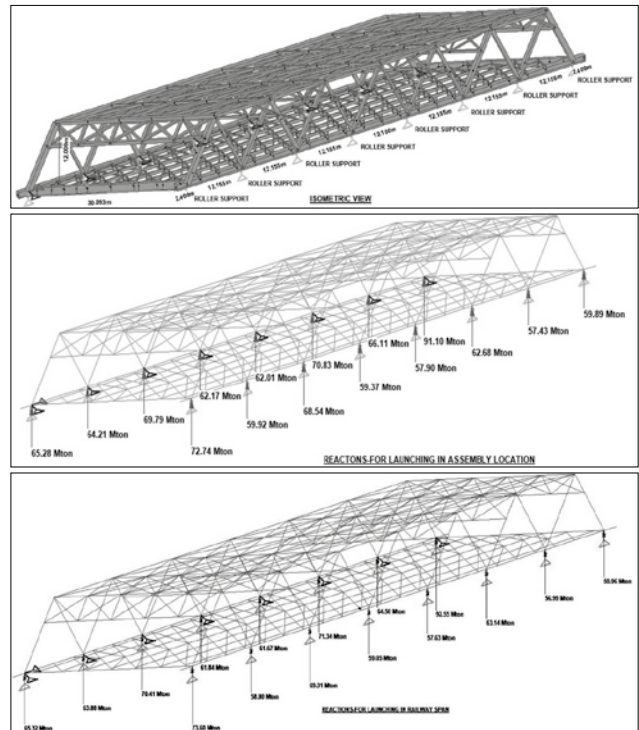


Fig: Analytical model of the launching arrangement



Fig: Temporary girders launched and resting on retained structure

Condition of Approach Retaining Wall and Rectification

At assembly location, the centerline of churchgate side truss of OWG was proposed to be located at a distance of 2.0m from the outer vertical face of retaining wall. Gravity masonry retaining walls were provided for existing approach road with longitudinal gradient of 3.1%. It was observed that the truss center line was located on the stepped masonry foundation of retaining wall. The load carrying capacity of the retaining wall was assessed and it was found that it was adequate to take surcharge load due to weight of assembled truss distributed at 8 nos. of nodal points. However, for pre-camber check when the girder is to be lifted on four end points, additional support was provided on the support location so that the wall is intact while lifting the OWG.

Displacement Control Pulling Arrangement.

As the skew arrangement of the girder posed various challenges in the design of OWG and the launching arrangement, pulling the girder along the temporary girders in the straight line was a big challenge as there was always possibility of girder moving in transverse direction. It was necessary to ensure that nodal points of both the girders travel with the same speed over the temporary girders, which was not possible through traditional pulling arrangements. Displacement control synchronized pulling arrangement through strand jacks was used for the first time over Western Railway to ensure that

or the supporting trestles. It was necessary to stop the pulling of girders in such case and rectify the issue, which is not easily possible in conventional pulling arrangements. In strand jacks the maximum limit of the load the jack can apply was per jack with provision of shutting of the operation if the pulling load requirement is more than the limiting value. The pair of pulling jacks were fixed on the west side of the temporary girders and pulling was controlled digitally where load transferred through each of the pulling jack at any given time can be seen on screen. This ensured a very safe and smooth movement of girder and ruled out possibility of any side swaying of the OWG.

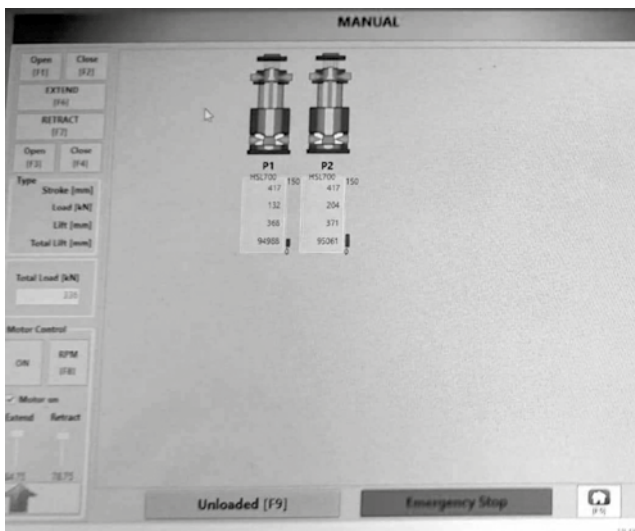


Fig: Strand jack output display on Laptop screen

the girder moves in straight line. Possibility of jamming of any rollers or any obstruction would mean applying more horizontal forces on the launching arrangements like temporary girders

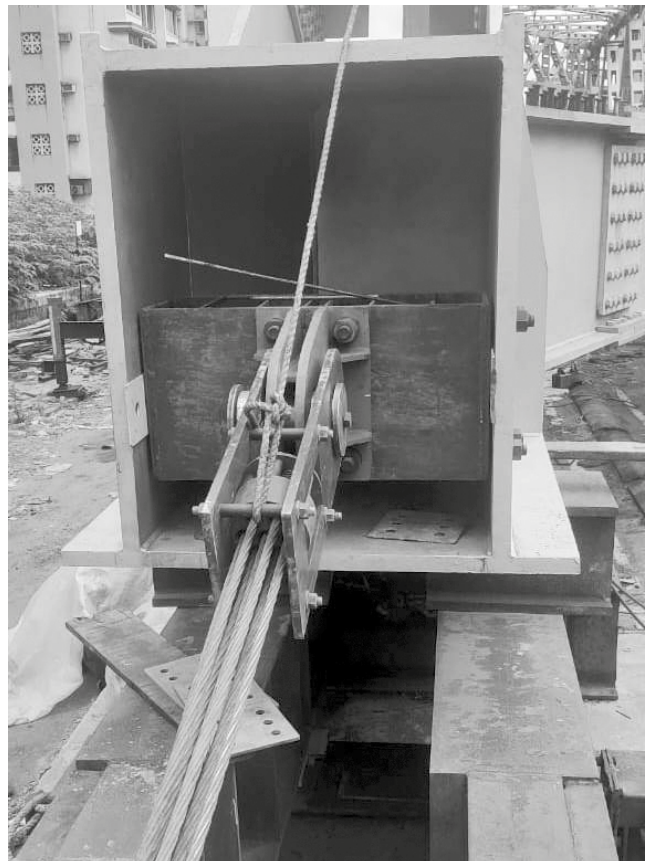


Fig: Strand jack assembly

Annex

DETAILED EXECUTION METHODOLOGY

Salient features: -

1. Total Length of the Span
 - a. Overall length of OWG :85.5m
 - b. Effective Span (C/c of bearing) :82.167m
2. Height of Through Truss :12.00m
3. Width of Through Truss
 - a. C/c of truss :13.00m (SQ)
 - b. Overall :14.00m (SQ)
 - c. Clear :12.00m (SQ)
4. Weight of Through Truss :1050MT
5. Weight of roller supports :20.0MT
6. Total weight to be pulled :1070MT
7. Nos. of roller supports below OWG :16 Nos.
8. Erection Method of assembled Through truss : One End Launching
9. Grade of Steel :Mild Steel Grade-E350-BO (IS-2062-2011)
10. Capacity of Hilman rollers for OWG launching :100MT-2 nos per support (16 nos. of support)
11. Capacity of Hilman rollers for side shifting : 300MT-2 nos per support (L0, L8 nodes of each truss) – 4 nos. of support)
12. Guide rollers @ each roller support : 10 MT per roller support (16 Nos. for OWG launching)
13. Co-efficient of Friction for Hilman rollers : 0.07
14. Total pulling force required for OWG launching :74.9 MT
15. Nos. of synchronized displacement controlled strand jacks proposed for pulling of OWG : 2 nos.
16. Capacity of each strand jack : 90T capacity
17. Total Force in strands per jack at one end $75/2$: 37.5 MT
18. Effective stroke of strand jack :400mm
19. Capacity of Hyd. Jack for side shifting (Total-2nos) :50MT, 1100 mm stroke



Fig: Trestle arrangement and Girder erection in progress

Construction Methodology:

1. Ground improvement, if required for crane movement for erecting trestle supports & erection of Main Truss members.
2. Foundation preparations for trestle support.
3. Erection of trestle support for truss assembly including bracings in transverse directions at end nodes of OWG.
4. Fixing of working platform on the top of trestle support.
5. Erection and fixing of cross beams and temporary girders on trestle support
6. Placing of hydraulic jacks, steel stools on the top of temporary girder at node locations of OWG for

assembly of Main truss

7. Assembling of all members of open web girder (OWG) of Virar side on trestle supports as per the sequence mentioned in the TAD.
8. Checking of bolting & pre-camber of OWG for self-weight of OWG
9. Lifting of main trusses at bearing locations and removal of temporary support stools and hydraulic jacks (camber jacks).
10. Inserting roller support frame and HILMAN rollers below each node of main truss.
11. Fixing of guide rollers at each roller support locations.
12. Strengthening of steel girders of old ROB at temporary girder support locations as per TAD
13. Erection of trestle supports, trestle cap beams and temporary girders in railway span portion including fixing of transverse bracing connecting temporary girders in transverse directions using crane.
14. Fixing of strand jacks, strands on the top of temporary girders beyond Abutment A1 and fixing anchor block for connection with bottom chord of OWG for pulling the OWG in front of each Main truss
15. Trial run of 44m of Main Truss (OWG) in Traffic and power block of railways by pulling the OWG using 2 strand jacks from front end.
16. Launching of OWG for 75m in railway span in subsequent traffic and power blocks of railways.
17. Side shifting of Virar side OWG towards Virar side to clear the launching girders (Temporary girders) for launching of Churchgate side OWG
18. Assembling of all members of open web girder (OWG) of Churchgate side on trestle supports as per the sequence mentioned in the TAD.
19. Checking of bolting & pre-camber of OWG for self-weight of OWG, fixing of roller support, lowering of OWG on HILMAN rollers for launching.
20. Launching of CHURCHGATE side OWG in railway span, in traffic and power block
21. Transverse shifting of CHURCHGATE side OWG to its desired location on bearing
22. Dismantling and removal of temporary plate girders, transverse bracing in railway span, from the gap between CHURCHGATE and VIRAR side trusses
23. Transverse shifting of VIRAR side OWG to its desired location on bearing.
24. Lowering of CHURCHGATE side open web girder (OWG) on temporary steel supports placed on

pedestals

25. Lowering of VIRAR side open web girder (OWG) on temporary steel supports placed on pedestals
26. Lifting of OWG and removal of temporary steel supports and placing of Bearings.
27. Fixing of sacrificial shuttering on stringers and cross beams and Casting of RCC deck slab.
28. Casting Of RCC Anti-crash barriers and bituminous work / road markings etc. on the top of deck for commencement of road traffic.

Reference Drawings: -

1. GAD Reference DRG. No. WR-15/REBUILDING-LOWER-PAREL-ROB/GEN/1501/ SH.1 OF 2/R0 and 2 of 2
2. TAD: Reference DRG No. TAD 01 to TAD-016, Latest revisions

SEQUENCE OF PRE-LAUNCHING ACTIVITIES, (without traffic block):-

Activity:-1 Marking the center line of Trestle supports, excavation for trestle support as per the bearing capacity requirement and casting of RCC footings for trestle supports and temporary staging as shown in the stage -1 of drawing.

Activity:-2 Erection of trestles using adequate capacity crane and temporary trestles TV1, TC1 in railway span at the locations shown in stage 1 of drawing.

Activity:-3 Fixing of horizontal and diagonal bracing connecting trestles in transverse directions.

Activity:-4 Assembly of Main Truss on the Temporary girder at assembly location using adequate capacity crane as per the erection sequence of members mentioned in TAD-01 to 04, stage-1A to stage-1G and checking of all bolting, alignment and pre-camber of main truss for self-weight.

Activity:-5 Inserting roller supports and transferring the load on HILMAN rollers at each node of OWG as shown in TAD-04, stage 1H.

Activity:-6 Erection of trestle supports on the top of abutment caps at A1 and A2, Trestle supports T4 adjacent to abutment transversely to the bearing center line on Virar side and temporary girders for transverse shifting arrangement, as shown in TAD-06

Activity:-7 Erection of trestle supports T5 and T6, temporary girders in between assembly location of OWG and abutment A2, in stage-2 as shown in TAD-05

Activity:-8 Installation of the strand jacks, strands

on the top of temporary girders beyond Abutment A1 and fixing anchor block for connection with bottom chord of OWG for pulling the OWG in front of each Main truss as shown in the drawing no. TAD-07 in stage 3 for pulling arrangement. Strand jacks are equipped with load sensors to monitor the pulling force and forward movement of each truss during pulling operations.

Sequence Of Pre-Launching Activities (With Railway Traffic Block):-

Activity:-1 Casting of RCC foundations in between existing stanchions of old bridge, Strengthening of existing cross girder and stanchion supports of old bridge as per TAD-012 R4, TAD-015 R3

Activity:-2 Erection of trestle supports TC1 & TV1, temporary plate girders, transverse bracings in railway span using crane as per TAD-05, stage-2.

Sequence Of Launching Activities:-

Stage:-4 (During traffic and power block on both UP and DN tracks)

- Ascertain and confirm the traffic and power block requirements as per schedule given in TA Drawing no.10 R4.
- In T & P Block of Railways, fix wire rope and diversion pulleys for front pulling arrangement
- In T & P Block of railways, Launch of Virar side OWG assembly by 44m for Test run behind abutment A2 to verify the adequacy of pulling arrangement.
- Lock the main truss & LN assembly in position and tighten the front end pulling wire rope to give tension of 1.5T in rope. Lock the front-end winch installed beyond abutment A1 to maintain the tension in wire rope till commencement of traffic and power block for launching of OWG across railway tracks.
- Rectify the discrepancies, if any, in the pulling system

Stage:-5 (During traffic and power block on both UP and DN tracks)

- In T & P Block of railways of 6 hours Start the launching of Truss assembly across Railway tracks from A2 (south end) to A1 (North end) with the help of pulling arrangements.
- Continue the launching till the front end of main truss (OWG) assembly reaches at the center line bearing on A1 abutment.

Stage:-6 (During traffic and power block on both UP and DN tracks)

- Avail T & P Block of railways of 4 hours for

transverse shifting of Virar Side OWG to clear launching track for launching of CHURCHGATE side OWG.

Stage:-8 (During traffic and power block on both UP and DN tracks)

- Similarly launch Churchgate side OWG In T & P block of 4 hours in trial run and launch it further by 75m in subsequent T & P block of 6 hours in railway span.

Stage:-9 (During traffic and power block on both UP and DN tracks)

- Avail T & P Block of railways of 4 hours for transverse shifting of Churchgate Side OWG to its desired location on bearing.

Stage:-10 (During traffic and power block on both UP and DN tracks)

- Dismantle & remove the temporary plate girders, transverse bracing in railway span

Stage:-11 (During traffic and power block on both UP and DN tracks)

- Avail T & P Block of railways of 4 hours for transverse shifting of Virar Side OWG to its desired location on bearing.

Stage:-12 (During traffic and power block on both UP and DN tracks)

- Place the main truss assembly on Steel Stools and wooden packing kept over pedestals at bearing locations.
- Lower the Churchgate side OWG on temporary stools by jacking and packing method.
- Lower the Virar side OWG on temporary stools by jacking and packing method.
- Fix bearings to bottom chord of main truss at bearing locations and Lower the OWG to rest bearings on pedestals with the help of 2x300MT capacity hydraulic jacks placed at jack locations below Bottom chord.
- Grout the bearing pedestals.

Sequence Of Post - Launching Activities:-

(No Traffic and Power Block required)

- Fix sacrificial shuttering on the top of stringer / cross beams
- Place and tie the Rebar for RCC deck slab.
- Fix side shuttering for casting of deck slab concrete.
- Cast deck slab concrete for the span
- Cast RCC anti-crash barrier.
- Complete bituminous work, wearing coat and road signs and marking

Regirdering of Existing Span No 28, 29, 30 & 30 BP Up & Dn Lines of Wadibunder Bridge on CSMT-CLA (HB) Section in Mumbai Division

By
- Nishith Kumar Mall¹
- Vivek Kumar²

SYNOPSIS

Wadibunder viaduct is located at Kms 1/19-2/13 on CSMT-CLA (HB) Section of BB division & it was constructed in 1923. This Viaduct carries harbor lines of BB division & crosses 4 lines (UP through main line, DN through main line, UP local line, DN local line) of CSMT-KYN Section. Elevated Sandhurst Road station is located on this viaduct. Girders were designed for ML Loading and were put on road in the year 1923. These Girders were fabricated as per GIPR drawings 41945 to 50. The Bridge consist of 39 spans of various length varying from 3.5 m to 24.5 m each on UP & DN HB Line.

Named after Lord Sandhurst, the Governor of Bombay between 1895 and 1900. The Sandhurst Road railway station (upper level servicing the Harbour Line) was built in 1923. The supporting pillars of the edifice bear the inscription "GIPR 1921 Lutha Iron Works, Glasgow". The fabricated metal was imported from the United Kingdom. It is India's first two-tier station with a 1,728 feet (527 m) long steel viaduct weighing 2,788 tonnes that carries the Harbour line. It cost Rs 20 lakh to build viaduct.

The saline environment of Mumbai has caused excessive corrosion to these steel girders of viaduct bridge resulting in loss of section in few spans. During inspection, it was found that span no.28, 29, 30 & 30BP (UP & DN lines) have corroded. It was therefore proposed to carryout re-girdering of these spans. Total 16 girders (08 on UP HB + 08 on DN HB) were required to be re-girdered.

The Girders have been fabricated at CEW Manmad workshop based on various drawings approved by HQ.

The location of these girders are not approachable by road, hence newly fabricated girders were placed at Wadibunder yard. These girders were lifted by crane and put on a dip lorry and then these were shifted to the desired locations on the adjacent line by pushing. The regirdering of existing span was done with the help of chain block with movable hoist attached to the portal frame.

The work was carried out under traffic and power blocks. Total 8 no. of mega traffic & Power block of 5 Hrs. duration each were permitted for harbor lines. Speed restrictions of 30 Kmph remained in-effect till the whole work was completed.

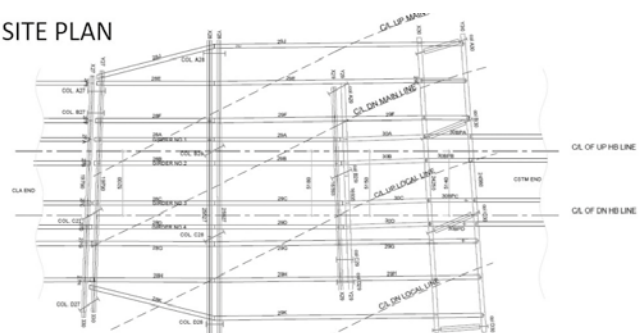
Introduction To Problem

The saline environment of BB had caused corrosion to this steel structure of bridge resulting in sectional loss of few spans. During inspection in 2010 it was found that span no.28, 29, 30 & 30BP UP & DN lines have corroded. Hence, it was proposed to re-girder these spans. Total 16 girders (08 on UP HB + 08 on DN HB) were required to be re-girdered.

Mumbai being a severely corrosion prone area results in corrosion of steel girders of bridges even after periodical maintenance. Due to heavy traffic on the bridge & below the bridge along with Live OHE wires (Just 500 mm below bottom of girders and connected to girders), it was very difficult to replace Girders of the bridge.

Proposal for the same had been included in LAW Book 2010-11 at Sr. no. 381. under PH-

SITE PLAN

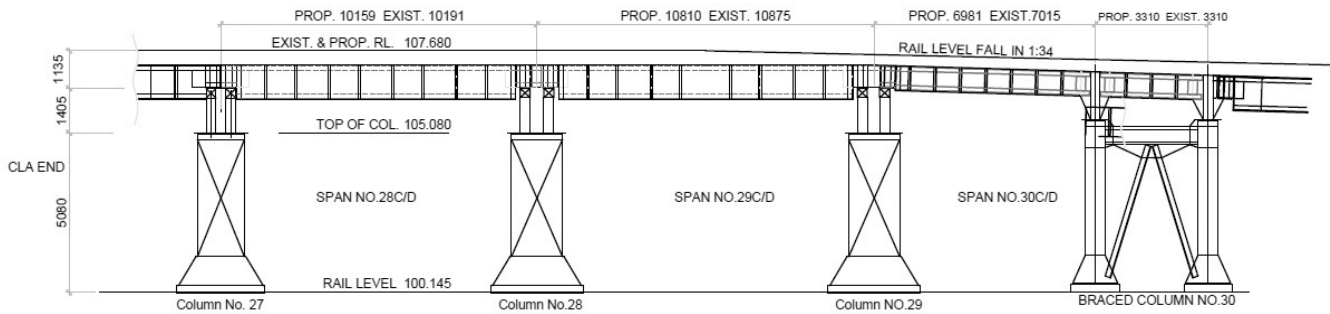


32 with the total cost of Rs.178 Lakhs. The work was awarded to M/s. S. P. Steel Maritech Pvt. Ltd, Navi Mumbai in the year 2017.

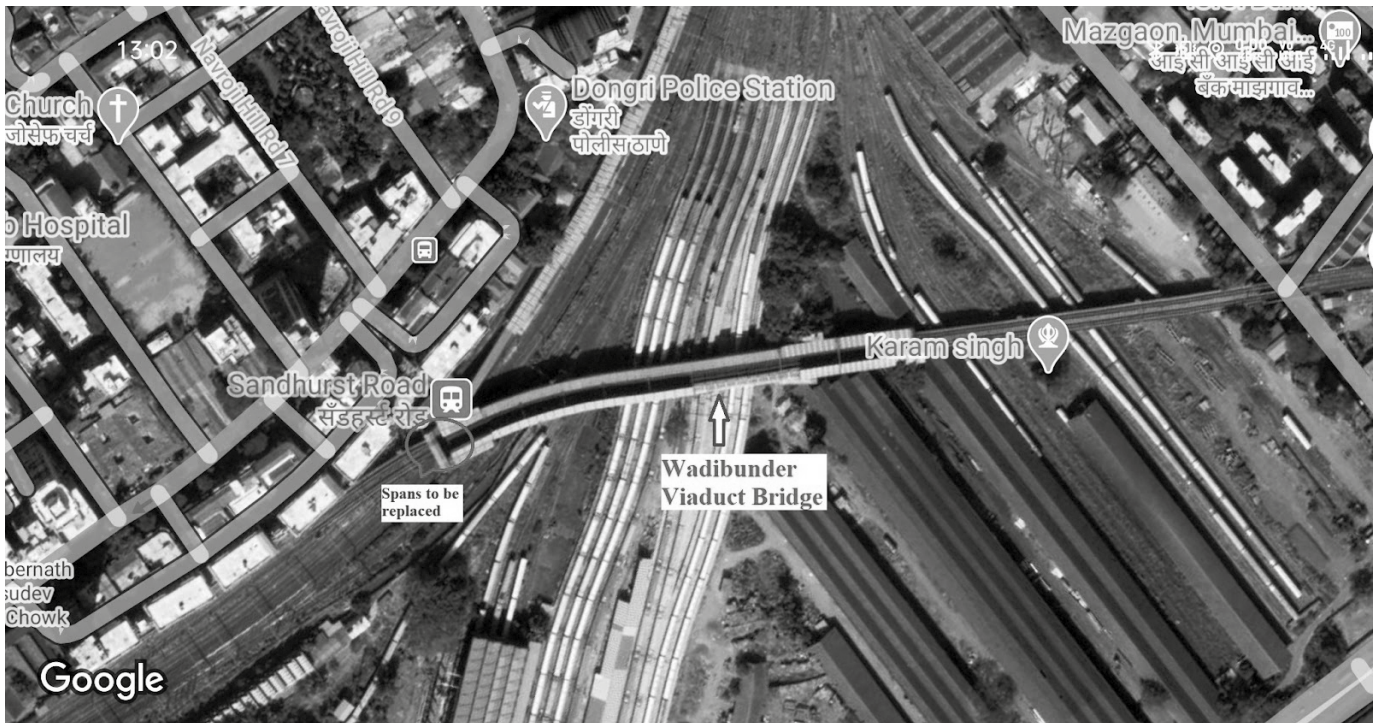
Four spans each from DN & UP harbor Line to be replaced.

¹ Dy.CE(Br.Line)HQ,CSMT

² SSE/Bridge/Byculla



Four spans each from DN & UP harbor Line to be replaced.



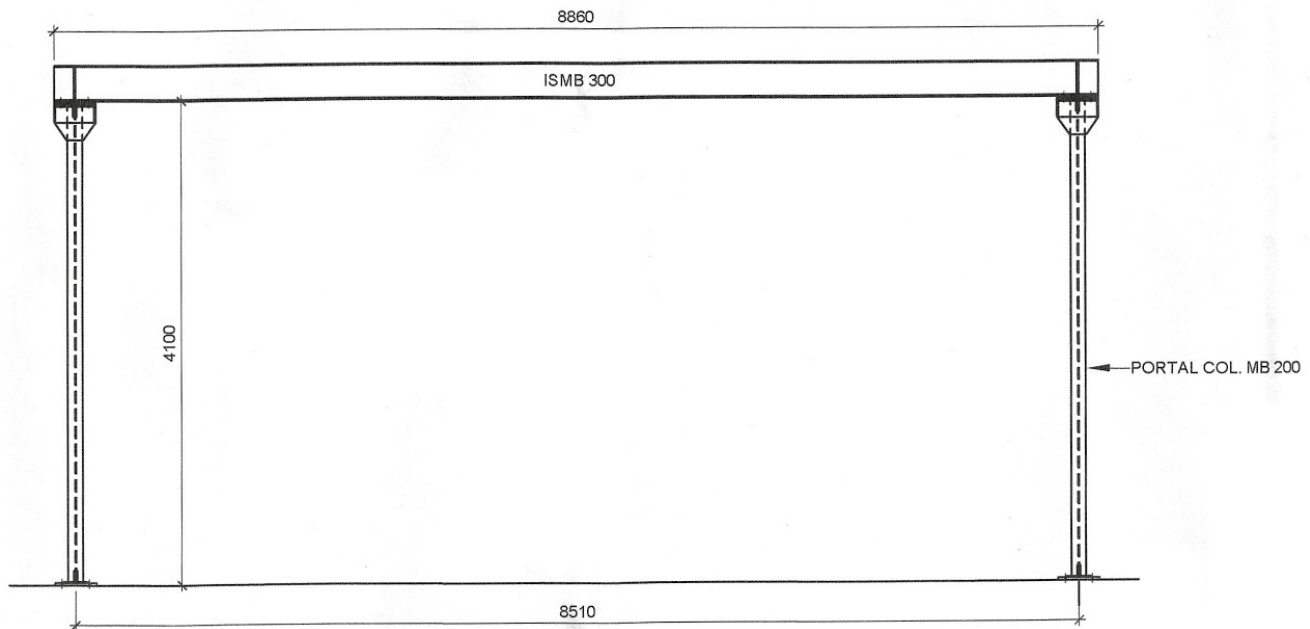
Wadibunder viaduct in HB line section of Mumbai Division.

Details of Weight of span & Length of span					
Sr. No.	SPAN NO.	Wt. of span (Old girders)	Wt. of span (New girders)	Overall length (Existing Girders)	Overall length (New Girders)
1.	28 UP(28A &28B)	10.063 MT	5.815 MT	10.083 M	9.989 M
2.	28 DN(28C &28D)	10.365 MT	5.899 MT	10.258 M	10.159 M
3.	29 UP(29A &29B)	10.264 MT	6.132 MT	10.757 M	10.625 M
4.	29 DN(29C &29D)	10.572 MT	6.224 MT	10.944 M	10.810 M
5.	30 UP(30A &30B)	5.346 MT	3.381 MT	6.937 M	6.858 M
6.	30 DN(30C &30D)	5.505 MT	3.435 MT	7.061 M	6.981 M
7.	30BP UP (30BPA &30BPB)	2.245 MT	1.669 MT	3.271 M	3.260 M
8.	30 BP DN (30BPC &30 BPD)	2.313 MT	1.691 MT	3.322 M	3.310 M

After due deliberation solution to problems encountered is summarized below :

- ❖ **Unapproachability of Machinery:** The location of the bridge is at elevated Sandhurst Road

station. The area surrounding it is densely populated to stop us from using cranes. The whole elevated station is a steel structure which was constructed in 1923 over steel columns. Being an old structure and no approach for



CROSS SECTION OF PORTAL

Portal Arrangement

Hydra, it took many deliberations to arrive at the launching scheme which would involve no machinery. It was decided to launch girders manually by Portal Beam Method. A portal of requisite capacity was erected on cross girders along with chain pulley block arrangement of sufficient capacity.

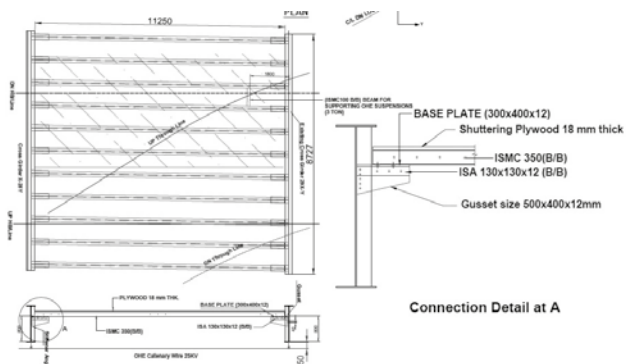


Loading of Newly fabricated upon Dip-Lorry @ Wadibunder Yard



- ❖ **Constraint in shifting of girders:** Due to inaccessibility of approach it was difficult to carry girders on site either by road or by rail. Being a very busy sub-urban station, it was quite impossible to place girders on the platform before regirdering too. The nearest location to place the girder was approx. 500 m away at Wadibunder yard. Therefore, it was decided to place the girder at Wadibunder Yard and shift the girders manually using dip lorrey during Mega block.04 Nos of dip lorries of suitable capacity was designed and deployed for shifting of girders.
- ❖ **Unavailability of working space:** The site condition was not at all favorable. There are 4 lines of CSMT- Kalyan section under the girders

(UP & DN Through, UP and DN Local) which carry all the locals of Mumbai Division with termination point at CSMT of long distance trains, while over the bridge Harbor line runs which connects CSMT - Panvel. It was not practically possible to take traffic and power blocks of all 6 lines because it would have caused enormous train cancellation and detention. Hence, it was decided to proceed with re-girdering without blocking the traffic under the bridge which was only possible by providing temporary staging under the girders over which the workers could work without risk of any induction. Isolation arrangement cum working platform was designed by HQ design wing as shown in drawing below. Additionally, the channels above OHE were provided with insulation paint to check any induction in the channels. The whole plywood layers were spun together using nylon wires to stop any displacement. Isolation arrangement platform for two spans was made simultaneously and once the regirdering of that span completed, platform cum isolation arrangement was shifted to the next consecutive span.



Isolation arrangement cum working platform

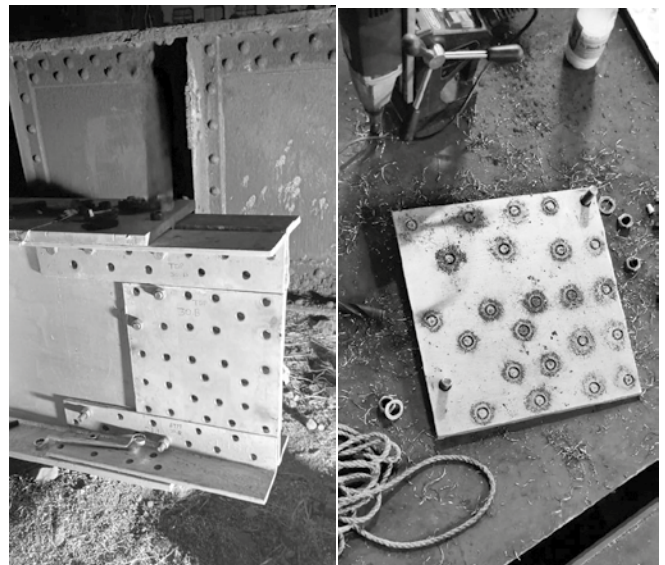


Temporary working platform cum isolation arrangement & OHE Fittings are shifted to staging channels coated with insulation paint.

- ❖ **Connection of OHE insulation/suspension with girders:** At seven locations, OHE fittings were connected to girders which were required to be replaced. The removal and placement of these fittings with new girders during the block would have necessitated the power block of lines under the bridge, which was practically very difficult. Above staging arrangement was also designed to cater

OHE load, during pre-block activity these fittings were shifted from girders to staging channels with the help of tower wagons and competent OHE staff.

- ❖ **Fix End connection of girders:** Out of 08 spans, 04 spans are simply supported over cross-girders, 02 spans having riveted fixed connection at one end and simply supported at other end, while remaining 02 spans having riveted fixed connections at both ends. It was very much difficult to match holes of the new girder with the existing gusset projecting outside from the cross girder. To overcome this problem a template was made by removing existing cover plate during block and the same was used for drilling of holes at one end of girders while the other end holes were drilled during block at site.



Templating of cover plate of Fixed end connection of Girder

- ❖ **High frequency of trains:** On an average daily 450-500 number of trains cross work site on UP & DN Harbor line, due to which working in a day time is quite impossible. Hence all types of pre-block activities carried out in Night during traffic & power block.



Curve & Gradient at working location

- ❖ **Curve & gradient:** Controlled movement of girders on Dip lorry from Wadibunder Yard to desired location as bridge site is in gradient of 1 in 37 with sharp curve. Anti-skid shoes & binding of dip lorry was ensured during girder stabilization.

Methodology of Execution

- ❖ **Fabrication of Girder:** The GAD No.GM(W) BB/P-14409, showing details of steel works of existing and proposed girders, was prepared and approved by HQ. Consequently, the structural drawing of steel work of new spans has been approved by HQ vide GM (W) MB - 6575 and these spans have been fabricated at CEW/MMR workshop followed by Sandblasting, Metallizing and painting as per provision laid down in para 218 of IRBM.



Newly fabricated Girders placed at Wadibunder Yard

❖ Pre-Block Activities:

1. To begin with the work, it was necessary to impose a Caution Order of 30 Kmph at Bridge site to avoid any unusual/incident.
2. As the shorter duration of Main Block was permitted, cutting of rivet connections of Rail Bearers to Cross Girders, Cross frames, footpath and Bracings etc and replacing the same by turn bolts was done in pre-block.
3. Similarly Cutting and punching of Rivets of top flange of cross girders for fixing of portal arrangement were done in pre-block activities during night in T&P block.
4. Channels along with supporting brackets are provided to stiffeners of cross girder for making temporary working platform cum isolation staging arrangement. Over these channels, plywoods of 18 mm thick were laid which would provide working space to the workers. Isolation arrangement platform for two spans was made simultaneously and once the regirding of that span completed, platform cum isolation arrangement was shifted to the next consecutive span.
5. Additionally, the channels above OHE were

provided with insulation paint to check any induction in the channels.

6. Shifting of S&T cables which were lying on the footpath to platform girders was done by making suitable fixing arrangements.
7. OHE fittings were connected to existing girders which were now shifted temporarily to channels of isolation staging arrangement.
8. Rivets connecting Stools and cross girder were replaced with turn bolt and made free.



Connection kept on Bolting before main block

Moreover arrangement was done for 4 sets of Dip Lorries for shifting of newly fabricated girders to worksite & shifting of existing corroded girders to wadi bunder yard where the girders are loaded & unloaded with the help of crane/hydra of requisite capacity during main block.

❖ Activities during Main Block

1. As soon as Traffic block was permitted, Erection & Fixing of Portal arrangement at both ends of

cross girder mounted with monorail traveling trolley with chain pulley block arrangement having capacity 05 Ton each is done.



Erection & Fixing of Portal Beam

2. Simultaneously, Lifting of Track was carried out with the help of Hydraulic Jack on adjacent sides of Cross-Girders by loosening of hook bolts, followed by Removing of Rubber Pads & Loosening of Hook Bolts of Panel under replacement.
3. To begin with replacement of the girder, first hold the existing girder with the help of chain pulley block arrangement provided on the portal. Now the connection of stringer with Cross Girder was removed. Total load was supported on Portal only. Slowly and steadily start side slewing the existing girders away from the centerline of the track. By Lifting existing girder with the help of chain pulley block above the Rail Level and load upon the Dip Lorry. Same method shall be adopted for another leaf of the existing girder.



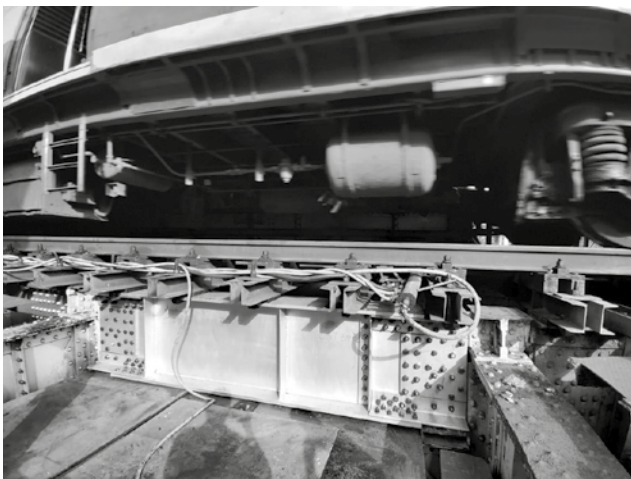
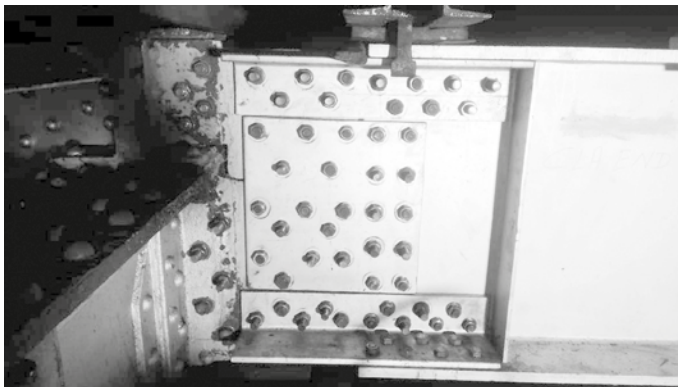
Removing existing girders by Portal & chain blocks

4. Both the dismantled existing girders were loaded upon Dip-Lorry and shifted to a location from where the old girders were unloaded at yard with the help of Hydra.



Existing girder was removed and kept on Dip-Lorry.

5. Launching of new girders was done, followed by providing diaphragm, bracings & footpath brackets etc. connected by turn bolts and the same shall be riveted after the main block is over.



Newly fabricated girder leaf launched one after another

6. Since the portal was infringing on the movement of the train, therefore removing the temporary portal and restoring track to the normal by providing rubber pad & necessary track fasteners in presence of competent SSE/P-Way staff.

❖ **Post Block activity**

1. After successfully regirdering of existing spans, all the bolted connections of cross frame, footpath bracket etc. were replaced by driving rivets. Laying of footpath decking plate was done thereon.
2. Re-fixing of OHE fittings to new girders was done in the traffic & power block by OHE staff.
3. Dismantling & removing the isolation staging arrangement. Rivets are driven in holes made on stiffeners for staging arrangement & on top flange of cross girder for portal fixing.
4. Apart from this, minor urgent structural repair work, such as strengthening of diaphragm of cross girder, strengthening of bottom flange of other spans also got successfully completed.

Safety Precaution Taken

1. Entire Work was carried out under a temporary speed restriction of 30 Kmph. Traffic & power blocks of 05 hrs. each were operated during the replacement of existing corroded girders.
2. Proper Protection was ensured during the work and caution boards were also provided as per G&SR.
3. It was ensured that all Tools & Plants used were in proper working condition & also available in spare to cater during any emergencies.
4. Safety of workmen & OHE wires below girders in the main line has been ensured by making a temporary isolation arrangement cum working platform.
5. Whereas the safety of Track is maintained by taking total Power & traffic Block of 40 hrs. during the Main Block, and sufficient no of T&P blocks for Pre & Post block activities.
6. Load Testing capacity of Crane was ensured before the Main Block prior to loading/unloading of Girders during.
7. Five coat high voltage insulation paint was applied on isolation cum staging channels for safety from OHE wires & fittings.

Lessons Learnt

1. Pulleys are to be used for lifting heavy weight portal beams on columns.
2. Proper match marking of holes to be ensured

- during templating of cover plates of fixed end connection.
3. Safety of OHE wire, fittings & running tracks should be ensured.
 4. Sequencing of activities along with time involved from the first block leads to time management & completion of work within block period from onward blocks.
 5. Freeness of stool connection from cross-girder should be ensured by lifting through jacks in pre-blocks.
 6. Slight slackening of P-Way fittings prior to main block can reduce block time for auxiliary works which leads to more block time for main re-girdering work.



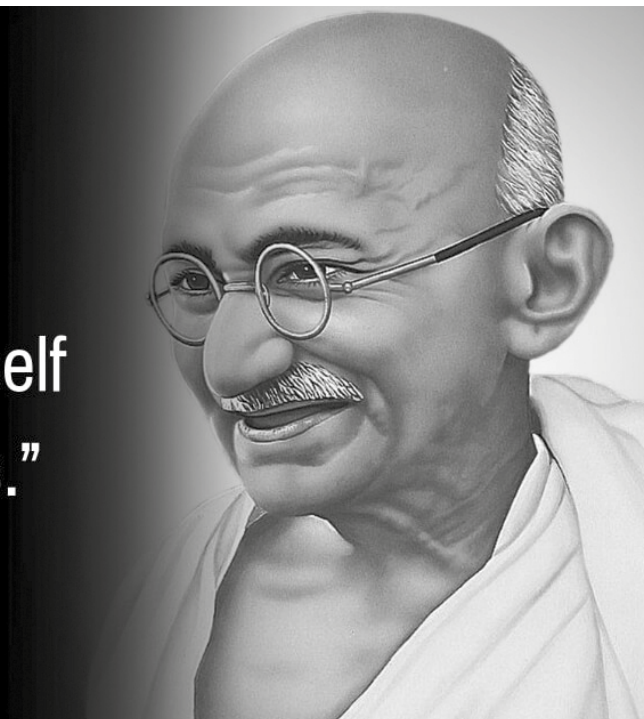
Progress Achieved

The preliminary works started from 26 November 2021 in regular night blocks. Total 08 Sunday mega blocks of 5 hrs. each of Harbor Line were taken (approx $5 \times 8 = 40$ Hrs) to complete the re-girdering work of 08 spans. The whole work was completed in time (March 2022) with full safety measures and not a single untoward incident has happened in the whole work.

In one of the most challenging and tedious work, Central Railway re-girdered 08 spans of Wadibunder Viaduct bridge by replacing 100 years old girders and It is learned that replacement of heavily corroded girders can be done easily by proper planning and close monitoring at each stage.

“The best way to find yourself is to lose yourself in the service of others.”

– Mahatma Gandhi



Experimental Study and Discussion on Multi-Twin-T-Girder-Deck for Road Bridges over Railway

By

Dr. Geetha M. P.¹

Dr. Girija K.²

S. Shanmughom³

ABSTRACT

Provision of grade separators, in the form of either road over bridges (ROBs) or road under bridges (RUBs), is the way of elimination of level crossings (LCs). RUB or subway is having the problem of drainage in the rainy season if the embankment height is very minimum in the range of 1.5 or 2m at the crossing location. Hence the provision of ROB is the best solution for the conversion of LCs. The authors developed a new cross-section of Twin-T (TT) shaped girders suitable for standardization and accelerated bridge construction to make any medium span highway bridges ranging from 15m to 45m. An experimental study conducted on two specimen TT girders-deck assembly and the corresponding structural performances are discussed in this paper. The capacity of the integrating deck slab to counteract the shear friction effect is accessed from the experimental study and is applied in designing the shear friction reinforcements embedded inside the deck slab above the joints between girders. Various advantages of the newly developed cross-section to make a ROB are also narrated in this study.

Introduction

The elimination of level crossings (LCs) is the need of the decade for any developing country. The completion of any highway network is always delayed at the LCs. Hence, converting an LC to a bridge across railways is essential and will smoothen the highway traffic and the railway traffic without major road vehicle-train collisions. By this, the social life of people around is also getting improved.

Provision of grade separators, either as the road over bridges (ROB) or as the road under bridges (RUB), is the way of elimination of level crossings. RUB or subway has a problem with drainage in the rainy season if the embankment height is minimum, like 1.5 or 2 m at the crossing location or if the high flood level (HFL) is above the proposed road level. Since the RUBs are generally economical compared to ROBs, engineers may be forced to go for RUB construction. To make the subway functional during the rainy season many remedial measures have to be adopted in the construction. These include the provision of a roof on both approaches [1] (including down water pipes from roof-gutter), hump at the entrance of downslope, reverse slope before the hump, French drain on either side of subway box structure with suitable slope to reach the nearest river (to reduce water pressure on reinforced concrete (RC) box structure), precast box segments suitable for pushing inside

under traffic block, compulsory service roads on either side (since digging makes house owners very panic), watertight construction, both side retaining walls (watertight), sumps with automatic pumping system with proper drainage system and its maintenance scheme, etc. In general, the cost increases on accounts other than main structure construction. The construction delay due to waiting for the dry season and the traffic blocks has also to be considered. Hence, the ROB with standardized girders of shallow depth is the best solution in place of level crossings. TT girder is the outcome of research intended for standardized restricted depth pre-stressed concrete (post-tensioned) girders with material high strength-high performance concrete (HS-HPC). The experimental study on two-TT girder-deck assembly and the various advantages in using these girders for making ROBs are discussed in the upcoming sections.

Need of the Study

New ROBs are constructed during increasing of railway tracks, conversion of level crossings into ROBs, construction of new railway lines and rehabilitation of existing ROB. In the first case, the span of the bridge increases, then correspondingly, the depth of the superstructure needs to be increased, and the same is not possible due to locked approaches in many cases. Accordingly, the construction depth must be restricted to avoid major land acquisition to

¹ Retired AXEN/Design/ Southern Railway.

² Professor, College of Engineering Trivandrum.

³ DEN/Special Works/ Madurai/ Southern Railway.

make the project viable and happen within the expected completion period. In the balance situations of ROB constructions, the depth reduction will help to reduce land acquisition. In all cases, the accelerated bridge construction should be ensured.

The Present Scenario

The ROB superstructures are generally of steel girder-RCC deck- composite construction interconnected between girders with steel diaphragms. Field bolts connect these steel diaphragms, and the slab and steel girder are connected using steel shear connectors or shear studs. The formwork for making the deck slab will be either consumable steel sheets (actually saving the reinforcements of the deck slab) or erected from the bottom flange of plate girders. Even though the in-situ constructions are less here, than in the concrete bowstring girder deck, the field connections require more traffic regulations. The figure 2.1 shows the erection of a composite girder over an electrified railway track; there will be a power block, train traffic block/ caution, feeder line block, if any, for 7 to 10 days for launching and integrated deck casting. Labour casualties are more in this case. Depth requirement is in the tune of span/10, and the cost is about five times that of PSC bridges.



Fig.1 : Erection of a composite girder over electrified railway tracks

The after effects can be seen in the figures 2 to 4 below:



Fig.2 : The level difference between old and new ROBs



Fig.3 : The modified junction to suit the level difference



Fig.4 : The steep slope visible on compound wall started after the gate of house

The RDSO has already provided steel bowstring girders with connecting cross girders and integrating deck slab, as standardised for crossing spans ranging from 30m to 72m with a depth of construction of only 1.385m. The erection time and hence the train traffic block timings are still more in this case. Space for crane erection of each assembled piece is also another constraint in adopting the steel bowstring girders. The cost of the bridge is also very high compared to the concrete bridges.

Construction management requirements.

Restricted depth type Precast Prestressed Concrete (PSC) girders are essential to make the ROB across a busy and electrified Railway track due to the following reasons;

- 1) To reduce the train traffic block time
- 2) To reduce the length of ROB
- 3) Thereby to reduce the land acquisition
- 4) To avoid disturbance to existing river bridge or junction in the approaches, if any.
- 5) The standardisation of cross-section of the superstructure is helping for Accelerated Bridge construction
- 6) Also to develop a competitive cross-section of

bridge to avoid risks of construction

- 7) If we can avoid the usage of bearings, the bridge becomes maintenance-free and hence highly fit for electrified track
- 8) In-situ construction above railway track has to be avoided since no formwork is possible from track

All these requirements are in addition to the safe, serviceable, and durable superstructure, the vital structural requirements.

Concept of Multi-Girder Bridge Deck

The concept of multi-girder bridge decks is mainly the segmentalisation of bridge deck in the lateral direction. The redistribution of the load is possible if there is a lateral connection between the girders. This lateral connection is possible either through shear keys and metallic diaphragms as in pi-girders developed by Federal Highways [2] or through integrating deck and metallic diaphragms as adopted in double T girder AASHTO type limited to a span range up to 25m [3]. Providing metallic diaphragms between two girders after erecting to the final position is not possible and unsuitable in the design situation of ROB. The potential issue of development of longitudinal cracks on overlay concrete above the shear keys provided in between two girders of multi-girder deck system [4] must be tackled with a proper solution. The method of cross pre-stressing is also not feasible for ROB construction. Hence, this can be tackled by properly designing the in-situ overlay concrete against the shear friction effects. The dead load of the girder can be reduced by adopting the multi-girder system. A standardised launching scheme can also be evolved. Hence the multi-girder deck system is decided for standardising the ROB superstructure. The different types of available cross-sections for multi-girder deck system are mainly multiple box girders, composite or non-composite, interconnected with transverse reinforcement rods fitted later after launching to position, multiple I-girders interconnected with precast diaphragms and integrated with a cast in place concrete deck slab laid over stay-in-place precast slabs, and double T girders integrated with deck slab as in PCI bridge manual [3].

General arrangement of Highway-Deck with Newly Developed Twin-T Cross-Section

Figure 5 to 8 shows the general arrangements of decks with 5, 6 & 7 Twin-T girders for 15m effective span.

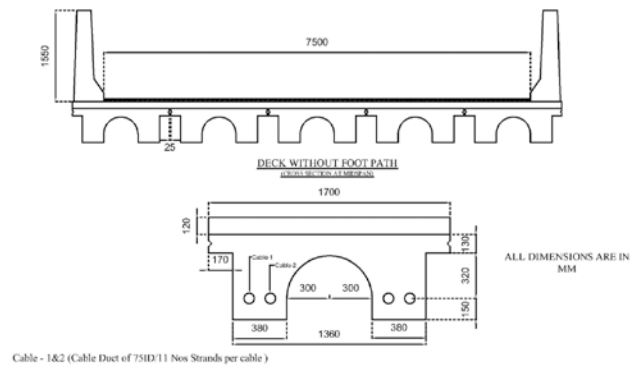


Fig.5 : General arrangement of five Girder Assembly

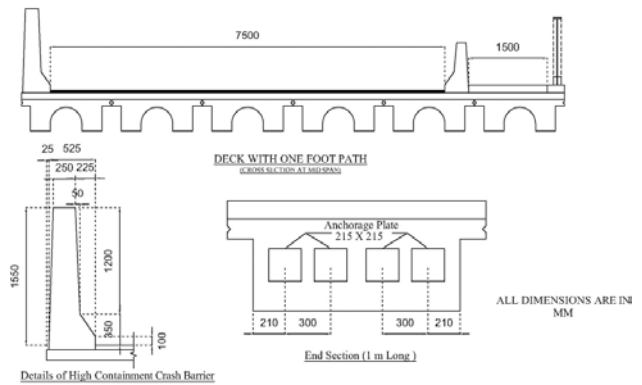


Fig.6 : General Arrangement of six girder assembly

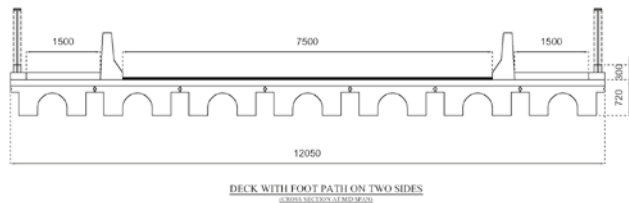


Fig.7 : General arrangement of seven girder assembly

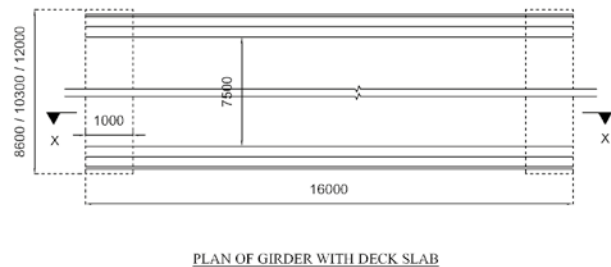


Fig.8 : GAD – Plan view & section of Deck- 15m span

From the views of arrangement, it is clear that the cross-section required to suit any span can be provided by just increasing the vertical sides and the extra length [5], as per design, as shown in figure 9. The inclination of the cables changes for different depths of girders. Hence, the end face of the shutter is to be changed for every span. A good designer can even plan to reduce this variation to the minimum.



Fig.9 : Proposed cross-section and bottom view of TT-girders of span varying from 15m to 45m (symmetrical dimensions in plan are avoided).

Shear Friction Reinforcement

Precast concrete multi beam bridges are constructed by placing precast concrete beams side by side and tying them together to form one integral structural component. The gap between adjacent units is filled with grout material to form a shear key. The grouted joints provide the means for constructing an integral structural element and allow for fabrication and construction tolerance. If a structural concrete composite overlay is placed, the gap between girders will be filled automatically. For adjacent precast multi beam bridges, the vertical shear is mainly transferred by grouted shear keys between girders. If there are longitudinal cracks in the shear keys and overlays as shown in figure 5.1, the connection between girders gets weakened, which is not favourable for the structural integrity and there by

leads to the condition of no load transfer between girders which is detrimental to the bridge safety.

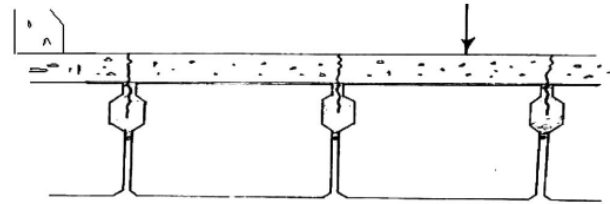


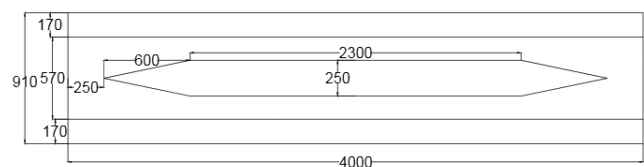
Fig.10 : Longitudinal cracking in the shear keys and overlay concrete of multi beam bridge deck

Provision of shear friction reinforcement is essential to ensure the integration between each girder units. When the vehicle load is above one girder and the other girder is not loaded, there is a chance of longitudinal crack on the deck, as in figure 5.1 as observed in the literature by Chung C.Fu, Zuanfeng Pan and Mohamed Sala Ahamed (2011) [4]. Transverse post-tensioning was the solution suggested to rectify this defect. The transverse pre-stressing is impossible to do at the site of bridge construction above railway tracks in running condition. Hence, it was investigated analytically on the effect of shear friction and found feasible to adopt the new detailing of reinforcement with N-type and reversed N-type fabricated reinforcement (M.P. & K., 2017) [6].

Experimental Study

General

In order to study the structural behaviour of TT-girders under various loading locations on a deck, the experimental study was conducted on a deck made with two specimen girders of length 4m made of high-performance concrete of M55 grade in the structural lab of College of Engineering Trivandrum. The total weight of each prestressed girder-deck slab assembly was within the capacity of a 5T crane available in the laboratory. The dimensioning of the girder was done to accommodate the minimum number of pre-stressing strands and end anchorages. The top slab and flanges had almost the same thickness and the projection as the same required for the prototype. Figure 11 shows the dimensions of specimen girder-deck assembly.



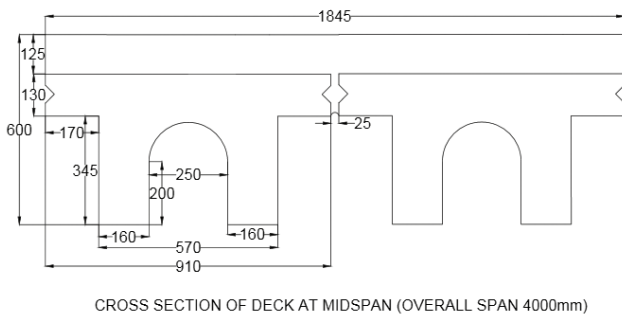


Fig.11 : Dimensional details of the specimen girder cast for the experimental study- Bottom view and cross-section

The Reinforcement Details of Girder Specimens and the Design Mix

The minimum steel is not required where the concrete is in compression due to pre-stressing. However, as depicted in figure 12 for other considerations such as early thermal and shrinkage cracking before the pre-stressing application, a minimum reinforcement was provided as per IRC 112-2011 [7]. At the end block, the designed reinforcement was provided as in figure 13. The special reinforcement in N-type and reversed N-type form was provided inside the deck slab above the shear key designed for the shear friction effect [8], as shown in figure 13. Both are to manage the position uncertainty of vehicles. The shape is to ensure the availability of diagonal steel.

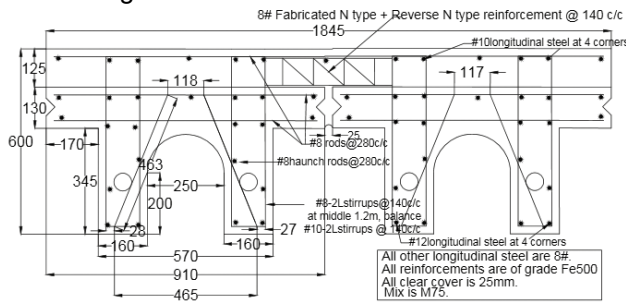


Fig.12 : Reinforcement details of specimen girder at mid-span

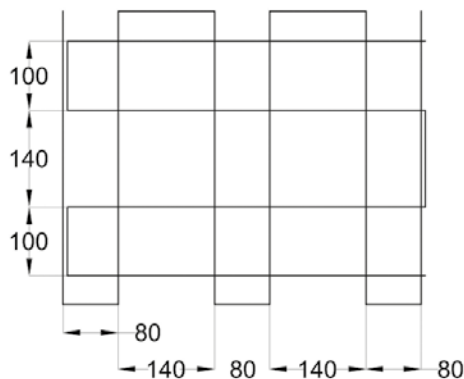


Fig.13 : Arrangement of end block reinforcement

The table 1 provides details of the mix design arrived for the study.

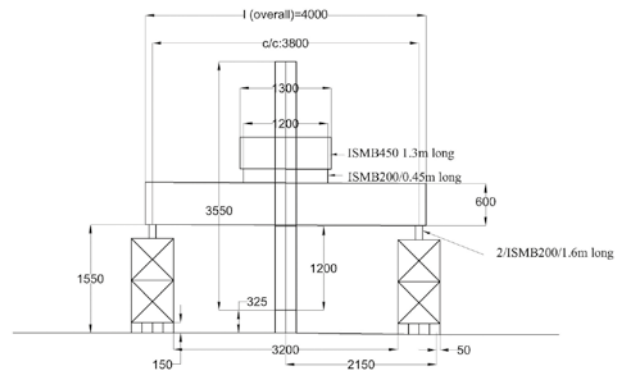
Table 1 The design mix of the study

Cement (Kg/m ³)	Crush sand (Kg/m ³)	Silica Fume (Kg/m ³) [9]	Coarse aggregate (Kg/m ³)		Plasticizer (Aurumix 500)	W/C ratio	Compressive Strength (MPa)
			20 mm	12 mm			
440	657	40	671	445	2.26	0.31	67

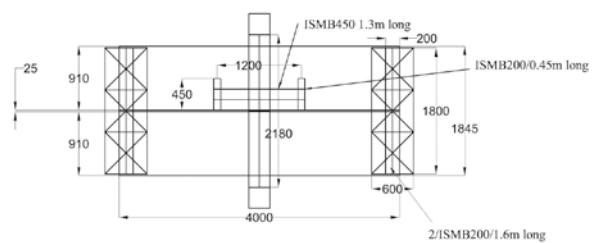
- The mean compressive strength of the mix adopted (third mix) was 65MPa.
- The corresponding characteristic strength was 55MPa.

The Test Set Up And Stages Of Casting

It was planned to cast the girders on the test floor of the structural laboratory. For conducting the load test, it was necessary to keep the girders at an elevated position below the loading frame available in the laboratory. The linear variable differential transformers (LVDTs) having the length of 1.2m were to be fitted below the webs at the mid-span of girders to measure the displacement of each web. The girders were supported over steel cribs. The arrangements for test set up was as given in the figure 14.



SET UP DIAGRAM OF LOAD TESTING



(a)

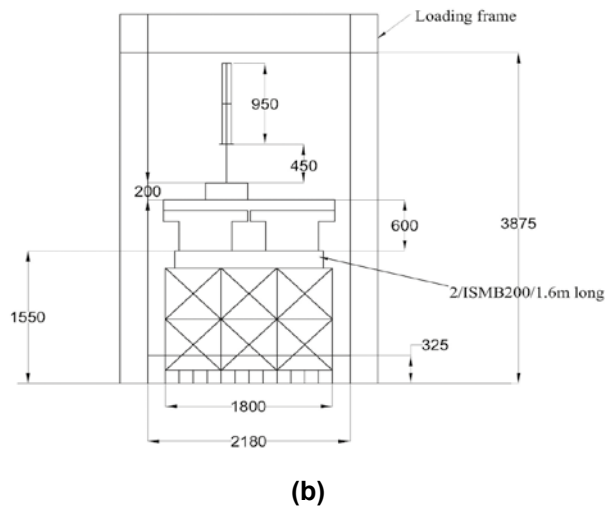


Fig.14 : Set up diagram of Load Testing, (a) Side elevation and plan (b) End view

Figure 15 shows stages before the deck casting



(a)

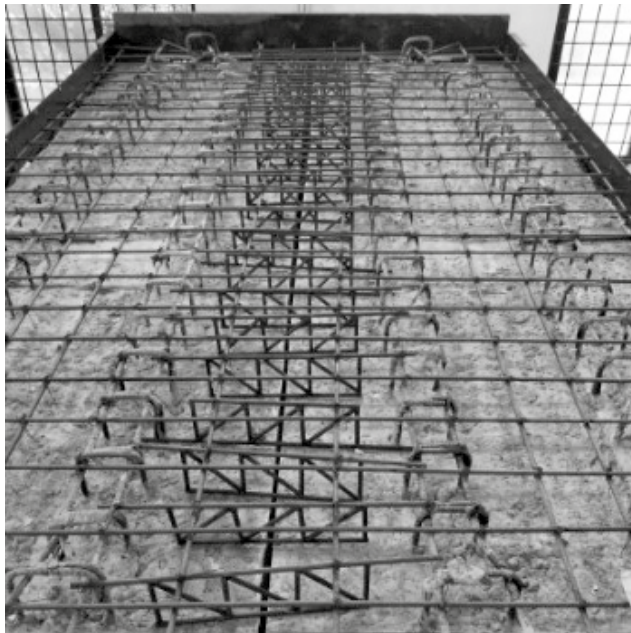


Fig.15 : Stages before the deck casting (a) Launching of Girders at 25mm gap (gap is concreted with same mix, with 12mm aggregate only), (b) Deck slab reinforcement including for shear friction.

Order of Load Testing

The following is the order in which the tests were conducted on the specimen girders and deck assembly made of PTGR1 and PTGR2.

- 1) Two-point load testing conducted on double girder deck assembly by placing load concentrically above PTGR1 and recorded all measurements (Test name PTGR111). Concentric load testing was conducted only up to 25 ton to limit for elastic behavior of deck assembly. This test helped to observe the load sharing nature of the girders if the load is away from the nearby girder.
- 2) Two point load testing conducted on double girder deck assembly by placing load eccentrically above PTGR1 (the load located above second web of PTGR1) and recorded all measurements (Test name PTGR112). This test was to observe the behaviour of the joint and to understand the structural behaviours of the girder in a simulating situation of the critical loading position on actual highway bridges.
- 3) After cutting the deck slab using a concrete cutter with blade diameter 300mm two-point load was placed again eccentrically on the same position of second test and recorded all the measurements (Test PTGR113). This test was to observe the capacity of shear key alone in sharing the load to the next girder.
- 4) Further to the above test, one more two-point load test was conducted on the same deck assembly of slab alone-cut, by keeping the load concentrically above PTGR1 (test PTGR114). This test was done to realize the effect of shear key alone causing to lift of exterior end.

Observations of Experimental Results

Test 1- The concentric load testing on double girder deck assembly (PTGR111)

A sample range of loading selected and the deflection of each web situated at fixed distance from one end has been plotted for each sample loading separately, in figure 16.

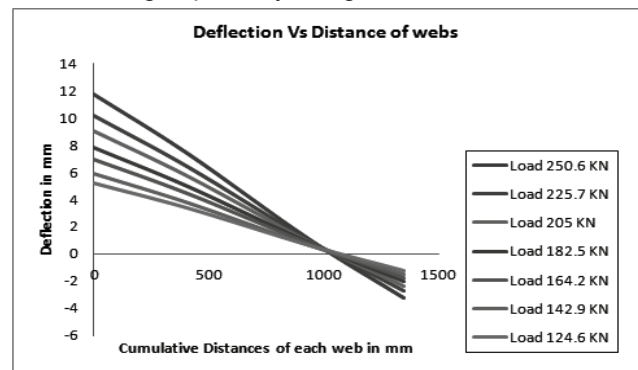


Fig.16 : Deflection of each web under different loading - Concentric

A linear pattern reflecting the excellent integration between girders is observed. It is due to the integration provided by the top deck slab, the shear friction reinforcement embedded inside the deck slab and the diamond shaped shear key. The load sharing between two girders is 85% to the loaded girder and 15% to the offloaded one as in table 2.

Table 2 Load share between specimen girders due to two point load testing concentrically on PTGR1 in double girder deck assembly (Data from test PTGR111).

Specimen girder	PTGR1 (loaded girder)		PTGR2 (off loaded girder)		Total
	Web 1	Web 2	Web 3	Web 4	
Deflection in mm of (Load applied on jack 25.06 tonne)	15.03	10.63	4.319	0	29.98
% deflection	50.0	35.0	15	0	100
% deflection/ % load share	85		15		100

Test 2 - The eccentric load testing on double girder deck assembly (PTGR112)

A sample range of loading selected and the deflection of each web situated at fixed distance from one end has been plotted for each sample loading separately, in figure 17.

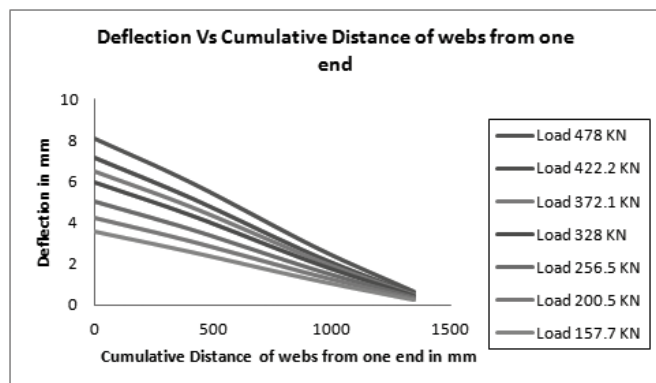


Fig.17 : Deflection of each web under different loading - Eccentric

A linear pattern reflecting the excellent integration between girders -due to the top deck slab, the shear friction reinforcement embedded inside the deck slab and the diamond shaped shear key. The load sharing between two girders is 77% to the loaded girder and 23% to the offloaded one as in table 6.3.

Table 3 Load share between specimen girders due to two point load testing eccentrically on PTGR1 in double girder deck assembly(Data from test PTGR112).

Specimen girder	PTGR1 (Loaded girder)	PTGR2 (offloaded girder)	Total
Deflection in mm of			
Load applied on jack 30.8ton (by random)	2.244	0.671	2.915
% deflection/ % load share	77	23	100

In test 1, uplift of the extreme outer web by 3.25mm was observed. This value was added to the values of all the other deflections to make the -3.25mm zero. Hence the readings are higher by 3.25mm in table 6.2. Otherwise also, the deflection values in test1 were found too much higher than that of test 2. It is due to the less load share between girders during test 1

Test 3 - The eccentric load testing on double girder deck assembly- slab alone is cut (Test PTGR113)

A sample data has been provided in table 6.4 to show the percentage load share between girders when the slab alone was cut. The two-point load was placed eccentrically above PTGR1. The capacity of shear key alone is arrived based on this table.

Table 4 Percentage load share between girders calculated from Test PTGR113-showing effect of shear key

Load	Average deflection of specimen girder PTGR1 (loaded)	Average deflection of specimen girder PTGR2 (offloaded)	Total	% load share to PTGR1	% load share to PTGR2
10.88	2.595	0.61	3.205	80.967	19.033
20.53	4.094	0.684	4.778	85.684	14.316
30.78	5.12	0.54	5.66	90.459	9.541
40.1	5.886	0.476	6.362	92.518	7.482
49.45	6.79	0.495	7.285	93.205	6.795
Average % load share to each girder				89 %	11 %

The above result shows that the capacity of shear key alone is approximately 50% in sharing the load between girders since the load share to PTGR2 was 23% in table 4 and that in table 5 it is 11%. This result is very useful in the design calculation of shear friction reinforcement which was embedded monolithically inside the integrating deck slab.

Test 4 - The concentric load testing on double girder deck assembly- slab alone is cut (Test PTGR114)

In this test the two-point load was placed concentrically above PTGR1. A sample data of this test is provided in table 5.

Table 5 Deflection of each web during load test PTGR114

Load in tonne	Deflection in mm of Web1	Deflection in mm of Web2	Deflection in mm of Web3	Deflection in mm of Web4
9.45	3.722	2.072	0.122	-0.978
20.34	6.164	3.624	0.334	-1.596
29.84	7.879	4.649	0.389	-2.131
40.32	9.876	5.776	0.166	-3.254
49.58	12.736	7.346	0.084	-4.762

The above result shows how effective the shear key in sharing the load to adjacent girders. It is even able to uplift the edge of the deck as seen in the above results.

7. Conclusions and salient features of TT girder-deck assembly

This paper deals with the development of Twin-T (TT) girders for the standardization of highway girders above the busy and electrified railway track. The experimental study on specimen girders could reveal the following structural performances.

1. The capacity of the shear key and the integrating slab are almost equal in sharing the load to the adjacent girders. This aspect is useful in designing the shear friction reinforcement embedded inside the integrating slab concrete.
2. The integration between girders is excellent due to the integrating deck slab, shear friction reinforcement embedded inside the deck concrete located above the joint and the diamond-shaped shear key in between adjacent girders. Due to this integrating effect, the load distribution between girders is in a linear pattern showing more deflection for the exterior web as in the usual bridge decks of grillage pattern [10].

Modelling with finite element method [11] was done as part of the research work and arrived TT girder cross-sections for various spans, ranging from 15m to 45m as given in figure 9. The vehicular deflection decides the depth of the girder, which is limited to span/800.

The salient features of TT girder-deck assembly are summarised as;

- The design is conforming to IRC standards

- The reduced depth of construction, stability during launching and casting deck slab without formwork except at sides are found possible. The newly developed cross-section has the shape of flanged inverted U at middle and flanged solid rectangular at ends with two slow transition zones before two end blocks.
- The potential issue of longitudinal cracking in the performance of the multi-girder deck system was solved by designing and providing special shear friction reinforcement embedded inside the cast-in-place deck slab laid monolithically above precast girders. Due to the embedded shear friction reinforcement, the suggested transverse pre-stressing in literature was avoided since it is impossible above running railway track.
- The diaphragm-less construction is possible by providing solid end blocks and providing a curved profile in the plan for the post-tensioning tendons. The inward lateral displacement resulting from the radial pressure from post-tensioning tendons is counteracting the spread of webs due to external loads.
- The width adopted for the developed cross-section of proto-type girder is 1.7m which is a typical dimension to generate usual deck widths of 8.6m, 10.3m and 12.0m. Keeping the webs vertical makes it easy to make any girder to suit any span length by simply adding the vertical shutter and shutter for extra length.
- The standardization of highway girders above the busy and electrified railway track is possible by adopting multiple units of modularized twin-T shaped girders due to the proper integration between girders and deck slab with the usage of special shear friction reinforcements and shear keys.
- The enhanced structural performances and durability of twin-T shaped girders were due to the usage of High-strength, High-performance Post-tensioned Pre-stressed Concrete.
- The minimized depth of construction was due to the evolved shape of cross-section and the HS-HPC PSC-PT girders, which in turn reduces the land requirements and any modifications of existing junction / bridges, if any, in the approaches.
- Due to the shape of the cross-section, the casting of integrating deck slab above the precast girders required no formwork, and hence no train traffic block is needed except for the launching of girders.
- Achievement of accelerated bridge construction becomes possible through standardization and

modularization.

- Useful to adopt for all bridges of highway standard of loading conforming to IRC 6 2014 [12]

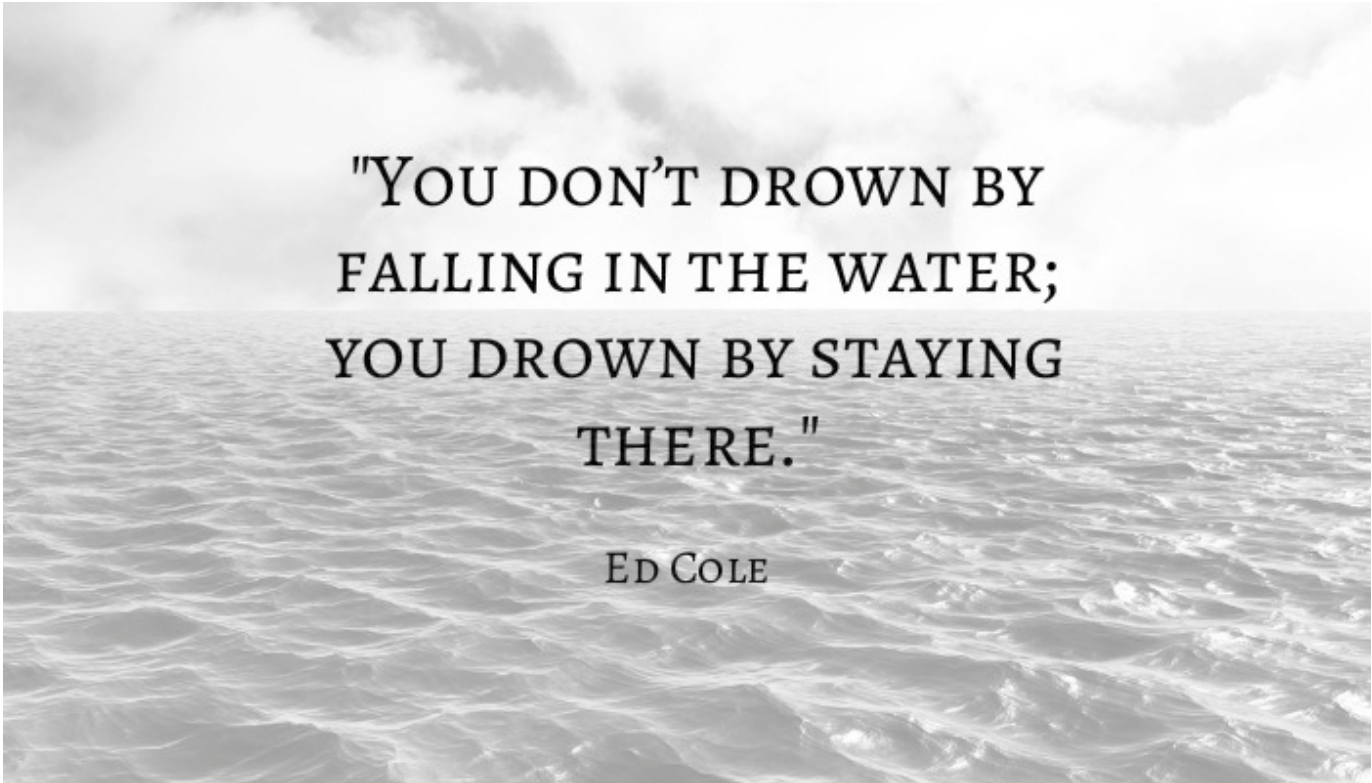
Acknowledgement

The experimental part of this research was funded by Technology Development and Transfer, Department of Science and Technology, India.

References

1. Railway board letter no. 2017/CE-IV/RUB/88 dated 04.10.2017
2. Chen, L. and Graybeal, B. A., (2012). Modelling Structural Performance of Second-Generation Ultrahigh-performance Concrete Pi-Girders (2012a). ASCE, Journal of Bridge Engineering.
3. PCI Bridge Design Manual (2014). 3rd Edition ed. Chicago: Precast/Prestresses Concrete Institute.
4. Fu, C. C., Pan, Z. and Ahamed, M. S., (2011). Transverse post tensioned design of adjacent precast solid multibeam Bridges. Journal of performance of constructed facilities.
5. M.P Geetha and Girija K, (2015). A standardized cross section for restricted depth girder for road bridges over railway track. SEWC conference at Singapore.
6. M.P Geetha and Girija K (IMMM 2017). Analytical Investigation on Effect of Shear Friction. Trivandrum, Taylor and Francis.
7. IRC:112(Idian Road Congress)(2011). Code of practice for concrete road bridges. New Delhi, India.
8. Pillai, U. S. and Menon, D., (2009). Reinforced Concrete Design. 3rd ed. Gautam Buddha Nagar, Uttar Pradesh: McGraw Hill Education(India) Private Limited.
9. IS:15338 (Bureau of Indiaan Standard)(2003). "Silica Fumes- Specification". New Delhi, India.
10. Victor, D. J., 1980. Essentials of Bridge Engineering. Third Edition ed. New Delhi: Oxford & IBH Publishing co.Pvt.Ltd..
11. Smith, M., (2009) ABAQUS/Standard User's Manual, Version 6.9. Providence, Rhode Island: Dassault Systèmes Simulia Corp.
12. IRC:6(Idian Road Congress)(2014). "Standard specifications and code of practice for road bridges." New Delhi,India.

□□□



"YOU DON'T DROWN BY
FALLING IN THE WATER;
YOU DROWN BY STAYING
THERE."

ED COLE

Uncracked Reinforced Concrete Rectangular, Circular and Hollow Circular Columns under Long Term Loading – A Review of Indian Bridge Codes

By
R.Sundaresan¹

ABSTRACT

Limit States Method of design was in practice in Indian railways from the year 2004. From the year 2011 onwards, the road bridges were also designed by using Limit States Method. The calculation methods for the evaluation of serviceability stresses for the railway bridges and road bridges are different. The additional stresses induced in reinforced concrete uncracked columns having rectangular, circular and hollow circular cross sections are analysed in this paper from the grounds of Indian Bridge Codes.

Introduction:

Under the actions of compression and bending, the Reinforced Concrete (RC) columns are subjected to bending compressive and tensile stresses. If the calculated bending stresses are compressive throughout the section of the column, the column is classified as uncracked column. In this case, the neutral axis will lie outside the column and hence the calculated stresses at any point of the column are compressive in nature.

Creep is the time dependent strain under constant stress. The volumetric change of concrete on drying and further hardening after the period of curing of concrete causes the shrinkage strain in concrete. Due to creep and shrinkage, the bending compressive stress in concrete slightly reduces with an appreciable increase in compressive stresses in reinforcement bars. The procedures for the calculation of changes in stresses in the uncracked RC rectangular, circular and hollow circular columns are presented below.

Need for the Study:

- ❖ The Indian Railway Bridge Code¹ uses the empirical modular ratios of $280/f_{ck}$, and $420/f_{ck}$ for the tension zone and compression zones respectively to partially account for the creep and shrinkage. The IRC:112-2011² provides for the Effective Modulus Method for calculating the time dependent stresses. Since two different approaches are used for the design of bridges, it becomes necessary to study the effects of creep and shrinkage based on the above two codes for ensuring their reliability in predicting the safe working stresses.
- ❖ Limitation and extension of the work:

For this study, a uncracked rectangular, circular and hollow circular RC column subjected to an axial load and uniaxial bending are considered. Since circular and hollow circular columns are symmetrical about the centroidal axis which is perpendicular the axis of bending, the circular and hollow circular columns subjected to axial load and biaxial bending can be treated as the column under axial load and uniaxial bending by replacing uniaxial moment by the resultant moment given by Eq.(1).

$$M_r = \sqrt{M_x^2 + M_y^2} \quad \text{Eq.(1)}$$

Distribution of Strains and Stresses:

The cross section of RC columns and distribution of strain across the depth is shown in Fig.1.

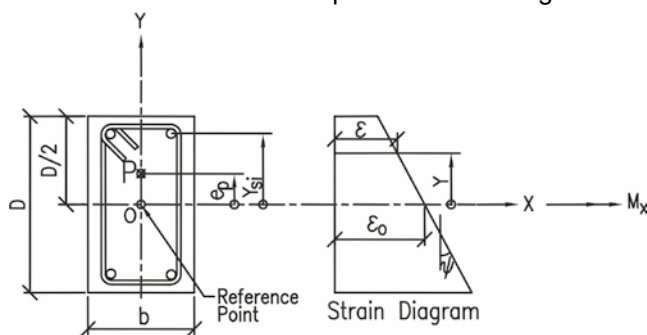


Fig. 1: Section of column and distribution of strain along depth

The strain at a distance, 'y' from the centre of circular column is given by Eq.(2)

$$\varepsilon = \varepsilon_0 + \psi y \quad \text{Eq.(2)}$$

ε_0 = strain at reference point; ψ = strain gradient

y = distance from reference point

¹ SSE/Drg., CAO/CN/O/MS, S.Rly

Hence the stress in concrete can be expressed as

$$\sigma_c = E_c (\varepsilon_0 + \psi y) \text{ if } -D/2 \leq y \leq D/2 \quad \text{Eq.(3)}$$

where E_c = elastic modulus of concrete

Similarly, the stress in reinforcement steel can be found as

$$\sigma_s = E_s (\varepsilon_0 + \psi y_s) \quad \text{Eq.(4)}$$

where E_s = elastic modulus of rebars and

y_s = distance of rebars from reference point

Methodology for Calculation:

The four steps analysis suggested in Ghali A, et. Al³ is used in this paper for calculating the time dependent stresses. The detailed methodology as applied to the cracked RC rectangular column can be found from Sundaresan R4. The equations for the calculation of time dependent stresses in RC solid and hollow circular columns which are cracked under axial and uniaxial bending are available in Sundaresan R5,6

Effective Sectional Properties of Column at Initial Time, t_0 :

For the uncracked columns, the neutral axis will lie away from the column section. Hence, the entire section of concrete is effective in resisting the externally applied loads and internally induced stresses arising from creep and shrinkage. The sectional properties of effective concrete areas of solid rectangular, circular and hollow circular columns can be calculated from the formulae given in the following sub-sections.

- ❖ 1 Effective concrete properties of RC solid rectangular column:

$$A_c = bD \quad \text{Eq.(5a)}$$

$$B_c = 0 \quad \text{Eq.(5b)}$$

$$I_c = \frac{bD^3}{12} \quad \text{Eq.(5c)}$$

where b & D are breadth and depth of rectangular column respectively.

- ❖ Effective concrete properties of RC solid circular column:

$$A_c = \frac{\pi}{4} D^2 \quad \text{Eq.(6a)}$$

$$B_c = 0 \quad \text{Eq.(6b)}$$

$$I_c = \frac{\pi D^4}{64} \quad \text{Eq.(6c)}$$

- ❖ Effective concrete properties of RC hollow circular column:

$$A_c = \pi (a^2 - a_1^2) \quad \text{Eq.(7a)}$$

$$B_c = 0 \quad \text{Eq.(7b)}$$

$$I_c = \frac{\pi}{4} (a^4 - a_1^4) \quad \text{Eq.(7c)}$$

where a & a_1 are outer and inner radius hollow circular column.

Transformed Properties of Column:

The transformed properties of area of the column section considering the area of reinforcement bars for the columns can be found from the following equations.

- ❖ Transformed properties of RC solid rectangular and circular columns:

$$A_{tr} = A_c + \alpha \sum_{i=1}^{n_s} A_{si} \quad \text{Eq.(8a)}$$

$$B_{tr} = B_c + \alpha \sum_{i=1}^{n_s} A_{si} Y_{si} \quad \text{Eq.(8b)}$$

$$I_{tr} = I_c + \alpha \sum_{i=1}^{n_s} A_{si} Y_{si}^2 \quad \text{Eq.(8c)}$$

where n_s is the number of reinforcement bars and α is the ratio of Young's modulus of steel to the initial modulus of concrete. Y_{si} is the distance of reinforcement bar from the axis through the reference point as shown in Fig.1. For circular column, Y_{si} can be calculated from the following formula

$$Y_{si} = (a - d'_c) \cdot \sin\left(\frac{2\pi(i-1)}{ns}\right); i = 1, 2, \dots, n_s$$

$$\text{and } d'_c = \text{Eff. cover} \quad \text{Eq.(8d)}$$

- ❖ Transformed properties of RC hollow circular column:

$$A_{tr} = A_c + \alpha \left(\sum_{i=1}^{ons} A_{osi} + \sum_{i=1}^{ins} A_{isi} \right) \quad \text{Eq.(9a)}$$

$$B_{tr} = B_c + \alpha \left(\sum_{i=1}^{ons} A_{osi} Y_{osi} + \sum_{i=1}^{ins} A_{isi} Y_{isi} \right) \quad \text{Eq.(9b)}$$

$$I_{tr} = I_c + \alpha \left(\sum_{i=1}^{ons} A_{osi} Y_{osi}^2 + \sum_{i=1}^{ins} A_{isi} Y_{isi}^2 \right) \quad \text{Eq.(9c)}$$

where 'ons' and 'ins' are respectively the numbers of reinforcement bars in the outer and inner cores.

A_{osi} & A_{isi} are the area of i^{th} reinforcement bar in outer and inner core respectively. The distances

of i^{th} reinforcement bar from the axis through the reference point can be calculated from the following formulae.

$$Y_{osi} = (a - d'_{oc}) \cdot \sin\left(\frac{2\pi(i-1)}{ons}\right); i = 1, 2, \dots, ons$$

...Eq.(9d)

d'_{oc} = Eff. cover to outer core rebar

$$Y_{isi} = (a - d'_{ic}) \cdot \sin\left(\frac{2\pi(i-1)}{ins}\right); i = 1, 2, \dots, ins$$

...Eq.(9e)

d'_{ic} = Eff. cover to inner core rebar

Calculation of Strains and Stresses at the Time of Initial Loading, t_0 :

The concrete and transformed sectional properties can be calculated from equations available in Sections 4 and 5 above. The initial

strain $\varepsilon_0(t_0)$ and strain gradient, $\psi(t_0)$ can be related to the external loadings in the Eq.(10).

$$\begin{Bmatrix} P \\ M \end{Bmatrix} = E_c(t_0) \begin{pmatrix} A_{tr} & B_{tr} \\ B_{tr} & I_{tr} \end{pmatrix} \begin{Bmatrix} \varepsilon_0(t_0) \\ \psi(t_0) \end{Bmatrix} \quad \text{Eq.(10)}$$

From the above equation, we can find the values of $\varepsilon_0(t_0)$ and $\psi(t_0)$ as given in Eq.(11) and Eq.(12) respectively

$$\varepsilon_0(t_0) = \frac{(I_{tr}P - B_{tr}M)}{E_0(t_0)[A_{tr}I_{tr} - B_{tr}^2]} \quad \text{Eq.(11)}$$

$$\psi(t_0) = \frac{(-B_{tr}P + A_{tr}M)}{E_0(t_0)[A_{tr}I_{tr} - B_{tr}^2]} \quad \text{Eq.(12)}$$

The stress in concrete and reinforcement steel bars can be found from Eq.(3) and Eq.(4) respectively from the above values and using the appropriate values of modulus of concrete and steel.

Modified Effective Sectional Properties of Column at Any Time, T:

The modified modulus of concrete and modified modular ratio considering the effect of creep can be found by

$$\bar{E}_c = \frac{E_c}{(1 + \varphi(t, t_0))}; \quad \bar{\alpha} = \frac{E_s}{E_c} \quad \text{Eq.(13)}$$

The sectional properties of effective concrete

alone can be calculated from the Eq.(5a)-Eq.(5c), Eq.(6a)-Eq.(6c), and Eq.(7a)-Eq.(7c) respectively for solid rectangular, solid circular and hollow circular columns. The transformed sectional properties modified to take care of creep of concrete in the solid rectangular, circular and hollow circular columns are given in the following sub-sections by Eq.(14a)-Eq.(14c), Eq.(15a)-Eq.(15c), and Eq.(16a)-Eq.(16c) respectively.

- ❖ Transformed concrete properties of RC solid rectangular column modified for creep effect:

$$\bar{A}_{tr} = A_c + \bar{\alpha} \sum_{i=1}^{ns} A_{si} \quad \text{Eq.(14a)}$$

$$\bar{B}_{tr} = B_c + \bar{\alpha} \sum_{i=1}^{ns} A_{si} Y_{si} \quad \text{Eq.(14b)}$$

$$\bar{I}_{tr} = I_c + \bar{\alpha} \sum_{i=1}^{ns} A_{si} Y_{si}^2 \quad \text{Eq.(14c)}$$

- ❖ Transformed concrete properties of RC solid circular column modified for creep effect:

$$\bar{A}_{tr} = A_c + \bar{\alpha} \sum_{i=1}^{ns} A_{si} \quad \text{Eq.(15a)}$$

$$\bar{B}_{tr} = B_c + \bar{\alpha} \sum_{i=1}^{ns} A_{si} Y_{si} \quad \text{Eq.(15b)}$$

$$\bar{I}_{tr} = I_c + \bar{\alpha} \sum_{i=1}^{ns} A_{si} Y_{si}^2 \quad \text{Eq.(15c)}$$

- ❖ Transformed concrete properties of RC hollow circular column modified for creep effect:

$$\bar{A}_{tr} = A_c + \bar{\alpha} \left(\sum_{i=1}^{ons} A_{osi} + \sum_{i=1}^{ins} A_{isi} \right) \quad \text{Eq.(16a)}$$

$$\bar{B}_{tr} = B_c + \bar{\alpha} \left(\sum_{i=1}^{ons} A_{osi} Y_{osi} + \sum_{i=1}^{ins} A_{isi} Y_{isi} \right) \quad \text{Eq.(16b)}$$

$$\bar{I}_{tr} = I_c + \bar{\alpha} \left(\sum_{i=1}^{ons} A_{osi} Y_{osi}^2 + \sum_{i=1}^{ins} A_{isi} Y_{isi}^2 \right) \quad \text{Eq.(16c)}$$

Restraining Stress to the Free Creep and Shrinkage:

The restraining stress in the concrete section against the free creep and shrinkage can be written as

$$\Delta\sigma_{res} = -\bar{E}_c \left\{ \varphi(t, t_0) [\varepsilon_0(t_0) + \psi(t_0)y] + \varepsilon_{cs} \right\}$$

...Eq.(17)

where $\varphi(t, t_0)$ is the creep coefficient and 'y'

is the ordinate where the restraining stress is required.

Resultant Force Developed by Restraining the Stress Due to the Free Creep Strain:

The forces induced at the reference point due to the artificial restraint to the free strain of creep on concrete section alone are given by the following Eq.(18).

$$\begin{Bmatrix} \Delta P_{crp} \\ \Delta M_{crp} \end{Bmatrix} = -\bar{E}_c \varphi(t, t_0) \begin{pmatrix} A_c & B_c \\ B_c & I_c \end{pmatrix} \begin{Bmatrix} \varepsilon_0(t_0) \\ \psi(t_0) \end{Bmatrix} \quad \dots \text{Eq.(18)}$$

Resultant Force Developed by Restraining the Stress Due the Free Shrinkage Strain:

On the application of restraint to the concrete section the free shrinkage strain will induce the following force at the reference point.

$$\begin{Bmatrix} \Delta P_{shr} \\ \Delta M_{shr} \end{Bmatrix} = -\bar{E}_c \varepsilon_{cs} \begin{Bmatrix} A_c \\ B_c \end{Bmatrix} \quad \dots \text{Eq.(19)}$$

Additional Strain Due to Creep and Shrinkage at Time, T:

The restraining force to prevent free creep and shrinkage strain can be found using Eq.(18) and Eq.(19) respectively. On summing up the additional axial forces and bending moments due to creep and shrinkage calculated from above equations can now be applied in reversed direction to nullify the effect of restraint. The mathematical equation for the above is expressed as in Eq.(20)

$$\begin{Bmatrix} \Delta \varepsilon_0(t, t_0) \\ \Delta \psi(t, t_0) \end{Bmatrix} = \frac{1}{\bar{E}_c} \begin{Bmatrix} \bar{A}_{tr} & \bar{B}_{tr} \\ \bar{B}_{tr} & \bar{I}_{tr} \end{Bmatrix}^{-1} \begin{Bmatrix} -\Delta P \\ -\Delta M \end{Bmatrix} \quad \text{Eq.(20)}$$

where $-\Delta P = -(\Delta P_{crp}) - (\Delta P_{shr})$, and

$$-\Delta M = -(\Delta M_{crp}) - (\Delta M_{shr})$$

Change in Stress in Concrete Due to Creep and Shrinkage at Time, T:

The stress due to restraint to creep and shrinkage can be found from Eq.(17) using modified modulus of concrete, creep coefficient, shrinkage strain and initial strain. Adding the above restraining stress to the stress caused by the change in strain due to creep and shrinkage, the final stress in concrete can be calculated by

$$\Delta \sigma_c = \Delta \sigma_{res} + \bar{E}_c \left[\Delta \varepsilon_0(t, t_0) + \Delta \psi(t, t_0) y \right] \quad \dots \text{Eq.(21)}$$

Additional Stress in Reinforcement Bars Due to Creep and Shrinkage:

Since the concrete in tensile zone is ignored, the changes in stress in reinforcement steel bars are calculated using the following equation.

$$\Delta \sigma_s = E_s \left[\Delta \varepsilon_0(t, t_0) + \Delta \psi(t, t_0) y_s \right] \quad \text{Eq.(22)}$$

Numerical Examples for Uncracked Columns Using Irc:112-2011 Code:

The grade of concrete for the column is M35 and the grade of steel for the reinforcement bars is Fe500D. The Initial modulus for concrete taken from the code is 32308MPa. The Young's modulus of reinforcement steel considered for this example is 200000MPa. Hence, the initial elastic modular ratio of concrete can be calculated as 6.19. The creep coefficient and the shrinkage strain considered for this study are 2.5 and -0.0003 respectively. The axial load while acting perpendicular to XY plane causing tension in the positive direction of Y-axis and bending moment acting about X-axis causing tension in the positive direction of Y-axis are taken as positive in this paper.

1 Rectangular column:

An RC column having the sectional properties shown in Fig.2 is taken for demonstration of application of theoretical equations given in the previous sections to the real structural member.

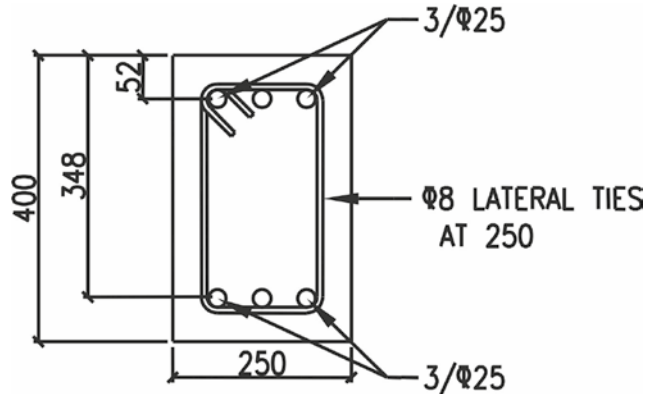


Fig. 2: Cross section of RC rectangular column

1.1 External loads acting on the column:

The column section is subjected to an external axial load of -832.5kN and bending moment of -49.26kNm acting permanently due to dead and superimposed dead loads. In addition to the above, an axial load of -277.5kN and bending moment of -16.42kNm are acting as transient loads due to live loads.

1.2 Initial stresses for the total loads:

The strain in concrete and its gradient can be formulated using Eq.(10) as given below

$$\begin{Bmatrix} -1.11E+06 \\ -6.57E+07 \end{Bmatrix} = 3.23E+04 \begin{pmatrix} 1.15E+05 & 0 \\ 0 & 1.67E+09 \end{pmatrix} \begin{Bmatrix} \varepsilon_0(t_0) \\ \psi(t_0) \end{Bmatrix}$$

The calculated strains and stresses are

$$\begin{aligned} \varepsilon_0(t_0)_{Total} &= -2.98E-04; \quad \psi(t_0)_{Total} = -1.22E-06 \\ \sigma_{ctopTotal} &= -17.50\text{MPa}; \quad \sigma_{cbotTotal} = -1.750\text{MPa}; \\ \sigma_{scminTotal} &= -80.22\text{MPa}; \quad \sigma_{scmaxTotal} = -19.73\text{MPa} \end{aligned}$$

1.3 Initial stresses for permanent loads:

The strain in concrete and its gradient can be formulated using Eq.(10) as given below

$$\begin{Bmatrix} -8.33E+05 \\ -4.93E+07 \end{Bmatrix} = 3.23E+04 \begin{pmatrix} 1.15E+05 & 0 \\ 0 & 1.67E+09 \end{pmatrix} \begin{Bmatrix} \varepsilon_0(t_0) \\ \psi(t_0) \end{Bmatrix}$$

The calculated strains and stresses are

$$\begin{aligned} \varepsilon_0(t_0)_{Perm} &= -2.24E-04; \quad \psi(t_0)_{Perm} = -9.14E-07 \\ \sigma_{ctopPerm} &= -13.13\text{MPa}; \quad \sigma_{cbotPerm} = -1.32\text{MPa}; \\ \sigma_{scminPerm} &= -60.16\text{MPa}; \quad \sigma_{scmaxPerm} = -14.80\text{MPa} \end{aligned}$$

1.4 Initial stresses for transient loads:

$$\begin{aligned} \sigma_{ctopTrans} &= \sigma_{ctopTotal} - \sigma_{ctopPerm} = -4.37\text{MPa} \\ \sigma_{cbotTrans} &= \sigma_{cbotTotal} - \sigma_{cbotPerm} = -0.43\text{MPa} \\ \sigma_{scminTrans} &= \sigma_{scminTotal} - \sigma_{scminPerm} = -20.06\text{MPa} \\ \sigma_{scmaxTrans} &= \sigma_{scmaxTotal} - \sigma_{scmaxPerm} = -4.93\text{MPa} \end{aligned}$$

1.5 Restraining stress in concrete to free creep and shrinkage strains:

$$\Delta\sigma_{cresTop} = 12.15\text{MPa}; \quad \Delta\sigma_{cresBot} = 3.71\text{MPa}$$

1.6 Equivalent forces to the restraining stress in concrete:

$$\begin{Bmatrix} \Delta P \\ \Delta M \end{Bmatrix} = \begin{Bmatrix} 5.16E+05 \\ 2.81E+07 \end{Bmatrix}_{crp} + \begin{Bmatrix} 2.77E+05 \\ 0 \end{Bmatrix}_{shr} = \begin{Bmatrix} 7.93E+05 \\ 2.81E+07 \end{Bmatrix}$$

1.7 Additional strain due to creep and shrinkage:

$$\begin{Bmatrix} 7.93E+05 \\ 2.81E+07 \end{Bmatrix} = 9.23E+03 \begin{pmatrix} 1.61E+05 & 0 \\ 0 & 2.67E+09 \end{pmatrix} \begin{Bmatrix} \Delta\varepsilon_0(t, t_0) \\ \Delta\psi(t, t_0) \end{Bmatrix}$$

$$\begin{Bmatrix} \Delta\varepsilon_0(t, t_0) \\ \Delta\psi(t, t_0) \end{Bmatrix} = \begin{Bmatrix} -5.34E-04 \\ -1.14E-06 \end{Bmatrix}$$

1.8 Additional stresses due to creep and shrinkage:

$$\Delta\sigma_{cTop} = \left(12.15 + (9.23E+03) \begin{pmatrix} -5.34E-04+ \\ (-1.14E-06)(200) \end{pmatrix} \right) = 5.11\text{MPa}$$

$$\Delta\sigma_{cBot} = \left(3.71 + (9.23E+03) \begin{pmatrix} -5.34E-04+ \\ (-1.14E-06)(-200) \end{pmatrix} \right) = 0.89\text{MPa}$$

$$\Delta\sigma_{scMin} = \left((2.00E+05 - 9.23E+03) \begin{pmatrix} -5.34E-04+ \\ (-1.14E-06)(148) \end{pmatrix} \right) = -134.10\text{MPa}$$

$$\Delta\sigma_{scMax} = \left((2.00E+05 - 9.23E+03) \begin{pmatrix} -5.34E-04+ \\ (-1.14E-06)(-148) \end{pmatrix} \right) = -69.58\text{MPa}$$

1.9 Final stresses considering creep and shrinkage:

$$\begin{Bmatrix} \sigma_{cFinalTop} \\ \sigma_{cFinalBot} \\ \sigma_{scFinalMin} \\ \sigma_{scFinalMax} \end{Bmatrix} = \begin{Bmatrix} -17.50 \\ -1.75 \\ -80.22 \\ -19.73 \end{Bmatrix} + \begin{Bmatrix} 5.11 \\ 0.89 \\ -134.10 \\ -69.58 \end{Bmatrix} = \begin{Bmatrix} -12.39 \\ -0.86 \\ -214.32 \\ -89.31 \end{Bmatrix}$$

2 Solid circular column:

An RC column having the sectional properties shown in Fig.3 is taken for demonstration of application of theoretical equations given in the previous sections to the real structural member.

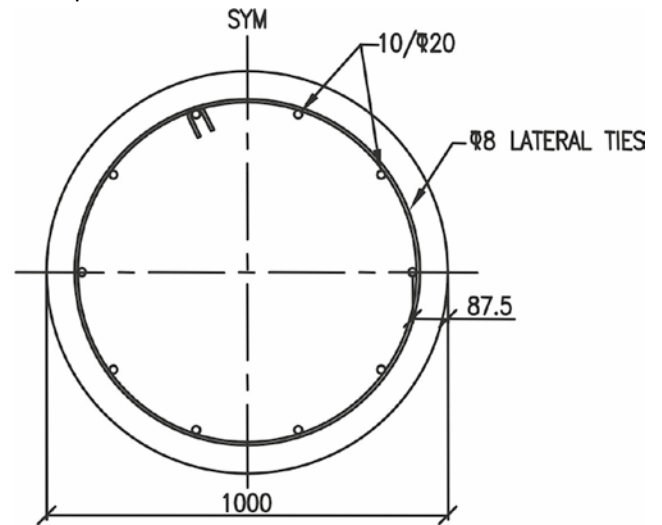


Fig. 3: Cross section of RC solid circular column

2.1 External loads acting on the column:

The column section is subjected to an external axial load of -5787kN and bending moment of -596.25kNm acting permanently due to dead and superimposed dead loads. In addition to the above, an axial load of -1929kN and bending moment of -198.75kNm are acting as transient loads due to live loads.

2.2 Initial stresses for the total loads:

The strain in concrete and its gradient can be formulated using Eq.(10) as given below

$$\begin{Bmatrix} -7.72E+06 \\ -7.95E+08 \end{Bmatrix} = 3.23E+04 \begin{pmatrix} 8.02E+05 & 0 \\ 0 & 5.05E+10 \end{pmatrix} \begin{Bmatrix} \varepsilon_0(t_0) \\ \psi(t_0) \end{Bmatrix}$$

The calculated strains and stresses are

$$\begin{aligned} \varepsilon_0(t_0)_{Total} &= -2.98E-04; \quad \psi(t_0)_{Total} = -4.88E-07 \\ \sigma_{ctopTotal} &= -17.50\text{MPa}; \quad \sigma_{cbotTotal} = -1.75\text{MPa}; \\ \sigma_{scminTotal} &= -82.03\text{MPa}; \quad \sigma_{scmaxTotal} = -17.88\text{MPa} \end{aligned}$$

2.3 Initial stresses for permanent loads:

The strain in concrete and its gradient can be formulated using Eq.(10) as given below

$$\begin{Bmatrix} -5.79E+06 \\ -5.96E+08 \end{Bmatrix} = 3.23E+04 \begin{pmatrix} 8.02E+05 & 0 \\ 0 & 5.05E+10 \end{pmatrix} \begin{Bmatrix} \varepsilon_0(t_0) \\ \psi(t_0) \end{Bmatrix}$$

The calculated strains and stresses are

$$\varepsilon_0(t_0)_{Perm} = -2.23E-04; \psi(t_0)_{Perm} = -3.66E-07$$

$$\sigma_{ctopPerm} = -13.12\text{MPa}; \sigma_{cbotPerm} = -1.31\text{MPa};$$

$$\sigma_{scminPerm} = -61.52\text{MPa}; \sigma_{scmaxPerm} = -1.31\text{MPa}$$

2.4 Initial stresses for transient loads:

$$\sigma_{ctopTrans} = \sigma_{ctopTotal} - \sigma_{ctopPerm} = -4.38\text{MPa}$$

$$\sigma_{cbotTrans} = \sigma_{cbotTotal} - \sigma_{cbotPerm} = -0.44\text{MPa}$$

$$\sigma_{scminTrans} = \sigma_{scminTotal} - \sigma_{scminPerm} = -20.51\text{MPa}$$

$$\sigma_{scmaxTrans} = \sigma_{scmaxTotal} - \sigma_{scmaxPerm} = -16.57\text{MPa}$$

2.5 Restraining stress in concrete to free creep and shrinkage strains:

$$\Delta\sigma_{resTop} = 12.14\text{MPa}; \Delta\sigma_{resBot} = 3.71\text{MPa}$$

2.6 Equivalent forces to the restraining stress in concrete:

$$\begin{Bmatrix} \Delta P \\ \Delta M \end{Bmatrix} = \begin{Bmatrix} 4.05E+06 \\ 4.14E+08 \end{Bmatrix}_{crp} + \begin{Bmatrix} 2.17E+06 \\ 0 \end{Bmatrix}_{shr} = \begin{Bmatrix} 6.22E+06 \\ 4.14E+08 \end{Bmatrix}$$

2.7 Additional strain due to creep and shrinkage:

$$\begin{Bmatrix} 6.22E+06 \\ 4.14E+08 \end{Bmatrix} = 9.23E+03 \begin{pmatrix} 8.50E+05 & 0 \\ 0 & 5.46E+10 \end{pmatrix} \begin{Bmatrix} \Delta\varepsilon_0(t, t_0) \\ \Delta\psi(t, t_0) \end{Bmatrix}$$

$$\begin{Bmatrix} \Delta\varepsilon_0(t, t_0) \\ \Delta\psi(t, t_0) \end{Bmatrix} = \begin{Bmatrix} -7.93E-04 \\ -8.22E-07 \end{Bmatrix}$$

2.8 Additional stresses due to creep and shrinkage:

$$\Delta\sigma_{cTop} = \left(12.14 + (9.23E+03) \begin{pmatrix} -7.93E-04+ \\ (-8.22E-07)(500) \end{pmatrix} \right) = 1.03\text{MPa}$$

$$\Delta\sigma_{cBot} = \left(3.71 + (9.23E+03) \begin{pmatrix} -7.93E-04+ \\ (-8.22E-07)(-500) \end{pmatrix} \right) = 0.18\text{MPa}$$

$$\Delta\sigma_{scMin} = \left((2.00E+05 - 9.23E+03) \begin{pmatrix} -7.93E-04+ \\ (-8.22E-07)(392.31) \end{pmatrix} \right) = -212.77\text{MPa}$$

$$\Delta\sigma_{scMax} = \left((2.00E+05 - 9.23E+03) \begin{pmatrix} -7.93E-04+ \\ (-8.22E-07)(-392.31) \end{pmatrix} \right) = -89.79\text{MPa}$$

2.9 Final stresses considering creep and shrinkage:

$$\begin{Bmatrix} \sigma_{cFinalTop} \\ \sigma_{cFinalBot} \\ \sigma_{scFinalMin} \\ \sigma_{scFinalMax} \end{Bmatrix} = \begin{Bmatrix} -17.50 \\ -1.75 \\ -82.03 \\ -17.88 \end{Bmatrix} + \begin{Bmatrix} 1.03 \\ 0.18 \\ -212.77 \\ -89.79 \end{Bmatrix} = \begin{Bmatrix} -16.47 \\ -1.57 \\ -294.80 \\ -107.67 \end{Bmatrix}$$

3 Hollow circular column:

An RC column having the sectional properties shown in Fig.2 is taken for demonstration of application of theoretical equations given in the previous sections to the real structural member.

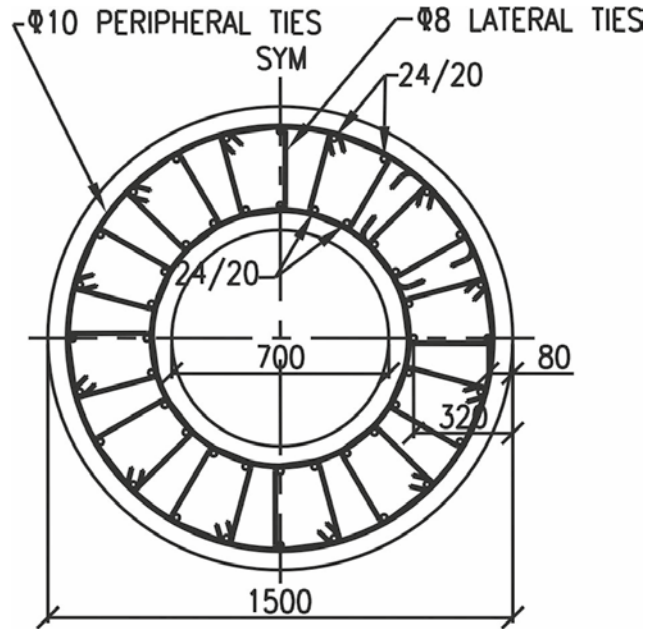


Fig. 4: Cross section of RC hollow circular column

3.1 External loads acting on the column:

The column section is subjected to an external axial load of -10543.5kN and bending moment of -1962kNm acting permanently due to dead and superimposed dead loads. In addition to the above, an axial load of -3514.5kN and bending moment of -654kNm are acting as transient loads due to live loads.

3.2 Initial stresses for the total loads:

The strain in concrete and its gradient can be formulated using Eq.(10) as given below

$$\begin{Bmatrix} -1.41E+07 \\ -2.62E+09 \end{Bmatrix} = 3.23E+04 \begin{pmatrix} 1.46E+06 & 0 \\ 0 & 2.49E+11 \end{pmatrix} \begin{Bmatrix} \varepsilon_0(t_0) \\ \psi(t_0) \end{Bmatrix}$$

The calculated strains and stresses are

$$\varepsilon_0(t_0)_{Total} = -2.98E-04; \psi(t_0)_{Total} = -3.25E-07$$

$$\sigma_{ctopTotal} = -17.50\text{MPa}; \sigma_{cbotTotal} = -1.750\text{MPa};$$

$$\sigma_{scminTotal} = -86.48\text{MPa}; \sigma_{scmaxTotal} = -13.44\text{MPa}$$

3.3 Initial stresses for permanent loads:

The strain in concrete and its gradient can be formulated using Eq.(10) as given below

$$\begin{Bmatrix} -1.05E+07 \\ -1.96E+09 \end{Bmatrix} = 3.23E+04 \begin{pmatrix} 1.46E+06 & 0 \\ 0 & 2.49E+11 \end{pmatrix} \begin{Bmatrix} \varepsilon_0(t_0) \\ \psi(t_0) \end{Bmatrix}$$

The calculated strains and stresses are

$$\begin{aligned}\varepsilon_0(t_0)_{Perm} &= -2.98E-04; \psi(t_0)_{Perm} = -3.25E-07 \\ \sigma_{ctopPerm} &= -13.13\text{MPa}; \sigma_{cbotPerm} = -1.31\text{MPa}; \\ \sigma_{scminPerm} &= -64.86\text{MPa}; \sigma_{scmaxPerm} = -10.08\text{MPa}\end{aligned}$$

3.4 Initial stresses for transient loads:

$$\begin{aligned}\sigma_{ctopTrans} &= \sigma_{ctopTotal} - \sigma_{ctopPerm} = -4.37\text{MPa} \\ \sigma_{cbotTrans} &= \sigma_{cbotTotal} - \sigma_{cbotPerm} = -0.44\text{MPa} \\ \sigma_{scminTrans} &= \sigma_{scminTotal} - \sigma_{scminPerm} = -21.62\text{MPa} \\ \sigma_{scmaxTrans} &= \sigma_{scmaxTotal} - \sigma_{scmaxPerm} = -3.36\text{MPa}\end{aligned}$$

3.5 Restraining stress in concrete to free creep and shrinkage strains:

$$\Delta\sigma_{cresTop} = 12.14\text{MPa}; \Delta\sigma_{cresBot} = 3.71\text{MPa}$$

3.6 Equivalent forces to the restraining stress in concrete:

$$\begin{Bmatrix} \Delta P \\ \Delta M \end{Bmatrix} = \begin{Bmatrix} 7.13E+06 \\ 1.33E+09 \end{Bmatrix}_{crp} + \begin{Bmatrix} 3.83E+06 \\ 0 \end{Bmatrix}_{shr} = \begin{Bmatrix} 1.10E+07 \\ 1.33E+09 \end{Bmatrix}$$

3.7 Additional strain due to creep and shrinkage:

$$\begin{Bmatrix} 1.10E+07 \\ 1.33E+09 \end{Bmatrix} = 9.23E+03 \begin{pmatrix} 1.69E+06 & 0 \\ 0 & 2.86E+11 \end{pmatrix} \begin{Bmatrix} \Delta\varepsilon_0(t, t_0) \\ \Delta\psi(t, t_0) \end{Bmatrix}$$

$$\begin{Bmatrix} \Delta\varepsilon_0(t, t_0) \\ \Delta\psi(t, t_0) \end{Bmatrix} = \begin{Bmatrix} -7.01E-04 \\ -5.04E-07 \end{Bmatrix}$$

3.8 Additional stresses due to creep and shrinkage:

$$\begin{aligned}\Delta\sigma_{cTop} &= \left(12.14 + (9.23E+03) \begin{pmatrix} -7.01E-04+ \\ (-5.04E-07)(750) \end{pmatrix} \right) = 2.19\text{MPa} \\ \Delta\sigma_{cBot} &= \left(3.71 + (9.23E+03) \begin{pmatrix} -7.01E-04+ \\ (-5.04E-07)(-750) \end{pmatrix} \right) = 0.73\text{MPa} \\ \Delta\sigma_{scMin} &= \left((2.00E+05 - 9.23E+03) \begin{pmatrix} -7.01E-04+ \\ (-5.04E-07)(670) \end{pmatrix} \right) = -198.10\text{MPa} \\ \Delta\sigma_{scMax} &= \left((2.00E+05 - 9.23E+03) \begin{pmatrix} -7.01E-04+ \\ (-5.04E-07)(-670) \end{pmatrix} \right) = -69.21\text{MPa}\end{aligned}$$

3.9 Final stresses considering creep and shrinkage:

$$\begin{Bmatrix} \sigma_{cFinalTop} \\ \sigma_{cFinalBot} \\ \sigma_{scFinalMin} \\ \sigma_{scFinalMax} \end{Bmatrix} = \begin{Bmatrix} -17.50 \\ -1.75 \\ -86.48 \\ -13.44 \end{Bmatrix} + \begin{Bmatrix} 2.19 \\ 0.73 \\ -198.10 \\ -69.21 \end{Bmatrix} = \begin{Bmatrix} -15.31 \\ -1.02 \\ -284.58 \\ -82.65 \end{Bmatrix}$$

Application of IRS Concrete Bridge Code:

In this method, the modular ratio is calculated based on the empirical relationship given this code. The effect of creep and shrinkage is partially considered in the above relationship.

15.1.1 Stress in concrete:

$$\sigma_{cTop} = \frac{P}{A_{tr}} + \frac{M}{I_{tr}}(D/2) \quad \text{Eq.(23a)}$$

$$\sigma_{cBot} = \frac{P}{A_{tr}} + \frac{M}{I_{tr}}(-D/2) \quad \text{Eq.(23b)}$$

For rectangular column,

$$\begin{aligned}A_{tr} &= bD + \left(\frac{420}{f_{ck}} - 1 \right) \sum_{i=1}^{ns} A_{si} \\ I_{tr} &= \frac{bD^3}{12} + \left(\frac{420}{f_{ck}} - 1 \right) \sum_{i=1}^{ns} A_{si} y_{si}^2\end{aligned}$$

For solid circular column,

$$\begin{aligned}A_{tr} &= \frac{\pi D^2}{4} + \left(\frac{420}{f_{ck}} - 1 \right) \sum_{i=1}^{ns} A_{si} \\ I_{tr} &= \frac{\pi D^4}{64} + \left(\frac{420}{f_{ck}} - 1 \right) \sum_{i=1}^{ns} A_{si} y_{si}^2\end{aligned}$$

For hollow circular column,

$$\begin{aligned}A_{tr} &= \pi(a^2 - a_1^2) + \left(\frac{420}{f_{ck}} - 1 \right) \left(\sum_{i=1}^{ons} A_{osi} + \sum_{i=1}^{ins} A_{isi} \right) \\ I_{tr} &= \frac{\pi}{4}(a^4 - a_1^4) + \left(\frac{420}{f_{ck}} - 1 \right) \left(\sum_{i=1}^{ons} A_{osi} y_{osi}^2 + \sum_{i=1}^{ins} A_{isi} y_{isi}^2 \right)\end{aligned}$$

1.1 Stress in reinforcement bars:

$$\sigma_{sc} = \left(\frac{420}{f_{ck}} \right) \left\{ \sigma_{cTop} - \frac{(\sigma_{cTop} - \sigma_{cBot})}{D} \left(\frac{D}{2} - y_{si} \right) \right\} \quad \dots\text{Eq.(24)}$$

Numerical Example for Cracked Hollow Circular Column Section Using IRS Concrete Bridge Code:

The example problems which is considered in section 1 and details of column shown in Fig.2, Fig.3 & Fig.4 for the analysis of stresses for rectangular, circular and hollow circular columns as per IRC:112-2011 are now also used for the calculation of stresses in concrete and reinforcement bars as per IRS concrete bridge code for the purpose of comparison of results. These results can be used for checking the correctness of manual calculation or computer programmes which can be made using the procedures mentioned in this paper.

1 Rectangular Column

The external loads acting on the column are the same loads given under section 14.1.1

1.1 Stresses for the total loads:

The stresses in concrete and reinforcement

steel bars can be calculated using Eq.(23) and Eq.(24). The calculated values are given below.

$$\sigma_{ctopTotal} = -14.58 \text{MPa}; \sigma_{cbotTotal} = -1.95 \text{MPa};$$

$$\sigma_{scminTotal} = -144.56 \text{MPa}; \sigma_{scmaxTotal} = -39.88 \text{MPa}$$

1.2 Stresses for the permanent loads:

The stresses due to permanent loads alone are

$$\sigma_{ctopPerm} = -11.1 \text{MPa}; \sigma_{cbotPerm} = -1.47 \text{MPa};$$

$$\sigma_{scminPerm} = -108.42 \text{MPa}; \sigma_{scmaxPerm} = -29.91 \text{MPa}$$

1.3 Stresses due to transient loads:

The difference between the stresses due to total loads and the permanent loads are equal to the stresses caused by the transient loads. The values of the stresses due to transient loads are

$$\sigma_{ctopTrans} = -3.70 \text{MPa}; \sigma_{cbotTrans} = -0.49 \text{MPa};$$

$$\sigma_{scminTrans} = -36.14 \text{MPa}; \sigma_{scmaxTrans} = -9.97 \text{MPa}$$

2 Solid circular column

The external loads acting on the column are the same loads given under section 14.2.1

2.1 Stresses for the total loads:

The stresses in concrete and reinforcement steel bars can be calculated using Eq.(23) and Eq.(24). The calculated values are given below.

$$\sigma_{ctopTotal} = -17.05 \text{MPa}; \sigma_{cbotTotal} = -1.77 \text{MPa};$$

$$\sigma_{scminTotal} = -169.45 \text{MPa}; \sigma_{scmaxTotal} = -37.57 \text{MPa}$$

2.2 Stresses for the permanent loads:

The stresses due to permanent loads alone are

$$\sigma_{ctopPerm} = -12.78 \text{MPa}; \sigma_{cbotPerm} = -1.33 \text{MPa};$$

$$\sigma_{scminPerm} = -127.09 \text{MPa}; \sigma_{scmaxPerm} = -28.18 \text{MPa}$$

2.3 Stresses due to transient loads:

The difference between the stresses due to total loads and the permanent loads are equal to the stresses caused by the transient loads. The values of the stresses due to transient loads are

$$\sigma_{ctopTrans} = -4.26 \text{MPa}; \sigma_{cbotTrans} = -0.44 \text{MPa};$$

$$\sigma_{scminTrans} = -42.36 \text{MPa}; \sigma_{scmaxTrans} = -9.39 \text{MPa}$$

3 Hollow circular column

The external loads acting on the column are the same loads given under section 14.3.1

3.1 Stresses for the total loads:

The stresses in concrete and reinforcement steel bars can be calculated using Eq.(23) and Eq.(24). The calculated values are given below.

$$\sigma_{ctopTotal} = -16.54 \text{MPa}; \sigma_{cbotTotal} = -1.62 \text{MPa};$$

$$\sigma_{scminTotal} = -142.81 \text{MPa}; \sigma_{scmaxTotal} = -56.96 \text{MPa}$$

3.2 Stresses for the permanent loads:

The stresses due to permanent loads alone are

$$\sigma_{ctopPerm} = -12.78 \text{MPa}; \sigma_{cbotPerm} = -1.33 \text{MPa};$$

$$\sigma_{scminPerm} = -127.09 \text{MPa}; \sigma_{scmaxPerm} = -42.72 \text{MPa}$$

3.3 Stresses due to transient loads:

The difference between the stresses due to total loads and the permanent loads are equal to the stresses caused by the transient loads. The values of the stresses due to transient loads are

$$\sigma_{ctopTrans} = -4.14 \text{MPa}; \sigma_{cbotTrans} = -0.41 \text{MPa};$$

$$\sigma_{scminTrans} = -35.70 \text{MPa}; \sigma_{scmaxTrans} = -14.24 \text{MPa}$$

Comparison of Results and Discussion:

The calculated maximum and minimum bending stresses in concrete and reinforcement steel bars using the Road and Railway Bridge Codes are tabulated in tables 1-3 given below. The ratio of stresses obtained from IRS concrete bridge code to the corresponding stresses obtained by IRC:112-2011 are given in column 4 of the above tables.

Rectangular column:

Table -1 Comparisons of stresses for rectangular column

Stress (1)	IRC:112-2011 (MPa) (2)	IRS concrete bridge code (MPa) (3)	Ratio of stresses (4) = (3)/(2)
Total loads at initial loading stage			
σ_c	-17.50	-14.58	0.83
σ_{sc}	-80.22	-144.56	1.80
Permanent loads at initial loading stage			
σ_c	-13.13	-11.11	0.85
σ_{sc}	-60.16	-108.42	1.80
Transient loads at all loading stages			
σ_c	-4.37	-3.70	0.85
σ_{sc}	-20.06	-36.14	1.80
Creep and shrinkage or time dep. stresses			
$\Delta\sigma_c$	5.11	-	-
$\Delta\sigma_{sc}$	-134.10	-	-
Total stresses + time dependent stresses			
σ_c	-12.39	-14.58	1.18
σ_{sc}	-294.80	-144.56	0.49

From the ratios of stresses calculated for rectangular column given in the above table, it can be seen that the IRS concrete bridge code underestimates the stress in concrete by 5% at the initial stage of loading and over estimates the stress in concrete by 18% after a long period of time. The stresses in compression reinforcement steel bars are overestimated by 78% by the railway bridge code at initial stage of loading. But, the long term stresses in the above reinforcement bars are under estimated by 33% by the IRS concrete bridge code.

Solid circular column:

From the above ratio, it can be seen that the IRS concrete bridge code underestimates the stress in concrete by 3% at the initial stage of loading and over estimates the stress in concrete by 4% after a long period of time. The stresses in compression reinforcement steel bars are overestimated by 107% by the railway bridge code at initial stage of loading. But, the long term stresses in the above reinforcement bars are under estimated by 43% by the IRS concrete bridge code.

Table -2 Comparisons of stresses for solid circular column

Stress (1)	IRC:112-2011 (MPa) (2)	IRS concrete bridge code (MPa) (3)	Ratio of stresses (4) = (3)/(2)
Total loads at initial loading stage			
σ_c	-17.50	-17.05	0.97
σ_{sc}	-82.03	-169.45	2.07
Permanent loads at initial loading stage			
σ_c	-13.12	-12.78	0.97
σ_{sc}	-61.52	-127.09	2.07
Transient loads at all loading stages			
σ_c	-4.38	-4.26	0.97
σ_{sc}	-20.51	-42.36	2.07
Creep and shrinkage or time dep. stresses			
$\Delta\sigma_c$	1.03	-	-
$\Delta\sigma_{sc}$	-212.77	-	-
Total stresses + time dependent stresses			
σ_c	-16.47	-17.05	1.04
σ_{sc}	-294.80	-169.45	0.57

Hollow circular column:

From the above ratio, it can be seen that the IRS concrete bridge code underestimates the stress in concrete by 10% at the initial stage of

loading and over estimates the stress in concrete by 3% after a long period of time. The stresses in compression reinforcement steel bars are overestimated by 73% by the railway bridge code at initial stage of loading. But, the long term stresses in the above reinforcement bars are under estimated by 48% by the IRS concrete bridge code.

Table -3 Comparisons of stresses for hollow circular column

Stress (1)	IRC:112-2011 (MPa) (2)	IRS concrete bridge code (MPa) (3)	Ratio of stresses (4) = (3)/(2)
Total loads at initial loading stage			
σ_c	-17.50	-15.75	0.90
σ_{sc}	-86.48	-149.22	1.73
Permanent loads at initial loading stage			
σ_c	-13.13	-11.81	0.90
σ_{sc}	-64.86	-111.91	1.73
Transient loads at all loading stages			
σ_c	-4.37	-3.94	0.90
σ_{sc}	-21.62	-37.31	1.73
Creep and shrinkage or time dep. stresses			
$\Delta\sigma_c$	2.19	-	-
$\Delta\sigma_{sc}$	-198.10	-	-
Total stresses + time dependent stresses			
σ_c	-15.31	-15.76	1.03
σ_{sc}	-284.58	-149.22	0.52

Scope for the Future Work:

Most of the non-circular columns used in bridges are subjected to axial load bi-axial moment. Hence, a separate study for the evaluation of stresses in concrete and reinforcement bars for the columns under the action of axial load and bi-axial bending is inevitable. Apart from the columns, the reinforced beams are also subjected to compressive stresses which in turn are affected by creep and shrinkage. The extent of changes in stresses in concrete and reinforcement bars need to be addressed in future.

Conclusions:

The following conclusions are made from the above study for the time dependent stresses in RC uncracked rectangular, solid and hollow circular columns by comparison of predictions of IRS concrete bridge code with IRC:112-2011.

- 1) The bending compressive stresses in concrete for the un-cracked RC columns of rectangular,

solid and hollow circular sections are slightly under estimated at the initial loading time ie., before creep and shrinkage strains are developed in concrete by the IRS concrete bridge code.

- 2) On the other hand, the bending compressive stresses in concrete for the above columns are marginally over estimated after a prolonged period of time ie., after creep and shrinkage strains are developed in concrete by the concrete bridge code of railways.
- 3) The compressive stresses in reinforcement steel bars in the RC hollow circular columns are over estimated by nearly 70% to 100% at the time of initial loading when the calculations are made using IRS concrete bridge code.
- 4) On contrary to the above, the compressive stresses in reinforcement steel bars in the above columns are under estimated by about 40% to 50% after a long period of time when IRS concrete bridge code is used for the prediction of stresses.
- 5) Due to large variations in stresses in concrete and reinforcement steel bars, it is required to reconsider the provisions of empirically based formula for considering the long term effect in IRS concrete bridge code.

Notations:

- A_c = Area of concrete section in compression zone alone.
- A_s = Cross sectional area of reinforcement steel bars.
- A_{osi} , & A_{isi} = Cross sectional area of *i*th reinforcement steel bars in outer and inner core respectively.
- $A_{tr} = A_c + \alpha A_s$ = Transformed area of column section.
- $\bar{A}_{tr} = \bar{A}_c + \bar{\alpha} A_s$ = Effective transformed area of column section.
- $a = D / 2$ = Outer radius of RC hollow circular column.
- $a_i = ID / 2$ = Inner radius of RC hollow circular column.
- B_c = First moment of area of concrete section in compression zone alone.
- B_{tr} = First moment of transformed area of column section.
- \bar{B}_{tr} = Effective first moment of transformed area of column section.
- D = Outer diameter of RC hollow circular column.
- ID = Inner diameter of RC hollow circular column.
- $E_c(t_0) = E_c$ = Elastic modulus of concrete at

initial loading time

$$\bar{E}_c(t, t_0) = \bar{E}_c = \frac{E_c}{[1 + \varphi(t, t_0)]} = \text{Effective modulus of}$$

concrete at time, *t*

E_s = Elastic modulus of reinforcement steel bars.

f_{ck} = Characteristic compressive strength of concrete.

I_c = Second moment of area of concrete section in compression zone alone.

I_{tr} = Second moment of transformed area of column section.

\bar{I}_{tr} = Effective second moment of transformed area of column section.

M = External uniaxial bending moment acting on the axis through the mid-depth of column.

M_x , and M_y = Uniaxial bending moment acting about X-axis and Y-axis respectively.

M_r = Resultant bending moment

$M_c, M_{c1}, \& M_{c2}$ = Bending resistance force offered by concrete alone.

M_s = Bending resistance offered by steel rebars.

M_{sc} = Bending resisting force offered by reinforcement steel in compression zone.

M_{st} = Bending resisting force offered by reinforcement steel in tensile zone.

ons , & ins = Number of reinforcement steel bars in outer and inner core respectively.

P = External axial load acting on column.

$P_c, P_{c1}, \& P_{c2}$ = Axial resisting force offered by concrete alone.

P_s = Axial resisting force offered by steel rebars.

P_{sc} = Axial resisting force offered by reinforcement steel in compression zone.

P_{st} = Axial resisting force offered by reinforcement steel in tensile zone.

t = Time elapsed after Initial loading.

t_0 = Initial loading time.

y = Distance of a point under consideration from the reference axis

y_n = Depth of neutral axis from the reference axis.

y_{si} = Distance *i*th reinforcement steel bar from the reference axis.

$\alpha = \frac{E_s}{E_c}$ = Elastic modular ratio for concrete

$\bar{\alpha} = \frac{E_s}{E_c}$ = Effective modular ratio for steel reinforcement bars at time, *t*

ε = Strain at any point under consideration.

ε_{cs} = Shrinkage strain at time, *t*.

$\varepsilon_0(t_0) = \varepsilon_0$ = Strain at the level of reference axis at initial loading time.

$\varepsilon_0(t_0)_{Total}$, and $\varepsilon_0(t_0)_{Perm}$ = Strain at the level of reference axis at initial loading time due to total loads and permanent loads respectively.

ε_{crp} = Creep strain at time, *t*.

$-\Delta M = -(\Delta M_{crp} + \Delta M_{shr})$ = Sum of the restraining bending moments to the creep and shrinkage acting in reverse direction at the reference point.

ΔM_{crp} , and ΔM_{shr} = Restraining bending moment to the creep and shrinkage respectively acting at the reference point.

$-\Delta P = -(\Delta P_{crp} + \Delta P_{shr})$ = Sum of the restraining normal forces to the creep and shrinkage acting in reverse direction at the reference point.

ΔP_{crp} , and ΔP_{shr} = Restraining normal force to the creep and shrinkage respectively acting at the reference point.

$\Delta \varepsilon_0(t, t_0)$ = Additional strain at the level of reference axis at time, *t*

$\Delta \sigma_c$ = Change in stress in concrete due to the creep and shrinkage.

$\Delta \sigma_{sc}$ = Change in controlling stress in compression reinforcement steel bars due to the creep and shrinkage.

$\Delta \sigma_{st}$ = Change in controlling stress in tensile reinforcement steel bars due to the creep and shrinkage.

$\Delta \sigma_{res}$ = Restraining stress in concrete to the creep and shrinkage.

$\Delta \psi(t, t_0)$ = Additional curvature at the level of

reference axis at time, *t*

$\varphi(t, t_0) = \varphi = \frac{\varepsilon_e + \varepsilon_{crp}}{\varepsilon_e}$ = Creep coefficient.

σ_c = Compressive stress at the level of reference axis.

σ_{sc} = Controlling compressive stress in reinforcement steel bars.

σ_{st} = Controlling tensile stress in reinforcement steel bars.

σ_{cTotal} , σ_{cPerm} , and σ_{cTrans} = Stress at the level of reference axis at initial loading time due to total loads, permanent loads and transient loads respectively.

$\sigma_{scTotal}$, σ_{scPerm} , and $\sigma_{scTrans}$ = Controlling stress in compression steel reinforcement bar at initial loading time due to total loads, permanent loads and transient loads respectively.

$\sigma_{stTotal}$, σ_{stPerm} , and $\sigma_{stTrans}$ = Controlling stress in tensile steel reinforcement bar at initial loading time due to total loads, permanent loads and transient loads respectively.

$\psi(t_0) = \psi$ = Strain gradient or curvature at the level of reference axis at initial loading time

12 References:

1. Indian Railways Standard code of Practice for Plain, Reinforced, and Prestressed Concrete for General Bridge Construction, Second Revision, Research Design & Standards Organisation, Lucknow, 1997
2. IRC:112-2011 Code of Practice for Concrete Road Bridges. Indian Road Congress, New Delhi
3. Ghali, A., Favre, R., and Elbadry, M., Concrete Structures-Stresses and Deformations Third edition. E & FN Spon, London and New York, 2002
4. Sundaresan, R., Time Dependent Stresses in Reinforced Concrete Rectangular Columns – A Review of Indian Bridge Codes, IRICEN Journal of Civil Engineering, Vol. 11, Dec. 2018
5. Sundaresan, R., Time Dependent Stresses in Reinforced Concrete Circular Columns from the view of Indian Bridge Code, IRICEN Journal of Civil Engineering, Vol. 12, June & Sept. 2019
6. Sundaresan, R., Effect of Creep and Shrinkage in Reinforced Concrete Hollow Circular Columns in the light of Indian Bridge Codes, Vol.13, Sept. 2020

Studies on Design Charts for RC Flexural Members of Railway Bridges

By
Dr. Amaravel. R¹

ABSTRACT

In this paper provisions for design of RC tension members pertaining to the bridges as per IRS concrete bridge code and bridge rule are discussed. The design parameters and procedures are reviewed. The reinforcement percentages for certain grades of steel and grade of concrete are studied for deducing the moment of resistance of slab. RC design calculation procedures with relevant codal provisions are described. The moment of resistance of the slab for the bridges with different grades of concrete and varying depth are also evaluated and tabulated. It is easy to design the RC bending tension members of various bridges i.e. RC slabs, RC T-Beam decks, RC box culverts, RC pipe culverts, RC piers and abutments, RC pile caps and piles, RC approach slabs and RC wing and return walls. The minimum percentage of steel and actual steel of particular span under some loading standard are detailed with model design example. The provisions in IRS concrete bridge code, 2014 IRC 112-2011 and IS:456-2000 are discussed.

RC members Slabs and Beams

❖ Effective Span of RC members

For RC slabs and beams, the effective span is minimum of following cases: For simply supported spans,

- 1 The distance between centres of bearings.
- 2 The distance between centres of supports
- 3 The clear span plus the effective depth.

For the framed structures, the distance between shear centres of the supporting members is the effective span. In the case of continuous members, the effective span is the distance between centres of supports. For the beams resting on wider columns the effect of column width is included in the analysis. For the cantilever beams, the effective span shall be as its length from the face of the support plus half its effective depth. If the cantilever is an extension of a continuous beam, then the effective span is the length to the centre of the support shall be used.

❖ Effective Width of Flanged Beams

Full width of flange shall be considered as effective width for analysing the structures. For analysing the cross sections under serviceability limit state, the width of the web plus one-tenth of the distance between the points of zero moment (or the actual width of the outstand if this is less) on each side of the web is the effective width. The points of zero moment at a distance of 0.15 times the effective span from the support shall be considered in the case of continuous RC

members. The full width of the flanges shall be used as effective width of flange while analysing sections at the ultimate limit state.

❖ Slenderness Limits for Beams

Simply supported or continuous RC members which are so proportioned that the clear distance between lateral restraints shall be below the value $60b_c$ or $\frac{(100(b_c)^2)}{d}$ whichever the minimum is. In the above formulae, d is the effective depth to tension reinforcement and b_c is the breadth of the compression face of the beam midway between restraints.

The cantilever RC members with lateral restraint provided only at the support are proportioned such that the clear distance from the end of the cantilever to the face of the support shall not exceed $25b_c$ or $\frac{(100(b_c)^2)}{d}$ whichever is lesser.

❖ Moment Resistance of Beams

Analysis of Sections

Assumptions made for analysing a cross section to determine its ultimate moment of resistance are detailed below.

- (i) The plane sections remain plane. Using this assumption, the strain distribution in the concrete in compression and the strains in the reinforcement, whether in tension or compression, are evaluated.
- (ii) The strain at the outermost compression fibre at failure is taken as 0.0035. The compressive strength shall be presumed as equal to $0.4 f_{ck}$

¹ SSE/Designs/CN/BNC, S.W. Railway

over the whole compression zone while assessing the stresses in the concrete in compression from the stress-strain curve shown in the Fig. 4A of IRS concrete bridge code, 2014, with $Y_m=1.5$. or, in the case of rectangular sections and in flanged, ribbed and voided sections where the neutral axis lies within the flange.

- (iii) The tensile strength of the concrete is neglected.
- (iv) Using stress-strain curves in Fig. 4B of IRS concrete bridge code with $Y_m=1.15$, the stresses in the reinforcement are derived. And also, if the ultimate moment of resistance, arrived with this clause, is not greater than 1.15 times the required value, the designed section shall be proportioned such that the strain at the centroid of the tensile reinforcement is greater than:

$$\left(0.002 + \frac{f_y}{(E_s Y_m)}\right) \quad \text{--- Equation A}$$

where, E_s is the modulus of elasticity of the steel.

- v) The calculated strain due to the application of ultimate loads at the outermost compression fibre of the concrete shall be less than 0.0035 and the strain at the centroid of the tensile reinforcement

shall be greater than $\left(0.002 + \frac{f_y}{(E_s Y_m)}\right)$ except where the requirement for the calculated strain in the concrete, due to the application of 1.15 times the ultimate loads, can be satisfied.

- vi) While analysing of a cross section of a RC member, the RC member has to resist a small axial thrust. The effect of the ultimate axial force may be neglected, when the axial force is less than $0.1f_{ck}$ times the cross-sectional area.

Design Formulae

The ultimate moment of resistance of a solid slab or rectangular beam, or of a flanged beam, ribbed slab or voided slab when the neutral axis lies within the flange are determined if the amount of redistribution of the elastic ultimate moments has been not greater than 10%. The flexural equations is indicated as given below.

$$M_u = (0.87 \times f_y) \times A_s \times z \quad \text{(equation 1)}$$

$$z = \left[1 - \frac{1.1f_y A_s}{f_{ck} b d}\right] d \quad \text{Step 1}$$

$$\frac{M_u}{b d^2} = [0.87 \times f_y] \times \left[\frac{P_t}{100}\right] - \left[\frac{0.87 \times f_y \times 1.1 \times f_y}{f_{ck}}\right] \times \left[\frac{P_t}{100}\right]^2 \quad \text{Step 2}$$

$$\frac{M_u}{b d^2} = [0.87 \times f_y] \times \left[\frac{P_t}{100}\right] - \left[\frac{0.87 \times f_y \times 1.1 \times f_y}{f_{ck}}\right] \times \left[\frac{P_t}{100}\right]^2 \quad \text{Step 3}$$

$$\left[\frac{0.87 \times f_y \times 1.1 \times f_y}{f_{ck}}\right] \times \left[\frac{P_t}{100}\right]^2 + [0.87 \times f_y] \times \left[\frac{P_t}{100}\right] - \frac{M_u}{b d^2} = 0 \quad \text{Step 4}$$

$$\left[\frac{0.87 \times f_y \times 1.1 \times f_y}{f_{ck}}\right] \times \left[\frac{P_t}{100}\right]^2 + [0.87 \times f_y] \times \left[\frac{P_t}{100}\right] = \frac{M_u}{b d^2} \quad \text{Step 5}$$

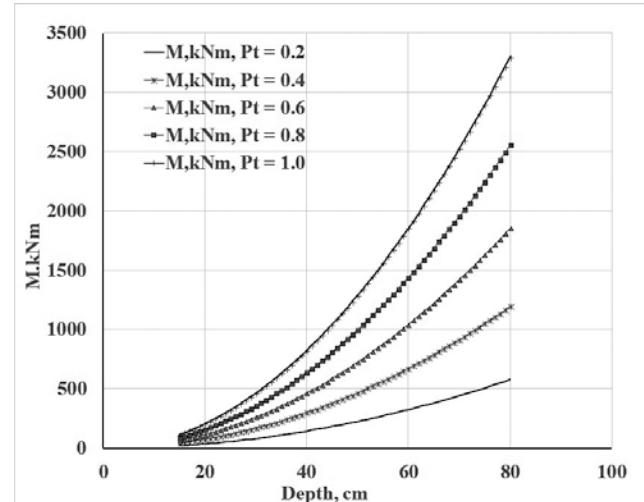
$$K_1 = \left[\frac{0.87 \times f_y \times 1.1 \times f_y}{f_{ck} \times 100000}\right] = 0.80$$

Step 6

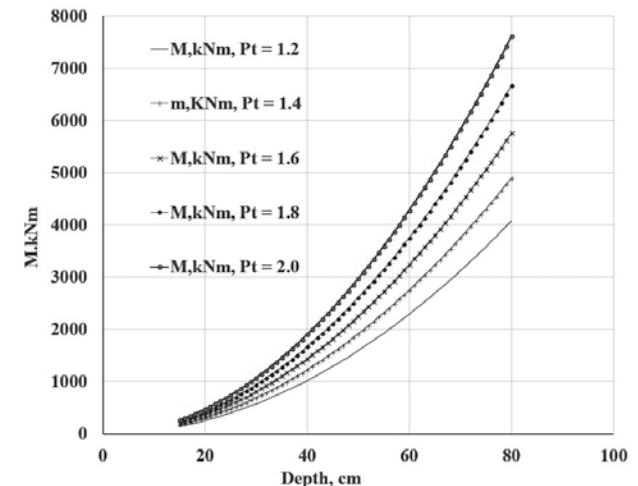
$$K_2 = \left[\frac{0.87}{100} \times f_y\right] = 4.35$$

Step 7

The Fig. 1 furnishes the moment of resistance of slab in kNm per m width for the depth of sections varying from 15 cm to 80 cm to the percentage of reinforcement (P_t) ranging from 0.2% to 2.0% for a beam with M30 and Fe500. These charts are developed for the parameters considered in the equation.no.1 cited above.



a. Moment of Resistance of slab per m width for P_t equal to 0.2,0.4,0.6,0.8 & 1.0.



b. Moment of Resistance of slab per m width for P_t equal to 1.2,1.4,1.6,1.8 & 2.0

Fig. 1 : Moment of Resistance of slab for P_t varying from 0.2 to 2.0 for RC slab with M30 and Fe500

$$M_u = (0.15f_{ck})bd^2 \quad \text{(equation 2)}$$

The ultimate moment of resistance may be considered as the lesser of the values obtained from the above equations 1 and 2 for sections without compression reinforcement. The moment

of resistance of slab for a width of 1000mm and various grades of concrete are arrived based on equation no.2 and furnished in Table 1 shown below. The moment of resistance from the Table 1 is limiting moment of resistance for a slab. If the moment of resistance exceeds this for any section, the slab section becomes over reinforced.

Table 1. Moment of resistance of slab, kNm. (for 1m width)

Depth of section, cm	Grades of concrete, N/mm ²					
	M15	M20	M25	M30	M35	M40
15	50.63	67.50	84.38	101.25	118.13	135.00
20	90.00	120.00	150.00	180.00	210.00	240.00
25	140.63	187.50	234.38	281.25	328.13	375.00
30	202.50	270.00	337.50	405.00	472.50	540.00
35	275.63	367.50	459.38	551.25	643.13	735.00
40	360.00	480.00	600.00	720.00	840.00	960.00
45	455.63	607.50	759.38	911.25	1063.13	1215.00
50	562.50	750.00	937.50	1125.00	1312.50	1500.00
55	680.63	907.50	1134.38	1361.25	1588.13	1815.00
60	810.00	1080.00	1350.00	1620.00	1890.00	2160.00
65	950.63	1267.50	1584.38	1901.25	2218.13	2535.00
70	1102.50	1470.00	1837.50	2205.00	2572.50	2940.00
75	1265.63	1687.50	2109.38	2531.25	2953.13	3375.00
80	1440.00	1920.00	2400.00	2880.00	3360.00	3840.00

Using the equations 3 & 4, the ultimate moment of resistance is arrived for sections with compression reinforcement under the assumptions that a rectangular stress block is of maximum depth $0.5d$ and a uniform compression stress is of $0.4f_{ck}$.

$$M_u = (0.15f_{ck})bd^2 + 0.72f_y A_s (d-d') \quad (\text{equation 3})$$

$$(0.87f_y) A_s = 0.2f_{ck} bd + 0.72f_y A_s \quad (\text{equation 4})$$

where,

M_u is the ultimate resistance moment;

A_s is the area of tension reinforcement;

A_s' is the area of compression reinforcement;

b is the width of the section;

d is the effective depth to the tension reinforcement;

d' is the depth to the compression reinforcement;

f_y is the characteristic strength of the reinforcement;

z is the lever arm; and;

f_{ck} is the characteristic strength of the concrete.

$\frac{d'}{d}$

For the values of $\frac{d'}{d}$ is greater than 0.2, equation 3 should not be used and the resistance moment shall be calculated as per the clause 1.4.1. The lever arm, z , in equation 1 may be calculated from the equation:

$$z = \left(1 - \frac{1.1f_y A_s}{f_{ck} b d}\right) d \quad (\text{equation 5})$$

The value z shall be normal taken as less than $0.95d$. The equations for sections other than rectangular sections.

$$M_u = (0.87f_y) A_s \left(d - \frac{h_f}{2}\right) \quad (\text{equation 6})$$

$$M_u = (0.4f_{ck}) b h_f \left(d - \frac{h_f}{2}\right) \quad (\text{equation 7})$$

The ultimate resistance moment of a flanged beam may be considered as the lesser of the values given by equations 6 & 7 where h_f is the thickness of the flange when the moment of resistance is to exceed the value given by equation.7, the section shall be analysed in accordance with 1.4.1.

Shear Strength of Beams

❖ Shear Stress

The shear stress, v , at any cross section is arrived from: -

$$v = \frac{V}{bd} \dots \dots \dots (\text{equation.8})$$

where,

V is the shear force due to ultimate loads.

b is the breadth of the section which, for a flanged beam, shall be taken as the rib width;

d is the effective depth to tension reinforcement.

In all the cases, the value of v shall not exceed $0.75\sqrt{f_{ck}}$ or 4.75 N/mm^2 whichever is the minimum, for the shear reinforcement provided in any form.

❖ Shear Reinforcement

Shear reinforcement shall be adopted as indicated in IRS concrete bridge code 2014. v_c is established from the following relationship:

$$v_c = \frac{0.27}{Y_m} \left\{ \frac{100A_s}{b_w d} \right\}^{\frac{1}{3}} \{f_{ck}\}^{\frac{1}{3}}$$

Only 50% of the shear force $(v+0.4-SV_c)bd$ shall be resisted by bent-up bars, on the occasion of stirrups combined with bent up bars for using as shear reinforcement. These bars shall be presumed to establish the tension members of one or more single systems of lattice girders in which the concrete creates the compression members.

The maximum permissible shear stress in any bar shall be taken as $0.87f_y$. The shear strength at any vertical section shall be taken as the sum of the vertical components of the tension and compression forces cut by section. Bars shall be checked for anchorage.

The value of A_s indicated in IRS concrete bridge

code is the area of longitudinal reinforcement which extends at a minimum distance equal to the effective depth beyond the section under consideration. At supports where the full area of tension reinforcement (A_s) may be adopted, provided the recommendations of 15.9.7 (IRS concrete bridge code) on Curtailment and anchorage of reinforcement are met. The area of A_s adopted in tension zone under the loading which induces the shear force is to be considered, when an RC member is provided with both top and bottom reinforcement. In the tension zone, the area of longitudinal reinforcement shall be equal to A_s .

$A_s \geq \frac{V}{(z(0.87f_y))}$ where, A_s is the area of effectively anchored longitudinal tension reinforcement (see 15.9.7);

f_y is the characteristic strength of the reinforcement; V is the shear force due to ultimate loads at the point of section considered.

- ❖ The spacing of the legs of stirrups/links.

In the spanning/barrel length direction shall be less than minimum of $0.75d$ and 450 mm. From the face of a support, front edge of a rigid bearing or centre line of a flexible bearing enhanced shear strength of sections close to supports for sections within a distance $\alpha_v < 2d$ are permitted to provide. Increase in the allowable shear stress SV_C to $\frac{SV_C \times 2d}{\alpha_v}$ due to this shear reinforcement enhancement shall be such that it shall be less than minimum of $0.75\sqrt{f_{ck}}$ or 4.75 N/mm². Anchorage equivalent to 20 times the diameter of bar is provided to the main reinforcement which continues to the support beyond the section where the enhancement of shear reinforcement is adopted. The value of s is as given below.

$$s = \left(\frac{500}{d}\right)^{0.25} \text{ or } 0.70, \text{ whichever is the greater.}$$

- ❖ Beams subjected to vertical loads at bottom near supports.

Suitable and sufficient vertical reinforcement to resist the vertical load applied at bottom near supports shall be provided in addition to any reinforcement required to resist shear.

Common Features of Torsional Reinforcements

Railway bridges are subjected to eccentric moment in transverse direction due to misalignment of track and other unsymmetrical actions. This increases the actual bending moment and shear to certain extent. The size of members is decided by the BM and SF due to main loads only not by the effect of torsion. Torsional moment may occur due to eccentric

loads/ geometry of sections with respect to sub and super structures. Additional torsional reinforcement in excess of the flexural and shear reinforcement are provided to cater for the effect of torsion.

Rectangular closed stirrups are used as torsional reinforcements along with longitudinal reinforcement as per the clause 15.9.6.4 of IRS Concrete Bridge Code.

The concept for calculation of torsional reinforcement considered is that the shear stresses induced due to torsion are combated by the longitudinal and transverse forces in thin walled tube analogues to rectangular closed rings.

Torsional Stresses and Reinforcement-

The concept of plastic stress distribution is utilized to arrive the torsional shear stress when the shear stresses in a section is increased considerably by the torsion.

The torsional reinforcement is to be provided, if the torsional shear stress, v_t , exceeds the value $v_{t(min)}$ from Table 17 of IRS concrete bridge code 2014. The sum of the shear stresses caused from shear force and torsion ($v+v_t$) should not exceed the value of the ultimate shear stress, v_{tu} from IRS concrete bridge code.

And in the case of small section ($y_1 < 550$ mm), the torsional shear, v_t shall not exceed, $\left(\frac{v_{tu} \times y_1}{550}\right)$ where y_1 is the larger centreline dimension of a stirrup/link. The Fig. 2 shows the details of V_{us}/d in kN/cm for various spacing to 8, 10 mm and 12 mm bars of Fe 415 and Fe500. Fig. 3 shows the details of V_{us}/d in kN/cm for various spacing to 8, 10 mm and 12 mm bars of $F_e 550$ and $F_e 600$.

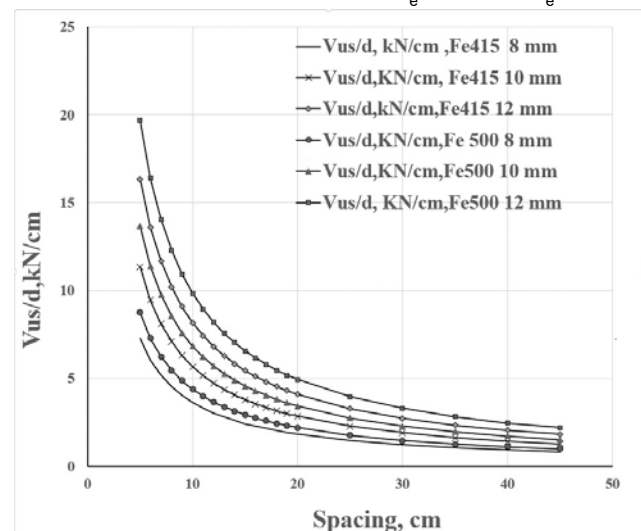


Fig. 2 : V_{us}/d , kN/cm vs. Spacing for 8, 10 mm and 12 mm bars of $F_e 415$ and $F_e 500$.

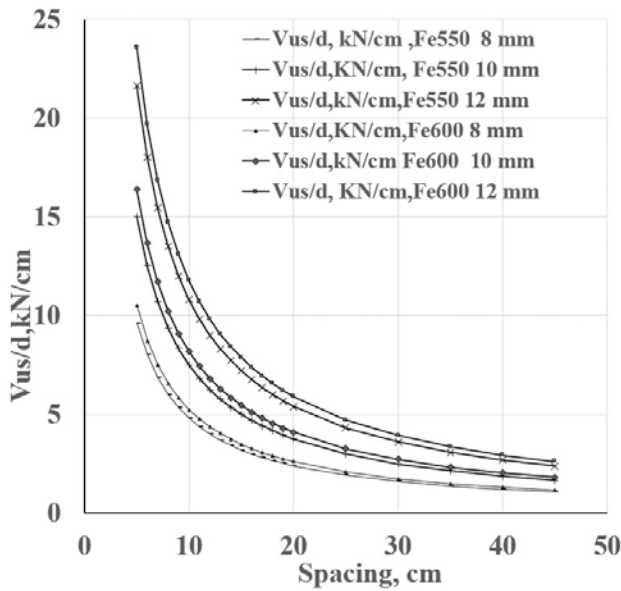


Fig. 3 : V_{us}/d , kN/cm vs. Spacing for 8, 10 mm and 12 mm bars of F_{e550} and F_{e600}

Illustrated Design Example with the use of Charts

❖ **Input Data for RC slab subjected to torsion**

Square span	= 1.800 m
Cushion due to ballast	= 0.400 m
Cushion due to earth fill	= 0.000 m
Total cushion	= 0.400 m
RCC Slab thickness	= 0.375 m
Depth of construction	= 0.775 m
Chamfer at the edge of bearing	= 0.000 m
Length of bearing	= 0.300 m
Total Bearing	= 0.300 m
Effective span	= 2.100 m
Dispersion width	= 4.195 m
Centre to center of track	= 5.800 m
Actual width of slab	= 5.800 m
Actual dispersion width	= 4.195 m
Overall square span	= 2.400 m

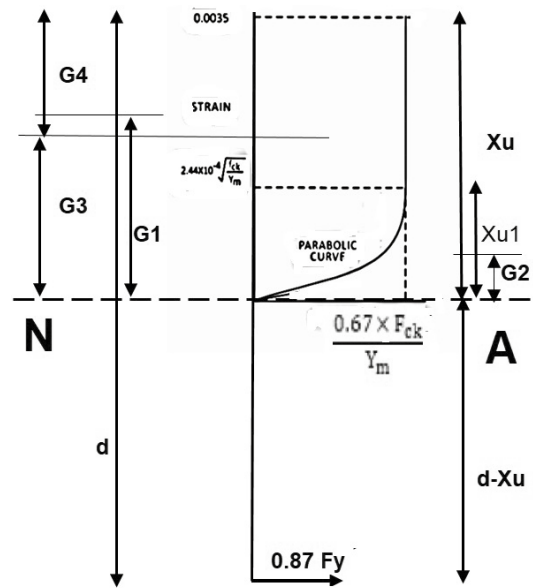
❖ **Loads and CDA**

Coefficient of dynamic augment(CDA)	=1.138
CDA1	= 0.885
App XXIIIa Bridge Rule, EUDL for BM for 400 mm ballast cushion	
App XXIIIa Bridge Rule, EUDL for SF for 400 mm ballast cushion	
Span,m ---- EUDL,kN	Span,m ---- EUDL,kN
2.0 0 ---- 409.9	2.00 ---- 410.4
2.5 0 ---- 425.9	2.50 ---- 489.7
2.10 ---- 413.1	2.40 ---- 473.84
Loads 25t, loading 2008 ,Load factors	

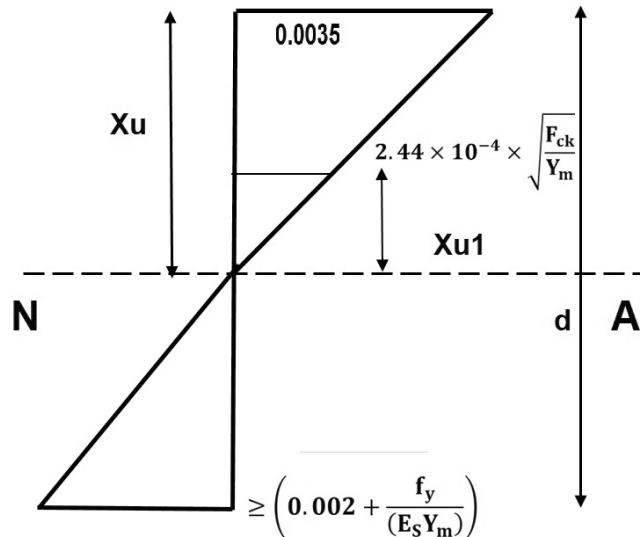
Case	Dead Load	Super Imposed Dead Load	Live Load with CDA	Earth Pressure
ULS	1.25	2.0	1.75	1.70

Live load from Appendix XXIIIa of Bridge rule for 2.100 m

Live load	= 413.100 kN
Live load on slab per m ²	= 46.893 kN/m ²
Live load+CDA1	= 154.674 kN/m ²
15% for derailment load	= 23.201 kN/m ²
Ballast 0.515 x 19.2 equal to	= 19.776 kN/m ²
Track , 12 T/M Hence	= 5.721 kN/m ²
Slab with ULS factor	
0.375 x 25 equal to	= 11.719 kN/m ²
Total load	= 215.091 kN/m ²



a. Stress Block Parameters for concrete (IRS)



b. Strain Parameters for concrete and steel (IRS)

Fig. 4 The variation of stress and strain parameters in concrete and reinforcement of RC slab bridge as adopted in IRS concrete bridge code, 2014.

❖ **Analysis and Design of RC section**

Bending moment M (without torsion)	=118.569 kNm
Diameter of bar	=2.000 cm
Clear cover	=5.000 cm
Effective depth d	=0.315 m
Maximum strain in concrete, ϵ_c	=0.0035
Strain at start of Parabola in concrete, ϵ_1	= $2.44 \times 10^{-4} \times \sqrt{\frac{F_{ck}}{Y_m}}$
Strain in C.G of tension steel ϵ_s	= $(0.002 + \frac{f_y}{(E_s Y_m)})$
Maximum stress in concrete S1 =	= $\frac{0.67 \times F_{ck}}{Y_m} = 13.4 \text{ MPa}$
Maximum stress in steel S2=	= $0.87 \times F_y = 435 \text{ MPa}$
Grade of concrete F_{ck} ,	=30 MPa
Partial safety factor for material strength (Concrete) $Y_{m\text{-steel}}$	=1.5
Partial safety factor for material strength (steel) $Y_{m\text{-con}}$	=1.15
Eoungs Modulus of concrete E_c	=28000 MPa
Maximum strain in concrete block ϵ_c	=0.0035
Strain in concrete at parabolic entry ϵ_1	=0.001091
Strain in tension steel not less than ϵ_s	=0.004174
Depth of parabola in stress block X_{u1}	=0.311 (X_u)
$(1 - X_{U1})=$	=0.688 (X_u)
$0.002/\epsilon_c =$	=0.571
$S1 \times (1 - X_{U1}) =$	=9.222 (X_u)
Rectangle area of con stress block, $A_r = S1 \times (X_u)$	=13.400 (X_u)
Bottom Parabolic area of con stress block $A_p = S1 \times (X_{u1}/3)$	=1.392 (X_u)
Total area of concrete stress block $A_c = A_r - A_p$	=12.007 (X_u)
C.G of A_r from bottom N.A, $G1$	=0.5(X_u)
C.G of A_p from bottom N.A, $G2$	=0.077 (X_{u1})
$C_1 = A_r \times G1 = 6.700 (X_u)^2$,	$C_2 = A_p \times G2 = 0.108 (X_u)^2$
$A_g = C1 - C2 = 6.591 \times (X_u)^2$,	$G_3 = \frac{A_g}{A_c} = 0.548 \times X_u$
$G4 \times X_u = (X_u - G3) = 0.453 \times X_u$	Lever. Arm = d -0.451 (X_u)
$A_c \times b$	=12.007 b(X_u), N
Effective depth of beam d	=315, mm
Width of beam b ,	=1000, mm
Bending moment , M_u	=1659 *10 ⁵ , Nmm
$\frac{M_u}{bd^2} = 1.672$,	$A_c \times (\frac{X_u}{d}) = -12.007 (\frac{X_u}{d})$
$A_c \times G4 \times (\frac{X_u}{d})^2 = 5.416 \times (\frac{X_u}{d})^2$,	$(\frac{X_u}{d}) = 0.149$, $X_u = 47.029$
Full compression force $C_{uf} =$	=5.64 X 10 ⁵ N
$A_{s,s} = C_{uf} / (0.87XF_y) =$	=1298.1 mm ²
$A_{st\text{-min}}$, mm ²	=630
Diameter of bar, mm	=314
Area of bar, mm ²	=241.88
Bar Spacing, mm	=20mm Dia @
Provided	190mm c/c

Minimum Compression Steel at top	= 472.500 mm ²
Area of 12 Diameter bar	= 113.040 mm ²
Spacing of top bar	= 239.238 mm c/c
	12 mm Tor @
	190.000 mm c/c

Distributors 12 mm Tor @ Minimum

A_{std}	=378.400 mm
Area of 12 Diameter of bar	=113.040 mm ²
Spacing of distribution bars, at top & bottom	=449.020 mm
	= 12 mm Tor @
	190.000 mm c/c

Calculation of Moment of Resistance

Provide 20 mm Diameter @	=190 mm c/c
A_{st} provided	=1652.632 mm ²
Revised N.A	= 59.908mm safe
calculation of Z	= 284.702mm
$Z < 0.95d$	= 299.250 mm safe
Check	

Ultimate moment of resistance	
Due to reinforcement (Fig.24)	= 192.152 kNm
Due to concrete (Fig.10)	= 446.513 kNm

❖ **Check for Shear**

EUDL for shear	= 473.840 kN
(appendix XXIIIa bridge rule)	
Load/m ² for shear	=53.787 kN/m ²
EUDL with CDA1	=101.381 kN/m ²
Total load	=263.178 kN
shear force V	=276.337 kN
shear stress t_v	=1.535 N/mm ²
$t_{v\text{max}1}$	=4.108 N/mm ²
$t_{v\text{max}2}$	=4.750 N/mm ²
Actual $t_{v\text{max}}$	=4.108 N/mm ²
$t_v < t_{v\text{max}}$	Safe
% of reinforcement provided(main)	=0.525
t_{vc}	=0.537
depth factor s1(as per 15.4.3.2 of Br.code)	= 1.122
s_2	= 0.700
Actual s	=1.122
s^*t_{vc}	= 0.603

$t_v > t_{vc}$ safe Safe
 $A_{sv} = K_v * S_v K_v = 3.063$
 Spacing of 12mm Diameter links $S_v = 194.213$ mm
 Provide links 12 mm Dia @190
 X 190 mm c/c

From Table 15 of IRS Concrete. $\%A_{st} \text{ --- } t_{vc}$ N/mm²
 Bridge. Code t_{vc} N/mm² 0.5 ----- 0.53
 1.0 ----- 0.67
 0.525 ----- 0.537

❖ Check for Torsion

Minimum eccentricity as per
 Bridge rule = 0.1 m
 EUDL for torsion effect = 413.100 kN
 Torsional moment = 41.31 kNm
 Torsional moment / m length = 19.67143 kNm
 Longitudinal Moment = 118.569 kNm
 Maximum shear force = 276.337 kN
 Equivalent BM = 165.9039 kNm <
SAFE 192.152 kNm
 Equivalent SF = 549.686 kN
 < **618.899 kN**
SAFE

❖ Shear Capacity

shear force V (without torsion) = 276.337 kN
 shear force V (with torsion) = 549.686 kN
 shear capacity of concrete = 189.832 kN
 shear capacity of links = 429.067 kN
 total shear capacity $V_{st} = 618.899$ kN
 $V_{st} > V$ safe

❖ Check for Deflection

Eoungs Modulus of concrete $E_c = 28000$ N/mm²
 Effective span = 2.100 m
 Total EUDL with CDA1 = 3039.233 kN
 Main, $A_{st} = 6932.789$ mm²
 Main, $A_{sc} = 2495.804$ mm²
 Mix = M30.000 N/mm²
 Modular ratio = 9.333
 Breadth of beam = 4195.000 mm,
 Effective depth, d = 315.000 mm

Effective cover, dc = 56.000 mm,
 Moment of Inertia = 44439502632.323
 Permissible Deflection mm⁴
 Actual Deflection = 4.200 mm
 = 0.067 mm

Table 2. IRS and IS code provisions of various aspects (for beams and slabs)

Clauses of codes	IRS concrete Bridge code 2014	IS 456-2000	IRC 112-2011
Minimum reinforcement for tension	$\frac{0.2 \times (b \times d)}{100}$ (Cl.15.9.4.1)	$\frac{0.85 \times b \times d}{F_y}$ (Cl. 26.5.1.1.a)	$0.0013 X bd$ (Cl.16.5.1.1.1)
Minimum % of steel for compression	$\frac{(0.3)}{100} \times (b \times d)$ (Cl.16.9.4.2.4.i)	Maximum of (i). $0.0012 \times bd$, (ii). $\frac{C_{ur}}{\min \text{ of } F_{ys}}$ (Cl. 25.1.11 & F _{ys} as in iii & iv of Table.22)	$0.01x b x dc$ (12.3.3.4 & 16.5.4.4)
Side face reinforcement	0.05% bd on each face (15.9.4.2)	0.1% of bd (Cl. 26.5.1.3)	> 150 mm ² (Cl.16.9.4)
Maximum compressive stress in stress block of concrete, σ_c MP _a	$\frac{0.67 \times F_{ck}}{Y_m}$ (Cl. Cl.15.4.2.1. b, Fig 4A)	$\frac{0.67 \times F_{ck}}{Y_m}$ (Cl.38.1. a, Fig.21)	$\frac{0.67 \times F_{ck}}{Y_m}$ (Cl.6.4.2.8, Fig.6.5)
Maximum stress in steel, MP _a	$0.87F_y$ (Cl. 15.4.2.1.d, Fig.4B)	$0.87F_y$ (Cl.38.1. f, Fig.23)	$0.8F_y$ (Cl.12.2.2)
Maximum strain in concrete block	0.0035 (Cl. Cl.15.4.2.1. b)	0.0035 (Cl.38.1. b)	0.0035 (Table 6.5, Sl.no.10)
Strain at start of parabola in concrete stress block, ϵ_1	$2.44 \times 10^{-4} \times \sqrt{\frac{F_{ck}}{Y_m}}$ (Cl.15.4.2.1.b, Fig 4A)	0.002 (Cl.38.1. a, Fig .21)	0.002 (Table 6.5, Sl.no.9)
Strain in steel not less than	$\left(0.002 + \frac{F_y}{(E_s \times 1.15)} \right)$ (Cl. 15.4.2.1.d)	$\left(0.002 + \frac{F_y}{(E_s \times 1.15)} \right)$ (Cl.38.1. f)	$\epsilon_{ud} = 0.02175$ (Cl.6.2.2 and Fig.6.2)
Concrete stress block shape	Rectangle with parabolic profile	Rectangle with parabolic profile	Rectangle with parabolic profile
Partial safety factor for material strength (Concrete)	1.5 (cl. 15.4.2.1.b)	1.5 (Cl.38.1.c)	1.5 (Cl.6.4.2.8, Fig.6.5)
Partial safety factor for material strength (steel)	1.15 (cl. 15.4.2.1.d)	1.15 (Cl.38.1. e)	1.15 (Cl.6.2.2, Fig.6.2, Note.1)
Spacing of main bar shall not exceed	300 mm (cl. 15.9.8.2.1)	300 mm (Table 15. Clear Distance Between Bars.)	300 mm (Cl.12.3.6, Table 12.3)
Spacing of stirrups shall not exceed	450 mm or 0.75 d (cl.15.4.3.2.4)	300 mm or 0.75 d (Cl. 26.5.1.5)	600 mm or 0.75d (Cl.16.5.2.7 & 16.5.2.9)
Maximum area of tension reinforcement	0.04 X B X D (Cl.15.9.5.1)	0.04 X b X D (Cl. 26.5.1.1.b)	(0.025) X Ac (Cl.16.5.1.1.2)
Maximum area of compression reinforcement	0.04 X B X D (Cl.15.9.5.1)	0.04 X b X D (Cl. 26.5.1.2)	(0.04/2) X Ac (Cl.16.5.1.1.2)

The various clauses of design aspects in IRS concrete bridge code 2014, IS: 456-2000 and IRC: 112-2011 are reviewed and given above in the Table.2. The most of the design provisions

are similar in the codes cited above except very few aspects with different details.

Conclusions

1. This paper provides Moment of Resistance of RC slab of width 100 cm for percentage of steel P_t varying from 0.2 to 2.0 for the grades of steel Fe500 and grades of concrete M30.
2. Moment of Resistance of RC slab for depth varying from 15 cm to 80 cm and width of 100 cm for the grades of concrete M15 to M40 is furnished.
3. It is easy to design the RC tension members of various bridges i.e. RC slabs, RC T-Beam decks, RC box culverts, RC pipe culverts, RC piers and abutments, RC pile caps and piles, RC approach slabs and RC wing and return walls.
4. Shear resistance in terms of balance shear force to be resisted and effective depth for grades of steel F_y 415, F_y 500, F_y 550 and F_y 600 for Diameter of bars (8, 10 and 12 mm) with respect to various spacing are developed.
5. A model calculation for 25ton loading 2008 with grade of steel F_y 500 and grades of concrete .M30 is furnished for guidance.
6. Various provision in IRS, IRC and IS codes are studied.
7. This design charts emphasizes the need of design aids to IRS concrete Bridge code, 2014 as available for IS:456-2000.

References:

1. Indian Railway Standard, "Bridge Rules", Research Designs and Standard Organization, LuckNow, 2014.
2. Indian Railway Standard, "Code of Practice for Plain, Reinforced & Prestressed Concrete for General Bridge Construction", Research Designs and Standard Organization, LuckNow, 2014.
3. Indian Standards 456-200, "Plain and Reinforced Concrete code of practice", Bureau of Indian Standards, New Delhi.
4. Indian Standards, "Design Aids for Reinforced Concrete to IS: 456-1978".
5. Indian Standards 1786-2008, "High Strength Deformed Steel Bars and Wires for Concrete Reinforcement— Specification (Fourth Revision)", Bureau of Indian Standards, New Delhi.
6. Indian Standards 383-2016, "Coarse and Fine Aggregate for Concrete Specification", Bureau of Indian Standards, New Delhi.
7. Ramamrutham, S., (1973) "Strength of Materials", Dhanpat Rai & Sons, Delhi-6.
8. Varghese., (1999), "Limit State Design of Reinforced Concrete", Prentice-Hall of India Pvt Ltd, New Delhi-110001.
9. Park.R., Paulay., (1975), "Reinforced concrete structures", John Wiley & Sons, New York.
10. IRC:112-2011., "Code of Practice for Concrete Road Bridges", Indian Roads Congress, New Delhi-110022.



A hybrid fault diagnosis scheme for railway point machines by motor current signal analysis

Proper analysis of point machine current signal provides pervasive information of health status of their internal components. Point machines are subjected to several failure modes during their operation. "Gearbox," "ball bearing," "lead screw," and "sliding chair" faults are among common mechanical failure modes. In this article, a two-stage prediction innovative process is proposed using Fault Detection based Decision Tree strategy (FDDT) where the healthy and faulty modes are first determined, followed by classifying the types of mechanical faults based on Parallel Neural Network Architecture and Fuzzy

System (PNNFS). To differentiate between faulty and healthy point machines, some relevant features are extracted from the motors' current signals which are used as input data for the proposed FDDT_PNNFS method. Feature selection has been performed using the ReliefF to select the dominant predictors in the point machine. Firstly, the Decision Tree (DT) algorithm is used to obtain a classifier model based on the offline training method for fault detection. The performance of DT is compared with the support vector machine algorithm. In the second stage, faulty data is fed to a bank of Neural Networks,

Designed in Parallel Neural Network Architecture (PNNA), which is used for identifying the type of failures. Each Neural Network Algorithm (NNA) is responsible for detecting only one type of failure and assessment of the NNA outputs shows the final failure of the point machine. If there is a discrepancy between the outputs of the NNAs, fuzzy logic plays the role of modifier and judges among outputs of NNAs and determines the more probable fault type. **Keywords** Point machine, fault detection, fault identification, decision tree, neural network, fuzzy logic **Introduction** Point machine is a type of equipment that switches the blades from one position to its opposite to set different paths for the trains. Defects in the operation of the point machine have a significant effect on train travels. Critically, it may lead to cataclysmic accidents resulting in casualties. In other words, real-time condition monitoring of railway point machines is highly significant. The subject of condition monitoring and fault identification in engineering systems has been noticed considerably in previous research over recent decades. These include research in the field of wind turbines, batteries, engines, point machines, pipelines, etc. Fault detection and identification

methods on point machines are developed in various researches that have been conducted pervasively and include signal-based and data-driven methods.

Regarding methods of condition monitoring, we can mention the use of vibration signals received directly from the point machine, sound signals, displacement and limit switches, image sensors, and motor current signals. Motor current signal approach has received the most attention in recent works, due to the potentials for remote monitoring of the system. Although early research in this field has used more basic methods.

By : Khadem Hossaini Narges, Mirabadi Ahmad and Gholami Manesh Fereydoun

Ref. : Rail and Rapid Journal, Oct- 22



Effects of the highway live load on the additional forces of the continuously welded rails of a long-span suspension bridge

High-speed running trains have higher regularity requirements for rail tracks. The track-bridge interaction of long-span bridges for high-speed railways has become a key factor for engineers and researchers in the last decade. However, studies on the track-bridge interaction of long-span bridges are rare because the bridges constructed for high-speed railways are mainly short- or moderate-span bridges and the effects of the highway live load on the additional forces of continuously welded rails (CWRs) have not been reported. In the present study, the effects of the highway live load on the additional forces of a CWR of a long-span suspension bridge are investigated through numerical simulations. A track-bridge spatial analysis model was established using the principle of the double-layer spring model and the bilinear resistance model. The additional stress and displacement of the rail are calculated, and the effects of the highway live load are analyzed and compared with those without a highway live load. The results show that the highway live load has an obvious effect on the additional forces of a CWR. Under a temperature force, the highway live load increases the maximum tensile stress and compressive stress by 10 and 13%, respectively. Under a bending force, the highway live load increases the maximum compressive rail stress and maximum displacement by 50 and 54%, respectively. Under a rail breaking force, when the highway live load is taken into consideration, the rail displacement at both sides of the broken rail varies by 50 and 42%,

respectively. The highway live load must be taken into consideration when calculating the additional forces of rails on highway-railway long-span bridges.

By : Xiangdong Yu, Nengyu Cheng, Haiquan Jing

Ref. : Rail and Rapid Journal, Oct- 22

Railway track support condition assessment—Initial developments on a vehicle-based monitoring solution through modal analysis

Nowadays, there are multiple initiatives showing a renewed interest on railway transport of goods and passengers around the world. Thus, an efficient management of railway infrastructures, both at the operational level and in terms of economic profitability, is not only desirable but also corresponds to an area of ongoing research. In order to contribute to these efforts, an alternative and novel methodology to evaluate railway track support conditions is presented here, based on modal analysis of the characteristic frequencies of the multi-element system composed by a railway infrastructure and an instrumented vehicle moving over it. This methodology belongs to the group of vibration-based structural damage identification methods, and is focused on observing the characteristic frequencies of this multi-element system, which can be correlated with changes in the physical properties of the railway infrastructure under analysis. An important feature of the proposed methodology is that it should enable the collection of information regarding the conditions of the substructure of a railway infrastructure. By performing this assessment of a railway infrastructure over its length, and over time by comparing different rides over the same railway stretch, important information can be gathered regarding the support conditions of the track. This paper presents a complete description on the current stage of development of the proposed methodology, along with the theoretical model that serves as the basis to interpret the collected data. Preliminary verification of this methodology is performed through the analysis of two case studies regarding the passage of an instrumented vehicle over two underpasses. The results obtained so far show that the proposed methodology can provide relevant information regarding the support conditions of railway tracks.

By : João Morais, Paulo Morais, Carlos Santos, André Paixão and Eduardo Fortunato

Ref. : Rail and Rapid Journal, Oct- 22

A review of research into aerodynamic concepts for high speed trains in tunnels and open air and the air-tightness requirements for passenger comfort

India will soon have its first line with trains operating at internationally defined standards of high speed (exceeding 250 km/h). On the MAHSR (Mumbai-Ahmedabad High Speed Railway) corridor modern high speed trains will routinely operate at speeds as high as 200 mph (320 km/h). At high speed, trains are capable of generating significant aerodynamic effects including wind gusts and air pressure changes, which makes it necessary to address HSTs' aerodynamics during the planning stage of high-speed rail (HSR) lines. The dynamic pressure tightness in train cars is also an important factor in the design of future railway tunnels, together with the medical health criterion and pressure comfort criteria. With increasing speed, the requirements of pressure tightness increases, which are explained and illustrated in this study. The current study is based on prior work done in the field of aerodynamic effects of HSTs, international standards, and design practice followed in existing HSR projects. Effort has been made to bring various studies in one place for ready reference. Parameters such as pressure comfort, optimized distance between center of track, wayside structural design, and tunnel cross-section requirements are explained. Based on the study and established relation by different authors, the pressure difference calculation is done for the MAHSR project for different scenarios, and passenger comfort was deduced. In this study, three major aspects of the aerodynamic pressure effect on the rolling stock and surroundings are examined, and each aspect is discussed distinctly: (1) open-air considerations: pressure effect on wayside structures,

(2) open-air considerations: two trains crossing in the open field,

and (3) open-air considerations: tunnel phenomenon: pressure wave effects on trains inside tunnels. The present study and a substantial portion of the existing knowledge base can be extrapolated for use in the future guidelines in India. This study examine the resultant pressures on wayside structures, the resultant pressures on adjacent trains, and pressure wave effects in tunnels (associated analyses were performed to determine the appropriate cross-sectional area of the tunnels), respectively. It includes basic aerodynamic concepts, influencing factors, measurement and calculation of pressure between trains, known and potential impacts, mitigations,

standards, conclusions, and recommendations.

By : Sandeep Srivastava, Govindu Sivasankar and Gautam Dua

Ref. : Rail and Rapid Journal, Oct- 22

Detection of rail local defects using in-service Trains

As track components deteriorate, their interaction dynamic response will alter accelerations on the train. Measuring acceleration on train components is a method to conduct condition monitoring of track defects. The measured signal can be used for the detection of rail surface defects which implement impacts on measured accelerations. In this paper, the axle-box acceleration (ABA) is measured in a subway as a case study. Fourier transform (FFT), empirical mode decomposition (EMD) and ensemble EMD (EEMD) methods are used to study accelerations relative to the track. Wheel frequencies are calculated using finite element method (FEM) to determine frequency couplings. Velocity-dependent/independent components and source of excitation of the measured signal are distinguished. Results indicated that the FFT approach can be applied for both velocity-dependent and velocity-independent vibration components for frequencies up to 680 Hz. Also, the EEMD method can be used to distinguish the impact component of the measured signal.

By : Morad Shadfar and Habibollah Molatefi

Ref. : Rail and Rapid Journal, Oct- 22

Development of metro track geometry fault diagnosis convolutional neural network model based on car-body vibration data

Traditional track geometry fault diagnosis methods, such as track geometry car, track detection trolley and manual measurement, suffer from low detection frequency. Therefore, using vibration data from in-service metro vehicles to diagnose metro track geometry faults can improve the efficiency of metro track condition detection. Hence, a metro track geometry fault diagnosis model using car-body vibration was established in this study based on a convolutional neural network model, and the effects of the structural hyperparameters on the model performance were analysed. First, the problem of car-body vibration data collection was addressed, and a mileage-locating model without the global navigation satellite system was developed. Then, the metro track geometry fault diagnosis model was derived using a convolutional neural network whose architecture is determined by four hyperparameters. Finally, a case

study was performed using the Beijing Subway 1 track geometry car detection data and car-body vibration data. The results demonstrated the effectiveness of the proposed model.

By : Zhipeng Wang, Rengkui Liu, Futian Wang and Yuanjie Tang

Ref. : Rail and Rapid Journal, Oct- 22

A review of snow melting and de-icing technologies for trains

Train icing may cause a series of problems to the safety of railway transportation in high and cold regions. Some important technologies on solving this issue are discussed in this paper, with the latest research landscape provided and the future development opportunities suggested. The hazards and principles of train icing are explained firstly, followed by a summary of several available methods of snow melting and de-icing, with their application and shortcomings indicated. The research progress of some basic issues such as the snow conditions of bogie parts and the optimal design of snow protection are discussed and analysed in detail. However, the problem of snow and ice accumulation during train operation has not been completely solved with the existing methods. At the end of this paper, suggestions on snow-resistance technology for trains are proposed for future study and development.

By : Liang Zhou, Liang Ding and Xian Yi

Ref. : Rail and Rapid Journal, Oct- 22

Safety of a high-speed train passing by a windbreak breach under different wind speeds

A derailment phenomenon could take place on the windward side of a 120 km/h high-speed train when it runs by a breach, between two windbreak walls, subjected to a normal wind speed of 32 m/s. To study the safety of a high-speed train under different normal speeds of crosswind, six wind speeds are investigated; 32m/s, 28 m/s, 25 m/s, 20 m/s, 15 m/s, and 10m/s. The wind forces and moments of the moving train are calculated using the Unsteady Reynolds-averaged Navier-Stokes (URANS) model, which are then applied to the train multi-body dynamics. The pressure fields around the train passing by the breach are analysed, which gives a reasonable explanation for the fluctuation of the wind loads. After an analysis on the response of the train, it is apparent that the risk of derailment on the windward side is much greater than the risk of overturning. The lateral distance of the first wheelset increases towards the windward side

as along with the yaw angle of the wheelset, which increases as well with wind speeds of higher than 20 m/s.

By : Zhuang Sun, Syeda Anam Hashmi, Huanyun Dai and Guiyu Li

Ref. : Rail and Rapid Journal, Oct- 22

Design method of worn rail grinding profile based on Frechet distance method

Due to the large volume and high running density of railway freight lines, rail deterioration occur frequently. Thus, it is necessary to grind the rail in time to improve the wheel-rail relationship. The profile data of the worn rail were measured at different measuring points in a section, and the Frechet distance method was adopted to analyze the data. The representative profile reflecting the overall condition of rail wear in this section is obtained. Combined with NURBS curve theory, a fitting algorithm in which the rail profile with certain discrete points was established. Taking the reduction of the amount of grinding material removed as the objective function, setting wheel-rail matching characteristics, and the reduction of rail wear as the constraint conditions, a calculation model for rail grinding profile was established. The dynamic characteristics of standard profile CN75 and g grinding profile OP75 were analyzed by the vehicle track dynamics model. The results showed that compared with the standard profile CN75, the amount of grinding material removed of the grinding profile OP75 is reduced by 44.7%, and the height reduction of the rail top is reduced by 0.39 mm. After 3 _ 104 km of running, the wear amounts of grinding profile OP75 is about 36.1%–36.5% less than that of standard profile CN75. In the small curve section, the derailment coefficient of grinding profile OP75 is reduced by 11.7% compared with that of standard profile CN75. The dynamic performance is improved. The grinding target profile has better dynamic characteristics and is beneficial to reduce wheel-rail wear.

By : Fengtao Lin, Liang Zou, Yang Yang, ZhenShuai Shi and Songtao Wang

Ref. : Rail and Rapid Journal, Oct- 22

A vision-based method for line-side switch rail condition monitoring and inspection

In railway systems, switch rails are one of the key

components of switches & crossings (S&C). They are controlled by switch machines to guide trains from one track to another. Due to the discontinuity in geometry, switch rails are exposed to high impact loads as train wheels pass through. The long-term impact loads can cause local plastic deformation. These faults, and general alignment changes, can lead to the development of a gap between the switch rail and the stock rail known as a toe gap, as well as non-optimal contact with the wheel flange, both of which can endanger the safe operation of passing trains.

Currently, periodic visual inspection is the main method for detecting these defects. This is not efficient or reliable enough to support the ever-shortening maintenance windows available in modern railway systems. The development of computer vision technologies and constantly improving processors make it possible to monitor the health status of such safety-critical components in real time. This research proposes a line-side condition monitoring approach for the switch rail. With the use of dedicated identification algorithms, the status of the switch rail, including movement, position, toe gap and the edge of the toes, can be monitored remotely in real time. This approach has been tested in a high-speed train testing centre in China. The results show a capability to further improve the safe operation of S&C while simultaneously reducing the cost and increasing the safety of inspection.

By : Jiaqi Ye, Edward Stewart, Qianyu Chen, Lei Chen and Clive Roberts

Ref. : Rail and Rapid Journal, Oct- 22

Visualization of wheel-rail contact area of running vehicle using film sensor

Proper evaluation of the wheel-rail contact is necessary to understand the dynamics of railway vehicles and the causes of wear and damage to components such as wheels and rails. Numerical methods are often used to evaluate the dynamic contact condition between the wheel and rail; however, there are few promising methods for experimental evaluation. It is important to develop a measurement method because the wheel-rail contact is easily changed owing to vehicle-track dynamic interactions. In this study, we used a film-based pressure sensor equipped with force-sensitive resistors to measure the contact area between the wheel and rail during vehicle operation. Using the film-based pressure sensor, we evaluated the geometry of the contact area and position. The validity of the measured contact position is evaluated by comparing it with the contact position based on the

cross-sectional profiles of the wheel and rail and the wheelset displacement during a vehicle running.

By : Shinya Fukagai, Takashi Toyama, Takayuki Tanaka, Masahito Kuzuta and Hisayo Doi

Ref. : Rail and Rapid August 22

Investigation into the braking performance of high-speed trains in the complex braking environment of the Sichuan-Tibet Railway

The Sichuan-Tibet Railway is an east-west rapid plateau railway under construction from Chengdu to Lhasa. One of its most remarkable features is the high altitude and notable altitude fluctuations. High altitudes will result in low atmospheric pressures and temperatures. The freezing caused by low temperatures will lead to low wheel-rail adhesions. Altitude fluctuations will generate complex spatial railway tracks. To investigate the braking performance of a train in such a complex braking environment, a train spatial dynamics model, a model of a direct pneumatic brake system and a model of a braking control strategy are constructed. A comprehensive analysis model for investigating the braking performance of high-speed trains in a complex braking environment is proposed based on the constructed train spatial dynamics model, direct pneumatic brake system model and braking control strategy model. A simulation computation platform for train braking performance analysis on the Sichuan-Tibet Railway is established based on SIMPACK, AMESim, Simulink and their interfaces. The braking performance under the different altitudes, different spatial railway tracks and low adhesions are analysed in detail and summarized. Computation time are compared in different altitudes and track conditions. Computational efficiencies of the dynamic model with multi-thread parallel computation are discussed. The results indicate that an increasing altitude and the alteration of railway track conditions have a remarkable influence on the braking distance, brake cylinder pressure, instantaneous deceleration, maximum wheel-load reduction rates and maximum longitudinal impact forces of high-speed trains. The track conditions in the dynamic model have a greater impact on the computation speed. Compared to single-thread parallel computation, the computational efficiency using 2-thread parallel computation can be promoted by 22.97%. These results will provide a reference for the Sichuan-Tibet Railway design and the optimization of train braking systems.

By : Wentao Zhao¹ , Jianming Ding¹, Qingsong Zhang¹ and Weiwei Liu²

Ref. : Rail and Rapid August 22

Augmented asset management in railways – Issues and challenges in rolling stock

Managing assets in railway, including infrastructure and rolling stock, efficiently and effectively is challenging. The emerging digital technologies and Artificial Intelligence (AI) are expected to augment the decision making in Asset Management (AM) and Fleet Management (FM). The AI technologies need to be adapted to the specific needs of any industrial domain, e.g. railways, to facilitate the implementation and achievement of the overall business goals. This adaptation is denoted as 'Industrial AI'(IAI). IAI for railways infrastructure and rolling stock, is dependent on an appropriate technology roadmap reflecting necessary know-hows. The IAI roadmap aims to provide a strategic and executive plan to augment managing railway assets i.e. 'Augmented Asset Management (AAM)'. AAM can be applied through an end-to-end secure platform for e.g. data sharing among stakeholders, the development of analytics, and model sharing through distributed computing. AAM in railways can be enhanced through implementation of a generic fleet management (FM) approach. In the FM approach, any population of assets with common characteristics and also the relationship of the asset to the fleet is considered. This paper aims to develop and propose a concept for AAM enabled through IAI and digital technologies to provide augmented decision support through a secure platform, for AM in railways. A FM approach towards a holistic operation and maintenance of assets, based on a System of Systems thinking, for AAM in railways is applied for population of infrastructure assets and rolling stock assets with common characteristics. Finally, a taxonomy of issues and challenges, in the application of AAM to FM in railways is provided. The data for this taxonomy has been collected from railway organizations through iterative rounds of interviews. This taxonomy can be used for research and development of frameworks, approaches, technologies, and methodologies for AAM in railways.

By : Jaya Kumari , Ramin Karim, Adithya Thaduri and Miguel Castano

Ref. : Rail and Rapid August 22



